The role of DNA repair gene *Ercc1* in the liver

Kristina Kirschner

Doctor of Philosophy

University of Edinburgh

2006

Für meine Eltern

Table of Contents

Declaration

The composition of this thesis and the work presented is my own, unless otherwise stated. All experiments were designed in collaboration with my supervisor Prof. David W. Melton.

Kristina Kirschner

Acknowledgements

There are many people who helped me during the work on this thesis, giving me advice and practical help on a professional basis as well as keeping me sane by providing out- of work entertainment. To all those people, I am truly grateful! One person whose door stood always open for me and who was always willing to listen to my many ideas, concerns and doubts was my supervisor Prof. David Melton. Not only did he provide a lot of encouragement and advice throughout the production of this thesis, he also offered an insight into the infamous Bristish humour. I felt very well looked after throughout my time in his laboratory and could always rely on him for support, something I came to appreciate many times when little obstacles came my way. I would also like to thank my second supervisor, Prof. David Harrison, whose very valuable comments helped me to gain a deeper understanding of all things liver related. I am grateful to Dr. Sandrine Prost for inviting me into her laboratory and teaching me a lot of methods used throughout this thesis. Without her providing the necessary help at a critical point of my Ph.D. this project would not have been possible in the current form. Along with that go many thanks to Helen Caldwell, Louise Treanor, Pin Lu and Stephen Boyce for always answering my many questions surrounding the liver work in vitro and in vivo. You made me very welcome in your laboratory at Teviot! I always appreciated our little coffee breaks at this evil American coffee house even though my bank account had to suffer. I would also like to thank Mr. Robert Morris for helping with the histology and always finding the time for a little chat on the way. Dr. David Brownstein offered valuable support with the pathological analysis of some of my samples. I am grateful to our collaborator Dr. Sing Raj who performed the malondialdehyde analyses on my samples. I would also like to thank Cancer Research UK for funding throughout my project.

I am obviously very grateful to all those great people from the Melton lab who were always willing to help me with experiments and taught me a lot about British society. Without my partners in crime at the student office, my time in the lab would only just have been half as much fun. Had Nicola Lawrence not provided many curious stories

picked out of the press, Oliver Maddocks not introduced me to the delights of Waitrose and Liang Song not made me laugh by being a bit too honest sometimes, it would have been a rather boring life! I hope that more initiatives like song competitions, sweepstakes and trips to Firbush will emerge from the student office and help to create a relaxed atmosphere in the lab. Our newest member in the office, Annelies Turksma, always supported me on all issues concerning the continent. A healthy working environment was provided by Lynn Morrice, Kate Britton and Nicola Lawrence. Many running trips helped to keep those cakes off my hips! Jennifer Doig not only introduced me to the pleasures of the mouse house, she also helped to keep my bench tidy and showed me what mountain biking is all about! Our little chats from bench to bench will be truly missed. I am extremely grateful to James Selfridge who solved the mystery of Southern blotting and will hopefully not suffer from further nightmarish consequences. Ann- Marie Ritchie was always willing to join in and fight the flow cytometer and other little bugs that came my way during tissue culture. Thank you! Thanks shall also go to Joanne Povey, Lesley Shaw, Helen Ibbotson, Vivien McGrath and Ewan Brown for providing excellent conversation material over coffee breaks!

I would like to thank Alexej Larionov for his help with the Real- time PCR. I would also like to thank the Abbott group for letting me use their wonderful Real- time PCR machine!

I am very grateful to the BRF staff, especially Ian and Chris, for always looking after my little mice and keeping me up on the mouse house gossip. I would like to thank Morweena and Susan for helping me with i.v. injections which are far harder to do than it looks!

Meine Eltern, meine Schwester und meine Oma haben immer an mich geglaubt und sind all die Jahre, die ich im Ausland verbracht habe, ununterbrochen für mich da gewesen. Ihr seid immer in meinem Herzen!

Without Alistair looking after me and making me laugh all these years, things would not have been the same. Thanks for all your support!

Abstract

The ERCC1/XPF complex is responsible for incision at the 5' side of the DNA lesion during nucleotide excision repair and is also involved in homologous recombination and inter-strand cross-link repair. The aim of the current study was to set up a better model for examination of *Ercc1* deficiency in the liver and to determine the DNA lesions responsible. Initially, we used the Cre/lox system with the floxed *Ercc1* gene and a tamoxifen- inducible liver- specific Cre transgene. However, only low and irreproducible levels of recombination were detected in vivo or in vitro with no consistent biological effects. We therefore switched to a cell culture approach using the loxP system and an AdenoCre virus. AdenoCre infection of hepatocyte cultures led to high levels of recombination with no ERCC1 protein remaining at 48 hours after infection. Flow cytometry failed to show high levels of polyploidy in knockout hepatocytes 1 week after infection. This differed from the premature polyploidy seen in this study in *Ercc1*- deficient livers. We used AdenoCre to reduce ERCC1 levels in adult liver in vivo. Low levels of recombination resulted in increased ploidy, indicating that polyploidisation may be a protective mechanism triggered by increased levels of DNA damage in *Ercc1*- deficient liver. *Ercc1*- deficient hepatocytes in vitro underwent higher levels of spontaneous, UV- and oxidative damage- induced apoptosis than control cultures, implying that *Ercc1* is essential for liver maintenance. Lipid accumulation was observed in older *Ercc1*- deficient hepatocyte cultures, one week after AdenoCre infection in vivo and also in young *Ercc1*- deficient and wild type livers. Lipids disappeared in the wild type controls with age, but persisted in *Ercc1* Null livers. These findings suggest that a reduced ability to repair oxidative DNA damage and a malfunction of oxidative pathways could be responsible for the *Ercc1*- deficient liver phenotype. Regeneration of liver following exposure to carbon tetrachloride in AdenoCre infected livers led to an increase in ploidy and S-phase independent of genotype, masking the increased ploidy resulting from AdenoCre induced *Ercc1* deficiency. Livers from simple *Ercc1* knockout mice showed no increase in malondialdehyde adducts. However, higher levels of reactive oxygen species were detected in young *Ercc1*- deficient livers compared to controls. RT Real- time PCR was used to determine differences in

expression of cell cycle regulation and survival genes between *Ercc1*- deficient and control livers. We succeeded in characterising *Ercc1* deficiency in the liver further.

Abbreviations

$(HhH)_2$: double helix- hairpin- helix

μ: micro

2n: diploid

^{3}H- Thd: ^{3}H- thymidine

4- OHT: 4- hydroxytamoxifen

4n: tetraploid

8n: octaploid

8-oxo-G: 8- oxo- guanine

A: adenosine

ATP: adenosine triphosphate

BER: base excision repair

bp: base pair

BrdU: 5- bromo-2- deoxyuridine

BW: body weight

C-: carboxyl terminal

C: cytosine

CCl_4: carbon tetrachloride

CDK: cyclin dependent kinase

CHO: Chinese hamster ovary

CM-H2DCFDA: 5-(and-6)-chloromethyl-2',7'-dichlorodihydrofluorescein diacetate, acetyl ester

CMV: cytomegalovirus

CS: Cockayne's syndrome

Da: Dalton

DEN: diethyl nitrosamine

DNA- PKcs: DNA- dependent protein kinase catalytic subunit

DNA: deoxyribonucleic acid

DSB: double strand breaks

E.coli: Escherichia coli

EGF: epidermal growth factor

ER: oestrogen receptor

ERCC: excision repair cross- complementing

ERK: extracellular signal regulated kinase

ES: embryonic stem

FACS: fluorescence activated cell scanning

Fas: apoptosis stimulating fragment

Fpg: formamidopyrimidine- DNA- glycosylase

g: gram

G: guanine

GAPDH: glyceraldehyde 3- phosphate dehydrogenase

GGR: global genome repair

GO: glucose oxidase

HCC: hepatocellular carcinoma

HGF: hepatic growth factor

HhH: helix- hairpin- helix

HNPCC: hereditary nonpolyposis colon cancer

HR: homologous recombination

i.p.: intraperitoneal

i.v.: intravenous

ICL: interstrand cross- link

IGF: insulin- like growth factor

Igfbp2: insulin- like growth factor binding protein

kb: kilo base

KO: knockout

m: messenger

M: molar

M_1dG: malondialdehyde deoxyguanosine

MAPK: mitogen- activated protein kinase

MER: murine oestrogen receptor

MMC: mitomycin C

MMR: mismatch repair

mt: mitochondrial

N-: amino terminal

NER: nucleotide excision repair

NFκB: nuclear factor kappa B

PCNA: proliferating cell nuclear antigen

PCR: polymerase chain reaction

pfu: plaque forming unit

PH: partial hepatectomy

PI3K: phosphoinositide 3- kinase

Rb: retinoblastoma protein

Ref-1: redox factor 1

RNA: ribonucleic acid

ROS: reactive oxygen species

rpm: revolution per minute

RT: reverse transcriptase

S. cerevisiae: Saccharomyces cerevisiae

SOD: Mn- superoxide dismutase

T: thymidine

TBP: tata- binding protein

TC- NER: transcription coupled nucleotide excision repair

TGFβ: transforming growth factor β

TNFα: tumour necrosis factor α

TS: translesion bypass

TTA: thioacetamide

TTD: Trichothiodystrophy

TTR: transthyretin

U: unit

UTR: untranslated region

UV: ultraviolet

V: volt

Wt: wild type

XP: Xeroderma pigmentosum

1. Introduction

1.1 Overview

DNA damage is one of the major causes of genome instability, mutation and carcinogenesis as well as ageing. Hydrolysis, oxidation and non- enzymatic methylation of DNA can be detected in vivo with 2,000-10,000 purine bases being subject to hydrolytic depurination in each human cell per day (Lindahl 1993). In order to deal with the various types of DNA damage and to ensure integrity of the organism, several pathways have evolved to protect the cell. Mismatch repair (MMR) is one of these pathways, dealing with unpaired and mispaired bases in the DNA (Marti et al. 2002). Another pathway is known as base excision repair (BER). It is involved in repair of smaller base modifications generated endogenously through hydrolysis or reactive oxygen species (Klungland et al. 1999a). More severe damage, caused by UV irradiation, psoralens, cross-linking agents and free radicals is dealt with by nucleotide excision repair (NER) (Sancar 1996). Homologous recombination (HR) dependent repair and non- homologous end joining (NHEJ) both repair double-strand breaks (DSB) produced during recombination events and by ionising radiation. In HR the homologous sister chromatid is used as a template. In contrast, NHEJ requires no such extensive homology (Sargent et al. 1997). Translesion bypass is a mechanism that allows the bypass of unrepaired DNA lesions by specific polymerases that lack a proof- reading capacity, helping to prevent a collapse of the replication fork during S- phase (Larsen et al. 2005).

In order to be able to extend the knowledge about human disorders involving defects in one of the repair pathways, investigations in lower organisms such as *Escherichia coli (E. coli), Saccharomyces cerevisiae (S. cerevisiae*) and mammalian cultured cells have been made. In addition, mouse models have been created using gene targeting as one of the major tools.

1.2 MMR

MMR pathways in *E. coli, S. cerevisiae* and humans have been described, with the methyl-directed MutHLS pathway of *E. coli* being the best-characterised (Marti et al. 2002). In this pathway, mismatches arising from replication errors, spontaneous or induced base modifications or during recombination, are recognised and repaired. Damage recognition takes place through MutS activation and formation of a repairosome consisting of MutS, MutH and MutL. The repairosome is responsible for excision at the mismatched site and seems to load helicase II onto the damaged DNA. The unwound DNA strand is then degraded by several factors including ExoX and ExoI, and eventually repaired by polymerase III and DNA ligase using the intact single stranded counterpart as a template (Marti et al. 2002).

Key proteins in MMR are highly conserved from bacteria to mammals and multiple homologues of MutS and MutL have been described in yeast and mammals (Buermeyer et al. 1999). Six MutS homologs have been identified in eukaryotes named MSH1-6, as well as MLH1-3, PMS1 and PMS2 showing homology to prokaryotic MutL (Prolla 1998). A model for the early steps of human DNA MMR has been proposed with the MSH2/MSH6 heterodimer initiating the repair process. The heterodimer binds to DNA mismatches and small insertion or deletion loops spanning 1-2 bp (Prolla 1998). Alternatively, MSH2 can form a complex with MSH3 and recognise 2-5 bp long insertion or deletion loops (Buermeyer et al. 1999). The initial step is then followed by ATP hydrolysis leading to a conformational change of either heterodimer, allowing the MLH1/PMS2 complex to bind to the lesion. A possible role in recruitment of other proteins and strand discrimination has been suggested for the eukaryotic MutS/MutL complexes (Buermeyer et al. 1999). Excision and re-synthesis of the damaged strand follows, involving EXOI/HEXI, DNA polymerases δ and ε as well as PCNA and RPA. The DNA ligase that completes the repair remains to be identified (Buermeyer et al. 1999).

Associations with mutations in MMR genes and human cancer have been made, especially with colon cancers from families with hereditary non- polyposis colon

cancer (HNPCC). HNPCC is an autosomal dominant, highly penetrant cancer characterised by early onset of colon carcinomas and cancers of the endometrium, stomach, upper urinary tract, small intestine and ovary after the fourth decade of life (Prolla 1998). Mutations in MSH2, MSH6, MLH1, PMS1 and PMS2 have been linked to HNPCC with MSH2 and MLH1 being the most frequently mutated factors in HNPCC patients (Buermeyer et al. 1999). Affected family members usually inherit one defective allele of the gene involved with an additional somatic mutation in the other gene being necessary for cancer to occur.

1.3 BER

BER mechanisms are highly conserved in evolution and help to maintain the DNA integrity. They evolved to deal with small base alterations that do not distort the DNA helix. Defects in key activities are lethal at an embryonic state (Klungland et al. 1999a). BER requires several distinct steps including a DNA glycosylase which releases the damaged base by cleaving the bond that connects the base to the deoxyribose (Klungland et al. 1999a). Different glycosylases deal with different types of damage (Krokan et al. 2000), leaving an abasic site (AP). This abasic site is then cleaved by hydrolytic AP endonucleases such as APE1 (= REF1) in mammalian cells resulting in a 5'- terminal abasic residue (Demple and Sung 2005). In short patch repair, dRp lyase, located in the N- terminal domain of mammalian polymerase β, excises this abasic residue and repair of the gap is undertaken by DNA polymerase β and others, replacing one single nucleotide. DNA ligation is then carried out. In contrast, two to eight nucleotides are replaced during long patch repair, where flap endonuclease I (FEN 1) excises the displaced flap. DNA ligase I or DNA ligase III in complex with XRCC1 finish the repair process (Demple and Sung 2005).

Although different enzymes and proteins central to BER and NER are used during the actual repair process, some functional overlaps, especially concerning the involvement of XPG in oxidative damage repair, have been reported (Klungland et al. 1999a). XPG is a structure specific endonuclease being responsible for the

cleavage of the 3' end of different types of lesions in NER. However, BER is the main repair pathway dealing with oxidatively damaged DNA bases. Typically, the DNA glycosylase-AP lyase hNTH1 performs the initial excision of the lesion with XPG facilitating the binding of hNth1 to the DNA substrate (Klungland et al. 1999a). Thus, XPG seems to be involved in both repair mechanisms carrying out different functions. Another example of functional overlap of the two systems is provided through studies of OGG1 DNA glycosylase. This glycosylase recognises the most frequent oxidative base lesion named 8- oxo-guanine (8-oxo-G) which is normally dealt with by BER (Klungland et al. 1999b). A report on *Ogg1* deficient mice reveals that these animals are viable but do not show any excision of the 8-oxo-G by an alternative glycosylase in cell free tissue extracts. However, in an *Ogg1* Null cell line, slow repair could nevertheless be detected, indicating a possible role for NER as an alternative system for repair of 8-oxo-G (Klungland et al. 1999b).

1.4 NER: global and transcription coupled repair

Dealing with many different kinds of DNA damage that occur in the form of bulky adducts, NER is one of the most flexible of all DNA repair mechanisms with similar principles in prokaryotes and eukaryotes (de Boer and Hoeijmakers 2000). After damage recognition, a dual incision is made at the damaged site to remove an oligonucleotide containing the lesion (Figure 0). Gap-filling repair follows by using the intact strand as a template (Sancar 1996). Two sub- pathways of NER have evolved with global genome nucleotide excision repair (GG- NER) removing lesions throughout the genome and transcription coupled nucleotide excision repair (TC-NER) ensuring a fast repair of lesions located on the transcribed strand of actively transcribed genes (Gillet and Schärer 2006). As structurally different types of DNA damage is repaired by NER, the system may not recognise the lesion per se, but an alteration in thermodynamic features of the DNA around a lesion might help to initiate NER.

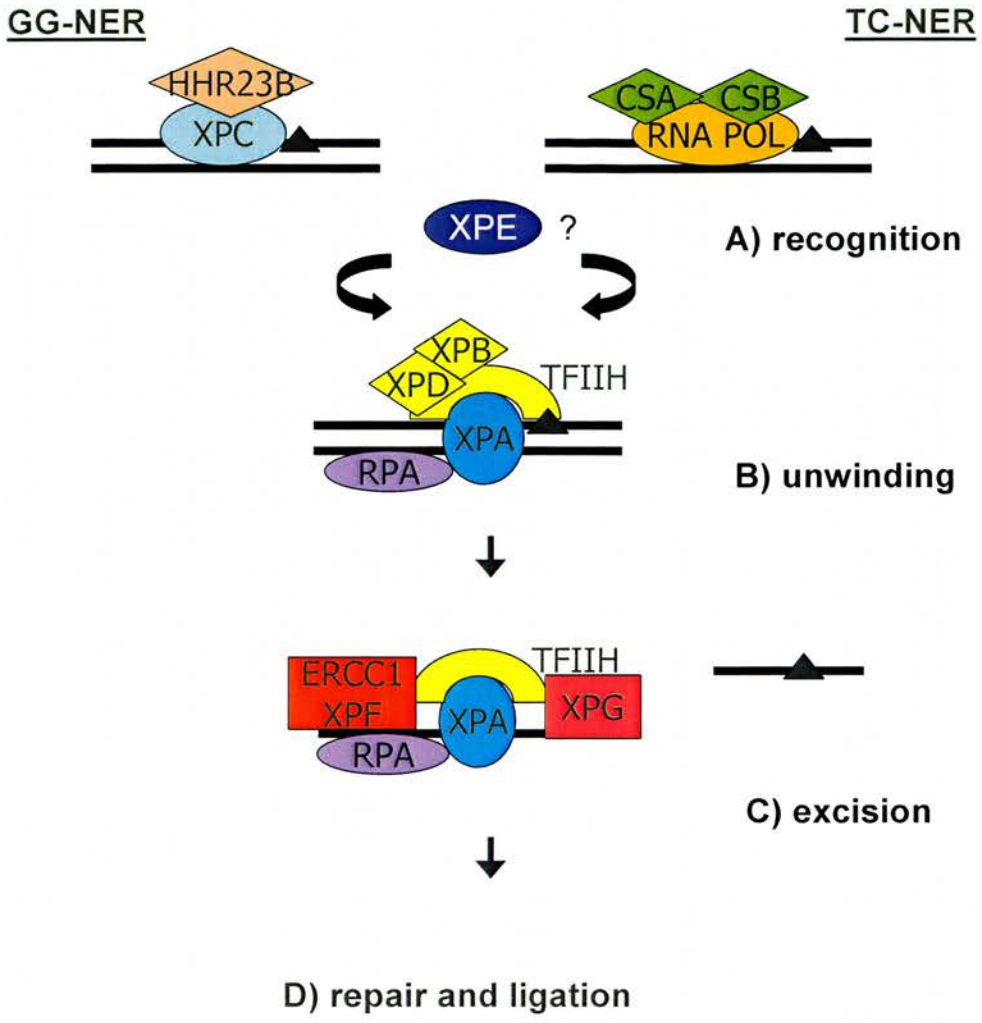

Figure 0: Global genome (GG) and transcription coupled (TC) nucleotide excision repair (NER) in vitro. A) Damage recognition. In GG- NER damage recognition occurs upon binding of XPC in complex with HHR23B. In TC- NER, stalled RNA polymerase (RNA pol) II in complex with CSA and CSB recognises DNA damage. In both pathways, other NER factors are then recruited to the site of the lesion, possibly with the involvement of XPE. B) DNA unwinding. In both pathways, transcription initiation factor IIH (TFIIH), consisting of ten subunits including XPB and XPD, and RPA protein are recruited to the complex to unwind the DNA around the lesion. XPA, RPA and XPG then help to form a pre- incision complex around the lesion. C) Excision. Upon recruitment of ERCC1/XPF complex to the damaged site, 3' incision is performed by XPG followed by 5' incision which is catalysed by the ERCC1/XPF complex. D) Repair and ligation. Immediate repair around the excision site might be initiated by the 5' incision through ERCC1/XPF. RPA, RFC, PCNA and DNA polymerases δ and ε are likely to carry out the gap- filling process. DNA ligase I completes the repair process. DNA strands are symbolised by black lines. DNA lesions are marked as black triangles.

Although the main features are evolutionarily conserved from bacteria to man, NER in eukaryotes involves around 20-30 proteins compared to prokaryotic NER which employs only three proteins. In general, a convergent evolutionary event seems to be represented in prokaryotic and eukaryotic NER with proteins sharing little structural homology but functional similarities (de Boer and Hoeijmakers 2000).

NER has been extensively studied in *E. coli* revealing some of the basic mechanisms. *E. coli* excision nuclease consists of three subunits: UvrA, UvrB and UvrC. The UvrA2UvrB complex tracking along the DNA performs the damage recognition step (Sancar 1996). In the event of DNA damage the rather unspecific binding of the complex to the DNA changes to a more specific binding. This first step involves unwinding of the DNA by UvrB followed by a conformational change of the protein. The conformational change of UvrB leads to the formation of an intimate complex between UvrB and the DNA (Sancar 1996). Dissociation of UvrA is then essential for dual incision by UvrB and UvrC. UvrB recruits UvrC to the damaged site as well as being responsible for the 3' incision of the single stranded DNA lesion. The 5' incision is made by UvrC releasing a 12-13 nucleotide oligomer. The final repair process is then initiated by binding of helicase II. After dissociation of UvrC, the 3'-OH at the 5' site is revealed and becomes accessible for polymerase I to fill in the gap and displace UvrB (Sancar 1996).

Studies in human NER have contributed to crucial understanding of global NER. In vitro, the damage recognition step initially involves the XPC/ HHR23B complex to recruit the whole repair machinery to the lesion (Gillet and Schärer 2006). XPE then arrives at the damaged site and is thought to be involved in verification of the lesion. XPC/ HHR23B complex recruits TFIIH which opens the helix locally (Gillet and Schärer 2006). This process is ATP dependent. TFIIH is a protein complex consisting of ten subunits, including XPB and XPD helicases. If XPD encounters a chemical modification of DNA during NER, the TFIIH complex stalls at the site of the lesion and signals for further assembly of other factors (Gillet and Schärer 2006). TFIIH plays a role in NER as well as in transcription, and is required for local unwinding of the DNA helix and the transcription initiation of RNA polymerase II at

the promoter (de Boer and Hoeijmakers 2000). Once the DNA is accessible, XPA, RPA and XPG are recruited to the XPC-HR23B/TFIIH/DNA intermediate platform and, upon protein to protein interaction, a stable pre- incision complex is formed, leading to XPC- HR23B being expelled (Gillet and Schärer 2006). RPA helps to load the ERCC1/XPF complex onto the damaged DNA site. The 3' incision is then carried out by XPG followed by the 5' incision made by ERCC1/XPF. In addition, the creation of a free 3'- hydroxyl end after ERCC1/XPF incision is thought to immediately initiate repair. Excision of the 24-32 nucleotide oligomer containing the lesion is followed by gap-filling carried out by RPA, RFC, PCNA and DNA polymerase δ and ε. DNA ligase I completes the final repair step (de Boer and Hoeijmakers 2000). In general, a multitude of weak protein protein interactions rather than a strong interaction between some factors only is crucial to ensure smooth transition during NER.

In vivo GG- NER is thought to require additional steps as chromatin remodelling is essential to access the site of the lesion. XPE (= DDB), a UV- damaged DNA binding factor, seems to be a central player in chromatin remodelling during NER with its strong affinity for UV- damaged DNA and its association with known factors involved in chromatin remodelling (Gillet and Schärer 2006). The re- assembly of chromatin after NER is thought to be mediated by the histone chaperone CAF-1 which seems to be recruited by PCNA after the repair is completed.

Although global genome NER takes place in a general manner, there is preferential repair carried out during transcription. This is not only true for eukaryotes but has also been detected in procaryotic cells (Sancar 1996). Transcription-coupled NER is essentially the same as global genome NER apart from the recognition step. On encountering a DNA lesion during transcription, RNA polymerase II stalls and signals the damage to the repair machinery. CSA and CSB are thought to help recruit the NER machinery to the site of DNA damage (Friedberg 2001). In order for the repair proteins to associate with the DNA, RNA polymerase II must first dissociate

from the site allowing the repair to take place.

In general, NER is carried out if bulky DNA damage is apparent in cells. TC-NER, with a preference for the transcribed strand of DNA, ensures that the transcription of genes can be carried out correctly acting in a short-term manner. In contrast, global NER repairs lesions in the overall genome more slowly, preventing mutations from being passed on to the next generation and keeping the integrity of the genome stable.

1.5 NER deficiencies in humans

NER deficiency in humans has been linked to several disorders with severe phenotypes. Three rare recessive diseases with photosensitive syndromes can occur from a defect in NER: Xeroderma pigmentosum (XP), Cockayne's syndrome (CS) and Trichothiodystrophy (TTD).

1.5.1 Xeroderma pigmentosum (XP)

XP is associated with very high photosensitivity and 1000- fold increased risk for skin cancer, as well as 10-to-20 fold higher risk for diverse internal cancers (Petit and Sancar 1999). The most common skin cancers seen during the development of the disease are basal cell carcinomas and squamous cell carcinomas with an average onset age of around 8 years (de Boer and Hoeijmakers 2000). Other characteristics in XP patients occur as ocular and neurological abnormalities with a rate of 40% and 30-40% of the cases being affected respectively (Petit and Sancar 1999). Seven complementation groups have been identified within the NER deficient group of XP patients, XPA to XPG. XP is a disease with defective overall NER.

1.5.2 Cockayne's syndrome (CS)

CS is characterised by a cutaneous photosensitivity along with increased sensitivity to some mutagenic agents in most patients. However, CS is a TC-NER defective disease and no predisposition to developing skin cancer can be observed (Petit and Sancar 1999). Instead, it is more likely that patients suffer from physical and mental retardation. CS patients generally display skeletal abnormalities and progressive neural degeneration (de Boer and Hoeijmakers 2000) giving rise to a possible link between defective TC-NER repair of oxidative lesions and CS features. Mutations in CSA and CSB seem primarily responsible for CS onset.

1.5.3 Trichothiodystrophy (TTD)

TTD patients show brittle hair and scaling of skin along with mental and physical retardation as characteristics of the disease. Photosensitivity is reported in most patients. Defects in TTD-A seem to be primarily causing the observed phenotype, although additional mutations in NER factors such as XPD and XPB can also cause photosensitivity in TTD patients (de Boer and Hoeijmakers 2000). TTD is a disease with broad clinical heterogeneity and has therefore been described in association with other syndromes. It is classed as a transcriptional syndrome.

Different mutations in the XPB, XPD and XPG genes give rise to a specific clinical outcome leading to either XP, XP/CS or TTD (Andressoo and Hoeijmakers 2005). This can be explained by the fact that those genes are not only involved in NER, but also play a role in transcription. XP patients suffer from a NER related defect in TFIIH resulting in photosensitivity and cancer development, while the basal transcription function of TFIIH is affected in CS and TTD patients, leading to a different range of symptoms (Andressoo and Hoeijmakers 2005). Moreover, combined XP/CS patients display mutations that affect both functions of XPD. In general, XPD complementation group patients are generally found to be heterozygous with one non-functional allele and a disease specific causative allele.

1.6 Double strand break repair: Homologous recombination and NHEJ

DNA DSB are one of the most severe forms of damage to the cell as chromosome rearrangements, loss of chromosome segments or even loss of the whole chromosome can take place. To minimise the risk of loss of genetic information, potent repair mechanisms have evolved using two different pathways.

One of these pathways, homologous recombination, has been extensively studied in *S. cerevisiae* and is regarded as being an error-free process. A template, usually a sister chromatid, is needed to carry out the repair event (Sargent et al. 1997). Therefore, HR is only functional in late S/G2 phase. A current model in *S.cerevisiae* suggests that after a DSB the 3' OH- end of the damaged DNA strand invades an unbroken double-stranded homologue to form a heteroduplex (Thacker 1999). According to this model, RAD50 along with other proteins form a complex that leads to nucleolytic resection in a 5' to 3' direction, enabling RAD51 to bind specifically to the 3' end of the damaged site (Jackson 2002). Other proteins such as RAD52 facilitate RAD51 binding. The RAD51 nucleoprotein is responsible for localisation of the homologous DNA template, promotes the initial invasion step and catalyses strand exchange events (Jackson 2002). Additional proteins of the RAD family help to complete this process. DNA synthesis by polymerase I occurs at the 3' end of the damaged strand, using the homologue as a template. Ends are joined by DNA ligase I. The cross-overs are finally resolved by cleavage and further ligation resulting in two intact DNA molecules (Jackson 2002). Mammalian homologues seem to exist for all HR factors, but recombination repair in higher eukaryotes is likely to be more complex.

Mammalian cells tend to make a more extensive use of NHEJ repair, the second pathway dealing with DSB (Sargent et al. 1997). This mechanism is not as accurate but has an advantage for eukaryotes as no extensive homology is required. This pathway is therefore able to operate in G1. Because of the increased complexity of

the genetic information in eukaryotes, appropriate homologous regions become harder to locate and alternative methods are necessary in order to carry out repair of DSB efficiently (Jackson 2002). Essential for NHEJ is the Ku heterodimer with its Ku70 and Ku80 subunits. The complex recognises and binds to DSB in a specific manner to then recruit other proteins to the damaged site (Jackson 2002). One of the recruited elements is the DNA-dependent protein kinase catalytic subunit (DNA-PKcs) that forms a holoenzyme along with the Ku heterodimer. Activation of this complex is triggered by the single-stranded DNA region at the damaged site itself, resulting in alteration of the complex's targets such as XRCC4 and replication factor A (Jackson 2002). XRCC4 itself is thought to interact in a tight complex with DNA ligase IV to stimulate end- ligation. Direct end- joining is most likely to lead to loss of information and slightly alters the DNA sequence at the DSB. As most DSB result from mutagenic agents, some DNA processing might be necessary before end-joining can take place. A likely candidate for the processing step is the mammalian MRE11/RAD50/NBS1 complex (Jackson 2002). Nevertheless, processing events often lead to deletion or introduction of some nucleotides. NHEJ does not seem to play a major role in yeast, but it seems to act as a complement to the homologous recombination pathway. There is now mounting evidence that complementary interaction of both pathways in prokaryotes and eukaryotes are a likely pattern to repair DSB (Driscoll and Jeggo 2005).

Several DSB deficiencies in mammals are known with many of them being involved in immunodeficiency related diseases. Severe combined immunodeficiency (Scid) is one of the sterner immunodeficiency diseases in humans with one half of the patients showing a defect in adenosine deaminase correctable by gene therapy (Weaver 2003). This form of the disease displays an autosomal recessive inheritance pattern and patients are prone to serious infections. Some Scid syndromes are classified as a disease with T and B lymphocyte (T^-B^-) defects and are linked to the X chromosome. T^-B^- Scid is thought to be caused by V(D)J recombination defects giving rise to an increased cancer risk in lymphoid tissues (Weaver 2003). Ig rearrangements have been observed from pre-B cells of B^- patients leading to extended deletions that destroy coding sequences. Additionally, chromosomal translocations with V(D)J

recombination site breakpoints are frequently found in lymphoid malignancies where the translocation alters the expression of genes such as c-MYC or BCL-2 (Weaver 2003). Patients with Ataxia Telangiectasia (AT) are at great risk for lymphoid malignancies because of the repair machinery being unable to recognise DSB as opposed to a lack of repair machinery (Weaver 2003). AT patients usually show perturbations of ATM, a kinase involved in activation of checkpoint responses following DSB (Lombard et al. 2005). Dysfunctional ATM leads to an accumulation of unrepaired DSB and a severe phenotype including premature ageing, immunodeficiency, cerebellar degradation and cancer (Lombard et al. 2005, Taylor and Byrd 2005). Other proteins have been associated with DSB repair defects leading to alterations of the cell cycle response. Phosphorylated BRCA1 or BRCA2 normally interacts with RAD51, participating in DNA damage dependent cell cycle checkpoint response (Zafonte et al. 2000). Mutations in BRCA1 and BRCA 2 may therefore lead to accumulation of damaged DNA because of a failure to trigger cell cycle arrest after DSB and contribute to increased cancer risk (Zafonte et al. 2000). In addition, BRCA 1 and BRCA2 are thought to be involved in RAD51- mediated invasion of homologous DNA during HR (Lombard et al. 2005). Defects in RAD51, BRCA1 and BRCA2 can therefore lead to genomic instability, chromosome aberrations and cancer (Thacker 2005).

1.7 Translesion bypass (TS)

TS allows the bypass of lesions by specific polymerases that lack a proof- reading capacity (Larsen et al. 2005). This mechanism helps to prevent a collapse of the replication fork during S- phase. In addition, TS is faster than NER and BER, but potentially mutagenic (Larsen et al. 2005). There are multiple specialised polymerases acting together during TS (Friedberg 2005). Specialised polymerase have a preferred substrate which leads to replacement of nucleotides in an error- free manner, but some specialised polymerases also allow repair in an error- prone manner. A limited processivity is characteristic for all specialised polymerases (Friedberg 2005). Usually, a switch from a high fidelity polymerase to a specialised polymerase occurs when the replication fork is stalled during replication. Once the

lesion is bypassed, the high fidelity polymerase resumes its activity around 1000 bp downstream of the lesion, leading to successful DNA replication. In *E. coli*, the replication fork helicase DnaB seems to be involved in the coordination of replication re- initiation signalling through DnaG (Heller and Marians 2006). PCNA acts as a DNA clamp and helps loading the specialised polymerases onto the DNA (Friedberg 2005). Mechanisms involved in signalling for polymerase switching have still to be discovered.

Interestingly, a defect in polymerase η function, a member of the Y- family of translesion bypass polymerases, has been linked to a clinical syndrome in humans. XP variant (XPV) patients display a XP phenotype with a late onset of around 30 years of age and much milder symptoms (Gratchev et al. 2003). In addition, NER is functional in patients suffering from XPV. Polymerase η has been implicated with correct bypass of thymidine- thymidine cyclobutane pyrimidine dimers (Friedberg 2005). In the absence of functional polymerase η, translesion bypass is catalysed by other DNA polymerases with a high likelihood of incorporating incorrect nucleotides. An increased mutation frequency is then responsible for the phenotype observed in XPV patients over time.

1.8 ERCC 1

In 1984 Westerveld et al. (1984) reported the successful cloning of human *ERCC1*. Since then, extensive genetic characterisation of the protein has been achieved. The *ERCC1* gene has been assigned to chromosome 19 with its exact location being at 19q13.2-13.3 (van Duin et al. 1987). The gene is about 15 kb in length and consists of 10 exons of which exon 8 is subject to alternative splicing (van Duin et al. 1987). The resulting mRNA products are 1.1 kb, 3.4kb and 3.8 kb in size with the 1.1 kb transcript being the major mRNA species (van Duin et al. 1987). The 3.4 and 3.8 kb mRNA transcripts most likely result from differential polyadenylation (van Duin et al. 1987). The *ERCC1* promoter is located at approximately 170 bp upstream of the transcriptional start site and does not show any of the classical promoter motifs such

as an AT-rich region or a TATA box (van Duin et al. 1987), indicating that this could represent a specific class of promoters. A striking homology between the 297 amino acids (aa) comprising human ERCC1 and the 210 amino acid *S. cerevisiae* RAD10 has been detected by van Duin and co-workers (1986). The C-terminus of RAD10 shows significant homology to the central 110 aa of ERCC1. These homologous regions are likely to display DNA- binding ability as structural comparisons to typical DNA-binding motifs show (van Duin et al. 1986). In contrast, the N-terminus of the ERCC1 product is not essential to carry out repair mechanisms in *ERCC1* deficient cells as the N- terminus deprived ERCC1 protein is still active (van Duin et al. 1986). In addition, ERCC1 carries a 53 residue long C-terminal extension that is not part of the RAD10 homology, but displays homology with the *E.coli* NER protein UvrC (de Laat et al. 1996). This region, being located to residues 236-289, consists of a double helix-hairpin-helix (HhH) motif. These motifs have been found in a lot of DNA break processing enzymes and are probably also involved in DNA binding (de Laat et al. 1998). This region is essential for ERCC1 endonuclease activity. Interaction with XPA is seen to be a crucial step in positioning the ERCC1/XPF complex onto the DNA, making the 93-120 residues in the ERCC1 protein, which bind XPA, an important part of the protein (de Laat et al. 1998). The regions responsible for binding XPF have been identified to be residues 224-297 in ERCC1 and 814-905 in XPF (de Laat et al. 1998).

Lately, part of the structure of the human ERCC1/XPF complex has been revealed, shedding more light onto the complex interaction between the two proteins (Tripsianes et al. 2005). This study showed that only XPF contains the nuclease domain of the complex but it does require ERCC1 for subsequent nuclease activity. Moreover, the interaction of the two proteins has been confirmed to lie in their C-terminal regions which both carry double helix- hairpin- helix $(HhH)_2$ domains (Tripsianes et al. 2005). However, only the $(HhH)_2$ domain of ERCC1 has been found to have DNA binding properties and is thus responsible to ensure correct positioning of the endonuclease upon DNA damage and interaction with other NER proteins such as XPA (Tripsianes et al. 2005) . These findings reveal that within the ERCC1/XPF complex, each subunit has got a specific function, ensuring error- free

processing of DNA lesions.

Comparison of mouse and human *ERCC1* genes showed a high similarity and the promoter region revealed a homologous sequence at 50-90 bp upstream of the transcriptional start (van Duin et al. 1988). The N-terminal of the mouse ERCC1 protein seems to be less conserved than the human protein and a functional protein arises even when the N- terminal of the protein is deleted. Moreover, the C-terminal extension is also prominent in the mouse protein (van Duin et al. 1988). The similarity between human and mouse ERCC1 offers the convenient opportunity to use mice with *Ercc1* deficiencies as a model for human defects.

1.9 ERCC1 in NER

The stable heterodimer formed by ERCC1 and XPF in vitro suggests that the two proteins are unstable in the absence of each other (Enzlin and Schärer 2002). XPA and RPA appear to have a role in damage verification and are also necessary to load and position the endonuclease correctly onto the damaged DNA. Interaction of ERCC1 and XPA at amino acids 93-120 of ERCC1 is thought to be required for NER (Enzlin and Schärer 2002).

A truncation of seven aa at the C-terminal of the ERCC1 protein has been reported to give rise to a decrease in the level of incisions. This leads subsequently to the accumulation of DNA breaks after unrepaired DNA damage persists in mouse cells heterozygous for the *Ercc1* mutation (Weeda et al. 1997). It also seems that overexpression of ERCC1 can be lethal for cells and only minimum amounts of the protein are available in the cell (van Duin et al. 1987). *ERCC1* expression does not seem to be UV-inducible (van Duin et al. 1988). So far, a defect of *ERCC1* has not been proven to lead to XP or any other human disease. This could be due to the consequences of such a defect being embryonic lethal.

1.10 ERCC1 in recombination and interstrand cross- link (ICL) repair

An additional role for ERCC1 is thought to be in homologous recombination. Evidence is given by the fact that RAD10 and ERCC1 share a significant homology and that RAD10 along with RAD1 is involved in recombinational repair in yeast. Moreover, ERCC1/XPF deficient cells are the only cells with a NER defect showing high sensitivity to interstrand cross-links created by mitomycin C. The repair of such damage is believed to require mitotic recombination (Melton et al. 1998).

Adair and co-workers (2000) reported a necessity of ERCC1 for removal of long non- homologous tails from 3'-OH ends of invading strands during targeted homologous recombination in Chinese hamster ovary (CHO) cells. These findings strengthen the assumption that recombinational repair is one of the functions for ERCC1. Kuraoka et al. (2000) proposed a new model for the repair of interstrand cross-links taking the incision properties of the ERCC1/XPF heterodimer into account. According to this model, a Y structure is created near the damage for example by the replication fork while in progression or by a DNA helicase. ERCC1/XPF then cleaves at the 3' side of one arm of the cross-link and then makes an additional incision at the 5' side. The fork collapses and recombination and NER events can take place to complete the repair (Kuraoka et al. 2000).

Although some involvement of ERCC1 in recombination repair pathways cannot be denied, it seems not to be an essential factor. Melton and co-workers (1998) induced inter-strand cross links in *Ercc1*-deficient murine cells and could only detect a moderate sensitivity to mitomycin C, concluding that ERCC1 is not essential for homologous recombination and that an additional pathway may exist to deal with the damage. In *S. cerevisiae* RAD1-RAD10 complex is involved in processing of non-homologous 3' tails during single strand annealing (Paques et al. 1999). Single strand annealing is a pathway that evolved to repair ICL which are located between direct tandem repeat sequences (Zheng et al. 2006). ICL induced single strand annealing

was decreased in a cell line lacking XPF (Zheng et al. 2006). In addition, Chipchase and Melton (2002) found that ERCC1- and XPF- deficient cells showed a lower incidence of chromatid exchange to DSB when compared to Wt and other NER-deficient cells after UV irradiation. UV- induced chromosome aberrations are thought to form when unrepaired DNA damage is present during DNA replication. These chromosome aberrations result from successful single strand annealing between non- homologous chromosomes in the presence of ERCC1/XPF. When ERCC1/XPF is absent, DSB accumulate as a consequence of impaired single strand annealing. Thus, ERCC1/XPF is involved in successful single strand annealing where the complex is most likely to trim non- homologous 3' tails arising during this process (Chipchase and Melton 2002).

In general, reports show that lower levels of ERCC1 complex are needed for elimination of cross-links compared to UV lesion removal (Sijbers et al. 1996). ERCC1 does not seem to be a rate-limiting step in interstrand cross- link repair. This could be explained by the assumption that ERCC1 displays a higher activity dealing with interstrand cross- links or that removal of this type of damage only requires low levels of the complex as the amount of interstrand cross- links in normal cells is very low (Sijbers et al. 1996).

Sarkar et al. (2006) examined interstrand cross- link repair in *S. cerevisiae* further, suggesting that a combination of pathways might be involved in lesion repair in G1 phase. Yeast cells are without homologous recombination substrate during the G1 stage of the cell cycle and can therefore not rely on the classical recombination based pathway of repair of ICL repair (Sarkar et al. 2006). Instead, NER factors, such as ERCC1/XPF and XPG, incise DNA around the ICL without removal of the lesion. When the high fidelity polymerase β stalls at the adducted oligo site, signalling to the RAD6 pathway occurs, leading to monoubiquitination of PCNA at K164. A polymerase switch to polymerase ζ, a B- family polymerase known to replicate through a variety of lesions, then occurs (Sarkar et al. 2006). Translesion synthesis and re-initiation of replication downstream of the lesion follows. An interplay between the predominant NER pathway and the translesion bypass pathway helps to

bypass ICL during G1 of the cell cycle in yeast. If this pathway is important in higher organisms remains to be elucidated.

Xu et al. (1998) found homologues of human *ERCC1* and yeast RAD10 in several plant genera, including lily. These homologues were able to correct mitomycin C induced lesions in Chinese hamster ovary cells, pointing to existing NER and recombination mechanisms in plants. These results have since been further confirmed and other NER factors similar to XPF have been found in *Arabidopsis* flower tissue (Liu et al. 2000).

1.11 ERCC1 deficiency in mice

With approximately 99% of the mouse genes having a homologue in the human genome, mice are a convenient model to investigate genetic disorders (Mouse genome sequencing consortium 2002). Mice have been used for biomedical research for a long time, and with the rediscovery of Mendel's law of inheritance in the beginning of the last century and the start of gene mapping, knowledge about the mouse genome has been extended (Mouse genome sequencing consortium 2002). Gene targeting has become a useful tool making it possible to alter particular genes and study the functional consequences of these alterations. The main principle of gene targeting is based on homologous recombination of a vector carrying, for example, a specific gene and a chromosomal locus that is targeted by the vector (Melton 2002).

Mouse models have increased the understanding of the mechanisms of ERCC1 deficiency during the past decade. *Ercc1* has been knocked out in strains of mice and consequences of *Ercc1* loss have been extensively studied. *Ercc1* knockout mice were reported to suffer from several abnormal features. They were runted at birth, died before weaning because of liver failure and displayed severe liver abnormalities (McWhir et al. 1993, Weeda et al. 1997). Liver cells were found to contain nuclei

with variable sizes and were polyploid with a development towards severe aneuploidy by three weeks of age (McWhir et al. 1993).

Polyploidisation is a general mechanism occurring in all cell types in mammals and is seen as a general physiological process. By providing duplicated genes, polyploidisation fuels long- term diversification and evolutionary success (Comai 2005). Advantages of polyploidisation include gene redundancy, which leads to a protective effect against deleterious recessive mutations in a bottleneck population. In addition, an increased performance of polyploids compared to inbred parents might occur as the fixation of a divergent parental genome is possible, leading to a more diverse genetic background which could adapt more easily to environmental changes (Comai 2005). On the other hand, a dosage imbalance could occur when the nucleus- cytoplasm ratio changes with increased polyploidy, causing a change in the relationship of tri- and bi-dimensional compartments of the cell to each other which could be of disadvantage. In addition, difficulties in meiosis might arise and an increase in abnormal chromosome segregation might be apparent (Comai 2005).

The onset of polyploidisation of the liver is associated with late foetal development and postnatal maturation and progresses with age (Gupta 2000). It is therefore seen as a sign of terminal differentiation and senescence of hepatocytes. Hepatocyte polyploidy in vivo is also associated with an increase in cell size and cytoplasmic complexity and an accumulation of lipid peroxidation products such as lipofuscin, an end product of intracellular oxidation, and a decrease in cell division potential (Gupta 2000). Polyploidy along with increased cytoplasmic density lead to a decline in cell division in vivo (Gorla et al. 2001). Liver polyploidy in humans is associated with an increase in age. Hepatocytes are mostly diploid in newborns with an increase in tetraploidy in adolescents and the onset of octaploidy in adults occurring with age (Biesterfeld et al. 1994). In mice, polyploidisation shows a similar pattern with the livers of foetal and suckling animals containing mainly diploid hepatocytes and tetraploidy being apparent in the majority of hepatocytes in young adult liver (Gupta

2000). Polyploidy is usually observed in older animals with nuclei being up to 16n towards their maximum life span.

The basis for polyploidisation is thought to be acytokinesis (Guidotti et al. 2003). Mononucleate cells have been shown to abort cytokinesis leading to a population of binucleate cells. Polyploidisation can occur when the two nuclei of a binucleate cell fuse. Alternatively, binucleate cells can give rise to two tetraploid cells during cell division with all chromosomes replicating once. Guidotti et al. (2003) showed that the latter is the case in hepatocyte cultures.

Liver polyploidy is normally seen in ageing hepatocytes and might have a protective role against DNA damage. The liver is naturally a target for many toxic agents and in order to deal with genetic damage, polyploidisation might occur to compensate for cellular losses (Weeda et al. 1997). Apart from being a protective mechanism, polyploidisation is also regarded to be a natural sign of ageing.

p53 levels were elevated in Ercc1- deficient liver, kidney and brain as p53 is involved in monitoring DNA damage. Further studies revealed changes in cell cycle and p21 involvement. p21 is one of the major downstream targets for p53, but can also be upregulated independently from p53. p21 acts as a cyclin-dependent kinase inhibitor, resulting in cell cycle arrest at G1/S and G2/M checkpoints, as well as a mediator in cell differentiation and senescence (Weeda et al. 1997). Overexpression of a p21 transgene in the liver produced a similar phenotype to that of Ercc1 deficiency (Wu et al. 1996), giving additional support to the idea that p21 is involved in ERCC1-dependent cross-link repair (Weeda et al. 1997). Moreover, arrest in G2 has been observed in hepatocytes deficient in *Ercc1* (Melton et al. 1998). The cell cycle arrest is thought to occur through misregulation of p21 as a result of uncoupling of S-phase and mitosis. DNA replication and normal binucleation events also seem to be reduced in Ercc1- deficient liver. This has been shown to be due to a protective role for p53 in ERCC1 deficient cells. It was suggested that p53 ensures

that cells with DNA damage do not proceed through replication or binucleation to reduce the risk of fixation of mutations and formation of chromosomal aberrations (Nunez et al. 2000).

The following model has been proposed to explain the growth arrest and early senescence in *Ercc1*- deficient rodent cells: ERCC1 is not essential for homologous recombination repair in rodents but seems to stimulate chromosome exchange in S-phase on a UV- damaged template during single strand annealing (Melton et al. 1998). Accumulation of DSB occurs where single strand annealing fails because of a defect in the *Ercc1* gene. This leads to upregulation of p53 although the main features of the observed phenotype are probably independent of it. Elevated levels of p21 arise because of the damage, where p21 seems to be independently induced in these cells. Increase of p21 results in G2 cell cycle arrest instead of arrest in G1/S (Nunez et al. 2000). Cells are therefore able to replicate and increase their DNA contents through rounds of endoreduplication without cell division or binucleation (Nunez et al. 2000). Genome instability and a rise in mutation frequency can be observed because of an increase in DSB and the lack of NER. In Ercc1- deficient liver, these events could be triggered by endogenous oxidative DNA damage, rather than by UV irradiation.

As *Ercc1* knockout mice die early after birth it is very difficult to study further consequences later during life such as cancer susceptibility and effects on tissues other than liver. Correction of liver dysfunction has recently been achieved through an *Ercc1* transgene, resulting in new opportunities to study more long term consequences of ERCC1 deficiency (Selfridge et al. 2001). A transgene was created under the control of a transthyretin (TTR) gene promoter to guarantee liver specific ERCC1 expression. The lifespan of these animals was extended to 61-88 days which still is not long enough for cancer susceptibility studies. However, runting was inhibited and liver function corrected by the transgene. The rise of oxidative damage along with liver polyploidy was reversed. Instead, polyploidy in the kidney could be detected and animals died with renal malfunction (Selfridge et al. 2001).

Prasher et al. (2005) investigated the haematopoietic system of *Ercc1* knockout mice and found the basal haematopoiesis and the reserve capacity of the system reduced in those mice. This functional decline of the haematopoietic system is normally found in humans aged 70 and older, where mild anaemia and reduced neutrophil production can be observed (Prasher et al. 2005). No such reduction in haematopoiesis could be noted in Xpa mice which are only malfunctional in NER. The hypersensitivity of *Ercc1* knockout mice to ICL and the reduced function of the haematopoietic system highlights similarities to patients with Fancomi anaemia and it has been suggested that *Ercc1* knockout mice are a model thereof (Prasher et al. 2005).

A mouse line with a truncated form of *Ercc1*, lacking the last 7 amino acids, on one allele, showed delayed onset of premature aging with an extended life span of 6 months (Dolle et al. 2006). Mutation frequencies were assessed using a lacZ reporter gene in *Ercc1* truncated livers and were found to be 2- fold increased when compared to Wt littermates at 28 weeks of age. Point mutations and deletions or inversions of over 50 bp were found in these livers. In addition, G:C to T:A mutations, an oxidative damage signature mutation, were the most common form of no- change mutations (Dolle et al. 2006). The increased genome instability found in mice with a truncated form of *Ercc1* was thought to be an effect of the impaired interstrand cross- link repair ability of *Ercc1* rather than its function in NER as livers of *Xpa* mice showed a lower mutation frequency and less severe genome rearrangements. *Xpa* mice display malfunctional NER pathways only and do develop spontaneous liver tumours (Ishikawa et al. 2004). Interestingly, only liver was affected by the truncated form of *Ercc1* with no mutations found in other organs such as kidney (Dolle et al. 2006). In addition, livers of 3 week old complete *Ercc1* knockout mice showed no increased genome instability and mutation frequency when compared to Wt littermates (Dolle et al. 2006). These findings suggest that mutation frequencies in *Ercc1*- deficient livers rise from weaning onwards, leading to large genome rearrangements thereafter. These large rearrangements could impact normal patterns of gene expression in liver and lead to age- related cellular

degradations and liver failure. Overall, the liver seems to be especially susceptible to loss of *Ercc1*. Further investigations are required to specify the reason for the importance of *Ercc1* in liver.

Xpf- deficient mice were created by Tian et al. (2004). Unsurprisingly, *Xpf*- deficient mice showed the same phenotype as *Ercc1*- deficient mice. Animals were runted, died before weaning and displayed an increase in polyploid hepatocyte nuclei. As ERCC1 forms a functional complex with XPF, these findings underline the importance of both factors to act simultaneously during NER, homologous recombination and inter strand cross- link repair.

1.12 Ercc1 and cancer

A skin- specific *Ercc1*- deficient mouse line has recently been established in our laboratory using the Cre/loxP technique. In short, mice carrying two loxP sites flanking exon 3 and 5 of the *Ercc1* gene were created. In *Ercc1* Flox/Null and Flox/Wt mice, a Cre recombinase under the skin- specific K5 promoter drove the recombination of the loxP sites, resulting in the excision of exons 3-5 of the *Ercc1* gene. *Ercc1* Flox/Null mice showed 50-70% recombination in the skin (Doig et al. 2006). When UVB was used as a DNA damaging agent, *Ercc1* Flox/Null mice showed a high incidence of skin tumours 8- 17 weeks after exposure to UVB with Wt littermates under the same protocol not showing any carcinogenic changes in the skin. This study underlines the role of *Ercc1* in cancer protection.

Liver cancer is the fifth most common cancer in men and the eighth most common cancer in women world- wide (Bosch et al. 2004). Rates of hepatocellular carcinomas (HCC) are 2-4- fold higher in men compared to women. Risk factors include hepatitis B and C, alcohol abuse and exposure to aflatoxin. Fautrel et al. (2005) have shown that ERCC1 is frequently overexpressed in HCC in patients and

that NER activity is upregulated which might account for the relative resistance of HCC to chemotherapeutic agents.

ERCC1 has also been implicated in resistance to platinum based chemotherapy in a variety of cancers and *ERCC1* status could be used as a predictive marker for chemotherapeutic outcome. *ERCC1* polymorphisms are known to occur at position 225 and 354 of the *ERCC1* gene. At position 225 a G:T substitution takes place and at position 354 C is substituted by T. Both mutations are silent and occur in heterozygous or homozygous form (Ford et al. 2000).

However, Yu et al. (2000) suggested that even silent *ERCC1* polymorphisms could lead to diminished mRNA and protein levels in ovarian cancer cell lines with functional consequences in cisplatin DNA removal capacity. In addition, a polymorphism in codon 118 in exon 4 leads to a C: T substitution without change in the polypeptide sequence (Isla et al. 2004).

However, predicted survival for cisplatin treated non- small cell lung cancer patients decreases when one allele contains the T variant of *ERCC1* at codon 118. The same polymorphism is also associated with decreased overall survival and time to progression of colorectal cancer on patients receiving chemotherapy (Moreno et al. 2006). Zienolddiny et al. (2006) propose that the 118 transition leads to differential *ERCC1* mRNA levels which might influence repair capacity. Yan et al. (2006) examined *ERCC1*- related cisplatin resistance in more detail. The upstream promoter region around 410 bp of the *ERCC1* gene contains a variety of transcription factor motifs and seems to be responsible for resistance to cisplatin. Upon exposure to cisplatin, the transcription repressor MZF1 was downregulated followed by *ERCC1* upregulation. Similarly, MZF1 overexpression led to lower levels of ERCC1 upon cisplatin administration, indicating a regulatory function for MZF1 on *ERCC1* expression (Yan et al. 2006).

In addition, human ovarian cancer cell lines and specimens were examined for the presence of a 42 bp splicing variant of *ERCC1* (Yu et al. 2001). The 5'- UTR region of *ERCC1* mRNA includes an untranslated region in exon 1. The loss of the 42 bp sequence was associated with a rise in *ERCC1* mRNA levels in ovarian cancer specimens, indicating a negative transcriptional regulatory effect of this region of *ERCC1* expression. These findings could not be confirmed in our laboratory when a variety of human cancer cell lines, including cisplatin resistant cell lines, were examined and the 42 bp splice variant was found ubiquitously (Winter et al. 2005). Therefore, the 42 bp splice variant was not cancer related. In general, deregulation of *ERCC1* and silent polymorphisms could give rise to higher incidences of cancer or to resistance to chemotherapeutic agents.

1.13 Objectives

The aim of the current study was to set up a better model for examination of *Ercc1* deficiency and premature polyploidy in the murine liver and to determine the DNA lesions responsible for this premature polyploidy. We used the Cre/lox system with an Adeno virus carrying Cre recombinase to conditionally induce *Ercc1*- deficiency and to reduce ERCC1 levels in adult murine hepatocytes in vitro and in liver in vivo. In addition, livers from simple *Ercc1* knockout mice were further characterised, examining their reactive oxidative species content and the occurrence of malondialdehyde adducts. Real- time RT-PCR was used to determine differences in expression of cell cycle regulation and survival genes between *Ercc1*- deficient and control livers. Moreover, lipid content was examined in *Ercc1*- deficient livers and in Flox/Null and Flox/Wt livers in vitro and in vivo after AdenoCre infection.

2. Materials and Methods

2.1 Laboratory reagents and suppliers

Ambion: RNase free water

Amersham Biosciences: Redivue (α-^{32}P)- dCTP (3000 Ci/mMole, 10 mCi/ml), Dextran sulphate, NICK column, ECL- plus Western Blotting detection system, Percoll, Bromodeoxyuridine (BrdU)

Applied Biosystems: 2x TaqMan©PCR mix, 20x Assays on demand Assay mix (containing Real- time PCR primers)

BDH ltd: Hydrochloric acid, Acetic acid

BioRad: Kaleidoscope pre- stained standards, Lowry protein assay, 96 well PCR plates, Coomassie brilliant blue R- 250

Greiner Bio: Petri dishes, 24- well plates

Fisher Scientific: 10% Sodium dodecyl sulphate (SDS), Boric acid, Ethanediaminetetraacetic acid (EDTA), Isoamyl alcohol, Sodium chloride (NaCl), Sodium citrate , Sodium hydroxide (NaOH), Potassium disulphite, Isopropanol, Methanol, Chloroform, Potassium chloride (KCl), Tri- sodium citrate

Fluka: Glucose oxidase (GO)

Invitrogen: 25 mM deoxyribonucleotides (dNTP), EcoRI, 10x Digestion Buffer for EcoRI, 1x Phosphate buffered saline (PBS), Oligo dT, Moloney murine leukaemia virus (MMLV) reverse transcriptase enzyme, RNase H, Dithiothreitol (DTT), Phenol, Low melting point agarose, Perfusion medium, modified Chee's medium, 10x Hanks buffered saline solution (HBSS), Insulin- Trans- Sel- G (ITS), Tris, L-glutamine, *4*-(2-hydroxyethyl)-1-piperazineethanesulfonic acid (HEPES), Gentamicin, 100 bp DNA marker ladder, 5-(and-6)-chloromethyl-2',7'-dichlorodihydrofluorescein diacetate, acetyl ester (CM-H_2DCFDA)

Millipore: Immobilon-P transfer membrane

LabTek: 2- well chamber slides, 4- well chamber slides

Oxford Technologies: anti BrdU antibody

Oswell: Polymerase chain reaction (PCR) primers

Packard Biosciences: Ultima Gold scintillation fluid

Perkin Elmer: Genescreen Plus hybridisation transfer membrane

Pfizer: Rimadyl, Halothane

Premier International foods: Marvel

Promega: 10x PCR buffer, 25 mM Magnesium chloride ($MgCl_2$), Taq DNA polymerase, DNA Polymerase I large fragment

Qiagen: RNeasy mini kit, DNase

Roche: DNase I

Virapur: AdenoCre virus

Sacura FineTek: OCT compound

Santa Cruz: Goat anti- rabbit IgG antibody

Severn Biotech: Acrylamide

Sigma: Carbon tetrachloride, Tamoxifen citrate, 4- hydroxytamoxifen, 20 mg/ml Proteinase K, RNase A, Trypsin, Trypsin inhibitor, Ribonuclease A, Propidium iodide (PI), Leibowitz 15 medium, Dulbecco's modified Eagle medium (DMEM), Mitomycin C (MMC), Sunflower oil, Electrophoresis grade agarose, Collagenase IV, Glasgow medium, Trichloroacetic acid (TCA), Tween 20, New- born calf serum (NRS), rabbit anti- rat Horseradish peroxidase (HRP) conjugated, Diaminobenzidine (DAB) solution, Cedarwood Oil, Propylene glycol, Hydrogen peroxide (H_2O_2), Fibronectin, Insulin, Linoleic acid (BSA), Epidermal growth factor (EGF), Dexamethasone, Tween 20, Lipid Lin-Trol Set, Dimethylsulphoxide (DMSO), Ethidium bromide, Glycerol, Herring sperm DNA, Formaldehyde, Triton X- 100, NP- 40, Bromophenol blue, β- mercaptoethanol, Feulgen's grade fuchsin, Ribonuclease inhibitor, Glycerine, N,N,N', N'- Tetramethylethylenediamine (TEMED), Ammonium persulphate (APS), Sucrose, activated Charcoal

Thermo Spectronic Corporation: ThermoTrace Triglyceride standard, ThermoTrace Triglyceride reagent

formamidopyrimidine- DNA- glycosylase (FPG) enzyme was a gift to Dr S. Prost.

2.2 Solutions

Bouin's fixative: 425ml Methanol, 25 ml glacial Acetic acid, 50 ml 40% formalin

Blocking solution (BrdU stain): PBS, 20% (v/v), normal rabbit serum (NRS), 0.05% Tween 20 (v/v)

Chloroform- isoamyl alcohol solution (CA): 24 parts chloroform (v/v), 1 part isoamyl alcohol (v/v)

Citrate Buffer: 8.55% sucrose (w/v), 5% DMSO (v/v), 40mM tri- sodium citrate (w/v), pH 7.6

Coomassie blue: 0.2% Coomassie (w/v), 7.5% Acetic acid (v/v), 40% Methanol (v/v)

Denaturing buffer (Southern blot): 0.5M NaOH, 1.5M NaCl

Electrophoresis solution (Comet assay): 0.3M NaOH, 1mM EDTA

Enzyme buffer (Comet assay): 40mM Hepes, 0.1M KCl, 0.5mM EDTA, 0.2 mg/ml BSA, pH 8.0

Fluorescence activated cell scanning (FACS) stock solution: 3.4M tri- sodium citrate, 0.5M Tris- HCl, 1% NP40, 0.52mg/ml spermine tetrahydrochloride, pH 7.6

FACS solution A: 30µg/ml trypsin in stock solution

FACS solution B: 0.5 mg/ml trypsin inhibitor, 0.1 mg/ml ribonuclease inhibitor in stock solution

FACS solution C: 0.42 mg/ml propidium iodide, 1 mg/ml spermine tetrahydrochloride in stock solution

Formalin: 10% (v/v) formaldehyde in phosphate buffered saline

Hybridisation buffer (Southern): 1 mg dextran sulphate, 10% SDS, 20x SSC, denatured sperm DNA and DDW

5x Loading buffer (gel electrophoresis): 20% (v/v) glycerol, 100mM EDTA, 0.1% (w/v) bromophenol blue

4x Lower Buffer (for lower, separating Western gel, 12%): 1.5M Tris- HCl, 0.4% SDS (v/v), pH8.8

Lower gel (Western): 12% Acrylamide (w/v), 0.006 % (w/v) APS, 0.002% (w/v) TEMED, 25% (v/v) Lower buffer

Lysis buffer 1 (Comet assay): 2.5M NaCl, 0.1M EDTA, 10mM Tris, 1% Triton X-100 (v/v), pH 10

Lysis buffer 2 (Comet assay): 2.5M NaCl, 0.1M EDTA, 10mM Tris, pH10.0

Lysis buffer (Western): 100mM Tris, 2% SDS (v/v), pH 8.2

Marvel solution: 5% Marvel (w/v), TBST

Neutralising buffer (Southern blot): 3M NaCl, 0.5M Tris- HCl, pH 7.0

Neutralising buffer (Comet assay): 0.4M Tris, pH to 7.5 with HCl

Solution A (Oligo labelling buffer): 1.25M Tris- HCl pH 8.0, 0.125M $MgCl_2$, 25mM β- mercaptoethanol, 0.5mM each of dGTP, dATP, TTP

Solution B (Oligo labelling buffer): 2M Hepes buffer adjusted to pH 6.6 with NaOH

Solution C (Oligo labelling buffer): Random hexadeoxyribonucleotides;

90 $OD_{260\ nm}$ units/ml in TE, 50 µg/ml DNA equals $OD_{260\ nm} = 1$

Definition OD_{260nm} unit: One optical density (OD) unit equals the amount of DNA that gives an absorbance reading of 1.0 at 260nm for a sample dissolved in 1 ml total volume of double distilled water.

Oligo labelling buffer: 50µl solution A, 125µl solution B, 75µl solution C

Percoll: 9 parts Percoll to 1 part 1xHBSS (v/v)

Phenol- chloroform- isoamyl alcohol (PCA) solution: 25 parts redistilled phenol, 24 parts chloroform, 1 part isoamyl alcohol

4x Protein sample buffer: 250 mM Tris- HCl, 2% SDS (v/v), 20% β-mercaptoethanol (v/v), 40% glycerol (v/v), 0.5% bromophenol blue (v/v), pH 6.8

5x RT buffer: 250mM Tris- HCl pH 8.3, 30mM $MgCl_2$, 200mM KCl, 5mM DTT

Schiff's reagent: 2.5g Feulgens grade Fuchsin, 5 g Potassium disulfite, 10ml 10% HCl, 2g activated charcoal

20x Standard saline citrate (SSC): 3M NaCl, 0.3M tri- sodium citrate, pH 7.0

Swelling buffer: 0.01M HEPES, 1.5 mM $MgCl_2$, pH 7.4

Tail lysis buffer: 400mM NaCl, 10mM Tris- HCl, 3mM EDTA, 1% (w/v) SDS

10x Tris- Borate- EDTA (TBE): 0.9M Tris- HCl, 0.9M boric acid, 20mM EDTA, pH 8.3

10x Tris buffered saline (TBS): 1M Tris base, 1M NaCl, pH 7.5

Tris buffered saline with Tween (TBST): 0.005% Tween 20 (v/v) in1x TBS

20% Trichloroacetic acid (TCA): Trichloroacetic acid in DDW (w/v)

Tris- EDTA (TE) buffer: 10mM Tris- HCl, 1mM EDTA, pH 8.0

Transfer Buffer (Western): 3 g TRIS, 14.4 g Glycine in 1 liter double distilled water (DDW)

4x Upper buffer (for upper, stacking Western gel): 0.5M Tris- HCl, 0.4 % SDS (v/v), pH 6.8

Upper gel (Western blot): 4% Acrylamide (w/v), 0.006% (w/v) APS, 0.002% (w/v) TEMED, 33% (v/v) Upper buffer

2.3 Cell culture media and conditions

Liver perfusion medium was obtained and 50 µg/ml gentamicin added to each 500ml bottle of medium.

Digestion medium consisted of 500 ml Leibowitz 15 medium to which 50 μg/ml gentamicin, 4 mM L- glutamine, 0.14 mM dexamethasone, 1.7 mM insulin and 50 mM Hepes were added. The pH was adjusted with 1M NaOH until pH 7.5 was reached. Before perfusion, 25 mg of collagenase IV and 600 mg DNase I were filter sterilised and added to 120 ml digestion medium.

Plating medium consisted of 500 ml DMEM to which 50 μg/ml gentamicin, 4 mM L- glutamine, 0.14 mM dexamethasone, 1.7 mM insulin was added. The pH was adjusted with 1M NaOH until pH 7.5 was reached.

Cell culture medium consisted of 500 ml modified Chee's medium to which 50μg/ml gentamicin, 4 mM L- glutamine, 0.14 mM dexamethasone, 0.1 ng/ml ITS and 12.5 ng/ml EGF, made up in 1x BSA, was added. The medium itself contained high amounts of amino acids to help proliferation in culture. The pH was adjusted with 1M NaOH until pH 7.5 was reached.

Hepatocyte cultures were maintained at 37°C in a 5% CO_2 atmosphere in a Sanyo incubator.

2.4 Primers

All primers are listed in Table 0. Conventional PCR primers were obtained from Oswell. Their sequence and the product size are indicated for all PCR assays. Real-time PCR primers were obtained from Applied Biosystems. The exact positioning and the sequence of those primers could not be obtained as Applied Biosystems does not provide this information. Instead, approximate positions and exon boundaries are given. The product size is indicated for each Real- time PCR assay. Real- time PCR primers are usually located around exon boundaries and PCR products are small to ensure amplification of cDNA only.

Table 0: PCR and RT Real- time PCR primers. Primer sequences for forward and reverse primers are indicated for all conventional PCR primers. The exon location of primers are given for RT Real- time PCR primers. The product size is given in base pairs (bp).

PCR assay (standard)	Forward Primer	Reverse Primer	Product size (bp)
TTRCre	5'- ATGAAATGCAA GAACGTGGTACCC-3'	5'- TCTAGAAGGAT CATATTCAGAATAG-3'	1350
Ercc1 KO	5'-GGTTCGAAATGA CCGACCAAGCG-3'	5'-CGAAGGGCGA AGTTCTTCCC-3'	800
Ercc1 Flox Wt	5'-TGCAGAGCCTG GGGAAGAACTTCGC-3'	5'- TCAAAGTATG GTAGCCAAGGCAGC-3'	500 (Flox) and 1050 (Wt)
Recombination	5'-TGTCTCCCTGG CTCTGGATCTGAC-3'	5'-TCAAAGTATG GTAGCCAAGGCAGC-3'	250

PCR assay (Real- time)	Exon location	Product size (bp)
Gapdh	1-1	107
Tbp	1-2	93
Igfbp2	2-3	85
p21	2-3	96
Tgf β	6-7	76
Bax	3-4	68
Pcna	3-4	117
Ref1	2-3	115
Polymerase β	3-4	97

2.5 Animal procedures

2.5.1 Breeding scheme

TTRCre mice were obtained from Mireille Vasseur-Cognet, Institut Cochin U567, Departement de Genetique, Developement et Physiopathologie Moleculaires, INSERM U567, 24 rue du Faubourg Saint Jacques, 75014 Paris, France. The mice were hemizygous for the transgene and were on a mixed background. We crossed TTRCre mice with our own *Ercc1* knockout stock (*Ercc1* Wt/Null) which was on a mixed genetic background. *Ercc1* Wt/Null animals containing the TTRCre transgene were then crossed with *Ercc1* Flox/Flox mice to obtain *Ercc1* Flox/Null and Flox/Wt animals with and without TTRCre transgene. For the AdenoCre experiments, *Ercc1* Wt/Null animals were crossed with homozygous *Ercc1* floxed animals to obtain *Ercc1* Flox/Null and Flox/Wt mice.

2.5.2 Animal husbandry

All animal procedures were carried out under the Home Office Animals (Scientific Procedures) Act 1986. All mice were maintained in accordance with established animal care guidelines (Poole 1989). Animals were kept at standard conditions with a 12 hour light cycle and an average temperature of 21°C. Water and food were given *ad libitum*. After weaning, animals were separated into single sex cages. Tail biopsies of less than 1 cm distal tail for genotyping were obtained after exposure to the analgesic rimadyle, and the anaesthetic halothane. At the same time each individual animal was marked with coded ear markings. In all experiments, littermates are used as experimental and control animals.

2.5.3 Tamoxifen injections

4-Hydroxytamoxifen was prepared in 50% ethanol to obtain a 40 mg/ml stock solution. All further dilutions were carried out in sterile sunflower oil until a final concentration of 10 mg/ml was reached. 1 mg of this solution was given i.p. to one group of mice once and subsequently to all other animals on 5 consecutive days.

In addition, tamoxifen citrate was prepared in 50% ethanol to obtain a 40 mg/ml stock solution. All further dilutions were carried out in sterile sunflower oil until a final concentration of 20 mg/ml was reached. 1 mg of tamoxifen citrate in solution was given to each animal i.p. daily for 5 consecutive days. All animals were 6-8 weeks old.

2.5.4 Carbon tetrachloride injections

Carbon tetrachloride was diluted in sterile sunflower oil to obtain a 23 mg/ml, 51 mg/ml and 102 mg/ml solution. 1 µl/g body weight (BW), which corresponds to 23, 51 and 102 µg/g body weight of solution, was injected i.p. into each mouse using a Hamilton glass syringe. Mice varied in age from 6-8 weeks.

2.5.5 AdenoCre injections

Sterile 1x PBS was added to the AdenoCre virus to obtain a pfu of $1x10^9$ and $4x10^9$ in a 200 µl volume. Mice were restrained in a plunger and the tail vein warmed with 37°C water. 200 µl of diluted virus was given i.v. to 6 week old male and female animals. Animals were sacrificed 1 and 3 weeks after AdenoCre injections.

2.5.6 Short term in vivo study

6 week old male *Ercc1* Flox/Null and Flox/Wt mice were injected i.v. with $1x10^9$ and $4x10^9$ pfu AdenoCre virus. 51µg/g BW of CCl_4 solution was given i.p. the next day once to one group of animals and weekly for three consecutive weeks to another group of animals. Animals were sacrificed 7 or 14 days after the last CCl_4 injection.

2.6 Tissue processing

2.6.1 DNA extraction

DNA from tail and tissue was extracted using phenol, together with chloroform, which separates nucleic acid from protein. Tail tips were incubated in 0.6 ml tail lysis buffer and 300 µg proteinase K solution on a shaker (Gallenkamp) at 37°C and 200 rpm over night. All centrifugation steps were done on a Mikro 20 centrifuge (Hettich) at 1300 rpm for 5 minutes. Separation of the solution and remains of hair was done by spinning. The samples were carried over into a fresh epppendorf tube and 0.6 ml Phenol- chloroform- isoamyl alcohol (PCA) was added to the samples to extract DNA. All sample tubes were attached to a Rotatest flatbed shaker (Stuart) at 80 rpm for 15 minutes. After an additional centrifugation step, the aqueous phase was carried over to a fresh eppendorf tube adding 0.75 ml of chloroform- isoamyl alcohol (CA) to eliminate any remaining phenol. Mixing was achieved through attachment of the tube to the rotatest flatbed shaker as above. The aqueous phase was carried over to a fresh eppendorf tube after a third centrifugation step using 0.75 ml propan-2-ol to precipitate the DNA. Samples were left at room temperature for 10 minutes and spun down to pellet the DNA. After washing the pellet in 70% ethanol, the DNA was dried and re- suspended in 100µl sterile water.

Isolation of DNA from mouse tissues was done as above using 5 ml tail lysis buffer and 2500 µg proteinase K solution as well as 5 ml PCA and CA respectively. Resuspension was done in 1ml DDW for liver DNA and 0.8 ml DDW for all other tissues.

2.6.2 Estimation of DNA concentrations

Concentration of DNA samples was estimated using spectrophotometry. The absorbance of diluted DNA was measured at 260 and 280nm using the Biomate 3 spectrophotometer (Thermo Spectronic). Double stranded DNA with a concentration of 50µg/ml equals an OD_{260nm}=1.0. In addition, the ratio of OD_{260nm}/OD_{280nm} is an indication of nucleic acid purity with a ratio of 1.8 indicating no significant contamination with protein.

2.6.3 Agarose gel electrophoresis

Agarose gel electrophoresis relies on the principle that negatively charged DNA moves towards a positive electrode. Agarose is used to create a porous gel to allow for DNA separation by size. Agarose gels were prepared using 1x TBE and electrophoresis grade agarose. 0.5µg/ml ethidium bromide, which intercalates with DNA and fluorescences under UV light, was added to each gel to visualise the PCR products. A 100bp DNA ladder was added to each gel for size comparison. TTRCre, *Ercc1* Null, Flox and Wt PCR products were run on a 1% agarose gel (w/v) for 1 hour at 100 V using 20µl of sample and 5µl of 5x loading buffer. The recombination PCR products were run out on a 2% gel (w/v) for 2 hours at 100 V using 20 µl of sample and 5 µl of 5x loading buffer.

All gel electrophoresis was carried out using a BioRad powerpack Junior. All samples were visualised on a Gel Doc 2000 from Biorad using the Quantity One software.

2.6.4 PCR assays

All PCR assays were carried out in 50µl volumes, using 5µl 10x PCR buffer, 2µl 25 mM $MgCl_2$, 1 µl 25 mM dNTP and 2.5 units of Taq DNA polymerase. All primers were used at 300 ng per reaction. To obtain 50µl of solution for the PCR assay, DDW was added accordingly. Typically, 100 ng of DNA were added to each reaction. All primer sequences are summarised in Table 0. All reactions were run on a Thermocycler (Biometra).

The TTR-Cre transgene was detected by PCR with the forward primer being Cre-derived and the reverse primer being MER- derived (see Figure 3). PCR conditions were as followed: 94°C for 5 minutes, 94°C for 1 min followed by 60°C for 1 minute and 72°C for 2 minutes for 30 cycles, 72°C for 10 minutes. The expected product size was 1350 bp.

For detection of the *Ercc1* Null allele, a PCR was performed using forward primer M4956 and reverse primer 035M (see Figure 2). The PCR reaction was run at 94°C for 5 minutes, 35 cycles of 94°C, 68°C and 72°C for 1 minute each and 72°C for 10 minutes. The expected band size was 800 bp.

For detection of the Flox and Wt alleles forward primer 432E and reverse primer F25732 were used to detect a 500 bp band for the Flox allele and a 1050 bp band for the Wt allele (see Figure 2). The PCR conditions were 94°C for 5 minutes, 35 cycles of 94°C and 63°C for 1 minute and 72°C for 2 minutes 30 seconds, 72°C for 10 minutes.

Recombination was visualised by PCR with the forward primer being F25731 and the reverse primer being F25732, giving a 250bp product (see Figure 2). The PCR conditions were as follows: 94°C for 5 minutes, 94°C for 1 minute followed by 68°C for 1 minute and 72°C for 30 seconds for 35 cycles, 72°C for 10 minutes.

For estimation of recombination by PCR, the amounts of DNA were matched using a spectrophotometer (Thermo Spectronic Biomate 3). In addition, EcoRI digestion (see Southern blotting below) was performed on all samples to further match the amounts of DNA used per sample for PCR. Under the above recombination PCR cycle conditions, the amount of PCR product is directly related to the input of DNA, giving this PCR assay a semi- quantitative quality. Densitometry was used to estimate the amounts of recombination between samples. Pictures were taken with the Quantity One software. The individual recombination PCR products were marked and the band intensities of the samples compared to the band intensity of the recombination control. The recombination levels in all samples were expressed as percentage of recombination compared to the control.

2.6.5 Histology

Liver samples were fixed in 10% formalin buffered in PBS and processed to obtain haematoxylin and eosin (H&E)- stained slides using standard histological methods. Histology was carried out by Mr Robert Morris. For Oil Red O analysis, liver samples were frozen in OCT compound and stored at -70°C until cryosections were cut. All sections were stained for Oil Red O as described below with assistance of Mr Robert Morris.

2.6.6 Microscopy

Images from slides were taken using an Olympus BX 51 microscope and the Olympus DP software. To estimate the amount of necrosis after carbon tetrachloride treatment, several pictures of the same liver were taken using a 20x objective. All necrotic islands were marked and the total amount of marked area was calculated. This amount was compared to the total amount of area examined and necrotic area expressed as a percentage of the total area examined.

2.6.7 Triglyceride assay

Triglyceride content was analysed as described in Morton et al. (2004). 100 mg liver was used per sample. Samples were homogenised using a hand- held Fisher homogeniser in a glass test tube in 2 ml isopropanol, taking care not to lose any fluid. The test tubes were covered and shaken in a flatbed shaker (Stuart) for 45 minutes to extract the lipids. Centrifugation (Sigma 4 k 15) at 3000rpm for 10 minutes was followed by assaying the supernatant. To 10µl of supernatant 1ml ThermoTrace Triglyceride reagent was added and all samples were incubated in a water bath (Grant) at 37° C for 5 minutes, allowing triglycerides to be recovered from all samples. A ThermoTrace Triglyceride standard was diluted with 1x PBS to obtain a standard curve. The absorbance of all samples was read on a Biomate 3 spectrophotometer (ThermoSpectronic) at 500nm. All calculations were performed in Microsoft Excel. The standard curve method was used to estimate the triglyceride content per liver sample. Before each run, a machine calibration check for linearity/limits of assay was performed using the Lipid Lin-Trol Set .

2.6.8 Malondialdehyde analysis

The immunoslot blot method is an antibody based approach to visualise DNA adducts in a variety of tissues. Malondialdehyde adducts were determined using the immuno slotblot technique with assistance of Dr R. Singh. 1μg of DNA was used per sample and the procedures followed as described by Singh et al. (2001). In short, single stranded DNA was prepared and pipetted onto a nitrocellulose filter. A 5% Marvel solution was used to block non- specific binding of antibodies before exposure to the primary deoxyguanosine malondialdehyde antibody. A horseradish peroxidase- conjugated secondary antibody was used to visualise the deoxyguanosine malondialdehyde adducts when exposed to a chemiluminescent reagent in combination with a X- ray hyperfilm. The band intensity was calculated using image analysis software. All samples were run in triplicate. A malondialdehyde-deoxyguanosine standard was created and used for comparison. The mean and the standard deviation were calculated for all samples using Microsoft Excel.

2.6.9 Reactive oxygen species (ROS) assay

Ercc1 Null and Wt livers were sampled and cut into small pieces. Collagenase IV treatment of the cells was performed using 10 mg of collagenase in 120 ml of plating medium ex- vivo. The dissected liver pieces were re-suspended in 1x HBSS and a centrifugation step at 500 rpm using Percoll (see below) performed to separate live from dead hepatocytes. Viability of the cell suspension was estimated using trypan blue and the hepatocytes were plated into 24 well plates at a density of 1.3 $x10^6$ live cells/ml. CM-H_2DCFDA, a cell permeable diacetate ester which fluoresces green upon reaction with ROS, was used to determine the amount of ROS in *Ercc1* Null and Wt hepatocytes obtained from animals aged 5-21 days. CM-H_2DCFDA was diluted in DMSO to give a 100μM stock solution. A 10μM solution of CM-H_2DCFDA was obtained by adding 1x HBSS. This solution was added to *Ercc1* Null and Wt hepatocytes. In addition, 100μU Glucose oxidase (GO) was added Wt

hepatocyte wells as a positive control. DMSO and 1x HBSS were added to Wt hepatocyte wells as a negative control. All samples were run in triplicate. The amount of ROS activated fluorescence was measured every minute over 1 hour at 37°C using a Synergy HT Fluorimeter (BioTek) with KC 4 software (BioTek). The excitation laser was set to 485 nm and the filter was set to 510 nm. The amount of ROS was normalised to the amount of protein in each well determined using the Lowry protein assay (BioRad). Cells were lysed in 100 mM Tris and 2% SDS and the manufacturer's instructions were followed. The amount of protein was determined using a MRX spectrophotometer (Dynex technologies) at an absorbance of 630nm. The mean and the standard deviation were calculated using Microsoft Excel.

2.7 Laboratory based methods

2.7.1 Southern blotting

To estimate the level of recombination in hepatocyte cultures and liver a Southern blot was carried out. Southern blotting was invented by E. M. Southern in 1975. This method can help with the determination of the molecular weight of a restriction fragment and the measurement of relative amounts in different samples (Alberts 1994). In short, genomic DNA is digested with a restriction enzyme and separated by gel electrophoresis. DNA samples are then transferred from an agarose gel onto a membrane which is then incubated with a single-stranded DNA probe. This probe will form base pairs with its complementary DNA sequence and bind to form a double-stranded DNA molecule. Before hybridisation of the membrane the probe is labelled with radioactive material or with an enzyme such as HRP. Detection of the probe is achieved by directly exposing the membrane to X-ray film or by chemiluminescent methods. 15µg of DNA was added to 80 units of EcoRI in 10 µl of 10x Digestion Buffer, 6 units of RNase A and 10 µg of 10x BSA. The solution was made up to 100µl with double distilled water (DDW). The digestion was carried

out at 37°C in a Grant water bath overnight. 50 µl of digested samples were run out onto a 0.8 % gel at 45 V overnight. The gel was denatured for 30 minutes in denaturing buffer on a Rotatest flatbed shaker (Luckham). The Genescreen Plus Hybridisation Transfer Membrane was soaked in DDW and denaturing buffer. The gel was then blotted onto the membrane in denaturing buffer overnight. The membrane was neutralised in neutralisation buffer for 20 minutes. The membrane was baked in a vacuum oven (Gallenkamp) at 80°C for 4 hours and prehybridised in 10 ml hybridisation buffer, containing 3.5 mg of denatured herring sperm DNA, in an incubator (Hybaid) at 65°C for 2 hours. The probe to detect the recombined and Wt allele was a 600 bp product spanning exon 1 and 2. The probe was denatured and labelled with ^{32}P using 10µl of Oligo labelling buffer, 20 µg of 10x BSA, 2 units of DNA polymerase I large fragment and 50 µCi of (α-^{32}P)- dCTP. The cleaning of the probe from unincorporated nucleotides was done through chromatography using a NIKK column. The column was equilibrated with 400µl of TE prior to use and 400µl of TE was added to the probe twice. 4.5 mg of denatured herring sperm DNA was then added to the flow through and used to hybridise the membrane in the rotator oven at 65°C overnight. The membrane was washed at room temperature in 2x SSC for 5 minutes twice and then washed in 2x SSC and 1% SDS in the rotator oven at 65°C for 2x 30 minutes. The last washing step was done in 0.1x SSC at room temperature twice. The membrane was sealed and exposed onto film (Kodak) at -70°C overnight. The Hyperprocessor (Amersham Biosciences) was used to develop the film. Alternatively, phosphoimagery was performed to visualise the Southern blot products. The membrane was exposed to a storage phosphor screen (Molecular dynamics) at room temperature overnight and signals visualised on a phosphoimager (Molecular dynamics). Data were analysed with the ImageQuant software. A titration curve of levels of recombination from 100%- 0% was obtained by diluting varying amounts of a cell culture sample with 100% recombination into genomic Flox/Flox DNA so that the total amount of DNA in each of the titration curve samples was 15µg. The 5.5 kb fragment is produced from the Wt, Null and non- recombined Flox alleles (this region on the gene is identical in these three alleles) and the 3.05 kb fragment is from the recombined Flox allele. Southern blotting was performed with assistance from Dr J. Selfridge.

2.7.2 Western blotting

Western blotting is an antibody based method that allows for determination of relative amounts of the protein between samples. Briefly, samples are homogenized in a buffer that protects the protein of interest from degradation. Separation of the proteins is achieved using SDS-PAGE (SDS polyacrylamide gel electrophoresis). The proteins are then transferred from the gel onto a membrane. The membrane is incubated with a blocking protein which binds to any remaining sticky places on the membrane. A primary antibody is added binding to the target protein. A secondary antibody, which can be visualised, recognizes the primary antibody, helping with the location of the protein in question. Cells were lysed with lysis buffer. 60 µg of total cell protein was subjected to SDS/PAGE. 4x Protein sample buffer was added to each sample to protect against denaturing of protein. The samples were loaded onto a 12 % acrylamide gel and run at 140V for 2 hours to separate proteins of different size. A Kaleidoscope prestained standard was used for comparison. The gel was then transferred onto an Immobilon-P transfer membrane using the Biorad (Hercules, CA) Trans-Blot SD semi-dry Transfer Cell at 12 V for 1 hour. Prior to the transfer, the membrane was soaked in transfer buffer to help protein transfer. In addition, the membrane was embedded in blotting paper, which was saturated with transfer buffer. A 5% Marvel solution was used to prevent non- specific antibody binding at 4° C overnight. The primary antibody was a crude rabbit anti- *Ercc1* antibody used at a 1:1000 (antibody: 1x TBST) dilution at 4° C overnight. The secondary goat anti-rabbit IgG antibody was used at a dilution of 1:200 000 (antibody: 1x TBST) at room temperature for 1 hour. The membrane was washed in 1x TSBT for 1 hour in between incubations. The membrane was exposed to ECL film after the ECL-plus Western blotting detection system was used to visualise the protein bands. The expected band size was 33 kDa. All amounts of protein were matched by eye using Coomassie stain to visualise the band intensity on a second gel with similar loading.

2.7.3 Flow cytometry

Flow cytometry is a method used to determine a single cell's characteristic as it passes in a fluid stream by a beam of laser light. Depending on the nature of the light scattered by the cell while passing the laser, cell size, granularity and more specific characteristics such as DNA content can be determined. The principles of flow cytometry for determining DNA content were first described by Vindelov (1977). DNA content was determined in hepatocytes and liver samples. Individual hepatocyte nuclei were prepared for flow cytometry. Tissue was cut into small pieces or dishes were scraped and re-suspended in 100 µl of citrate buffer. Cells were trypsinised for 10 min in 450 µl of solution A. Trypsin was subsequently inhibited by 320 µl of solution B containing trypsin inhibitor and ribonuclease A to degrade cellular RNA. Cells were incubated in 250 µl of solution C containing propidium iodide at 4°C for 10 min. Propidium iodide is a nucleic acid dye that intercalates in the DNA double helix. It fluorescences red when exposed to laser light (488nm). Depending on the DNA content, the extent of the fluorescence captured by the FACScan varies. Typically, 10 000 nuclei per sample were analysed on the Coulter Epics XL machine using Expo 32 (Beckham Coulter) and Multi cycle (Phoenix Flow Systems) software.

2.7.4 RNA isolation

Total RNA for RT Real- time PCR was isolated using the Qiagen RNeasy kit. The manufacturer's instructions were followed. In short, samples were stored at -80 °C in RNA*later* until processed. RNA was extracted from ca.10 mg of liver sample. The tissue was homogenised in 300 µl Buffer RTL using a hand– held homogeniser (Fisher). Buffer RTL contains guanidine isothiocyanate and β- mercaptoethanol ensuring denaturing of the tissue and inactivation of RNases. Ethanol was then added to the lysate, helping selective binding of total RNA to the silica- gel membrane. In

addition, samples were treated with 2 units DNase to remove any DNA contamination. All samples were re-suspended in 80 µl of DDW and stored at –70°C.

2.7.5 Estimation of RNA concentrations

Concentration of RNA samples was estimated using spectrophotometry. The absorbance of diluted RNA was measured at 260 and 280nm using the Biomate 3 spectrophotometer (Thermo Spectronic). 40µg/ml of RNA represents an OD_{260nm}=1.0. In addition, the ratio of OD_{260nm}/OD_{280nm} is an indication of nucleic acid purity with a ratio of 2 indicating no significant contamination with protein.

2.7.6 Reverse Transcription (RT)- PCR

cDNA for Real- time PCR was obtained using RT- PCR. MMLV reverse transcriptase was chosen as its cDNA synthesis rate is up to 40 times greater than that of avian myeloblastosius virus (AMV) reverse transcriptase (Bustin 2004). In addition the choice of a random oligo dT primer, which anneals to the polyadenylated 3' (poly- A) tail found in most mRNAs, rather than a specific primer, allows the amplification of a number of different mRNA from the same cDNA. RNase free water and 50 ng oligo dT was added to 3 µg of RNA to give a total volume of 11µl and incubated at 70 °C for 10 minutes. The samples were subsequently chilled on ice. 4 µl of 5x synthesis buffer, 10 mM dNTP mix, 0.1M DTT and 200 units of MMLV reverse transcriptase enzyme was added to each sample. All samples were incubated for 10 min at room temperature. The tubes were heated to 37 °C for 60 minutes to allow cDNA synthesis. The reaction was finally terminated by heating to 90 °C for 10 minutes. After chilling the tubes on ice for 10 minutes, 1 unit of RNase H was added to the reaction followed by 20 minutes incubation at 37 °C to ensure elimination of remaining mRNA. All samples were stored at -70 °C.

2.7.7 Real- time PCR

Real- time PCR requires a specific, fluorescence probe for detection of cDNA levels. In the TaqMan assay, a probe longer than the primers contains a fluorescent dye on the 5' base along with a quenching dye on the 3' base. In the intact probe, the energy of the excited fluorescent dye is transferred to the quencher rather than resulting in detectable fluorescence. TaqMan probes are designed to anneal to an internal region of a PCR product. During PCR amplification, the 5'- 3'- exonuclease activity of Taq DNA polymerase separates the fluorphore and the quencher leading to an increased fluorescent signal. This fluorescent signal increases with each cycle proportional to the rate of probe cleavage. Real- time PCR exploits the characteristics of a PCR reaction where 4 phases can be distinguished: the 1^{st} phase consists of an exponential amplification of fluorescence hidden under the background fluorescence level. In the 2^{nd} phase, an exponential amplification can be detected above the background which then increases during the 3^{rd} step where the fluorescence intensity is linear to the amplification efficiency. A plateau is then reached in the 4^{th} step (Bustin 2004). The amount of amplified target is known to be directly proportional to the input amount of target during the exponential phase of the PCR amplification. Therefore, selection of the threshold should be placed within this region. All sample cDNA was diluted 1:9 in RNase free water. A standard curve using Wt liver cDNA was created for each gene of interest. Serial dilutions were carried out to give 1:1, 1:3, 1:9, 1:27, 1:81, 1: 243 of cDNA in RNase free water. The Taq Man© system with 2x Taq Man© universal PCR mix and 20x Assays on demand Assay mix was used for all reactions. The Assay on demand mix contained the primers for each reaction and the probe with the fluorescent FAM- 490 (Table 0). Each reaction contained 10µl of PCR mix and 1µl of Assay mix with 9 µl of diluted cDNA. All samples were done in triplicate and 20µl/reaction was loaded onto a 96 well plate. Each plate contained a no template control (NTC) without cDNA. RNA only was loaded once per sample to check for RNA quality. We wanted to exclude the possibility that DNA contamination, resulting from the RNA isolation procedure, rather than actual

amplification of cDNA was responsible for the signals obtained. The PCR was carried out on a Biorad My iO single colour PCR detection system (Biorad). The PCR protocol used was 2 minutes 50°C, 10 minutes 95°C, and 15 seconds 95°C and 2 minutes 60°C for 40 cycles. All samples were analysed using Microsoft Excel and the standard curve method following Larionov et al. (2004). The threshold was selected automatically, a standard curve created and all means and variances were calculated for the PCR replica using MyiQ software. *Tbp* and *Gapdh* were chosen as reference genes for which the geometric mean was calculated to receive a single normalisation factor for each sample. Non- normalised values were divided by the normalisation factor. The final results were expressed as the ratio between *Ercc1* Null and Wt samples, showing the mean of two different plates and the standard error of the mean.

2.8 Cell culture methods

2.8.1 Hepatocyte isolation

A two-step perfusion protocol was established to isolate hepatocytes from mice. Livers were perfused with a Ca^{2+}- free Perfusion medium to allow opening of desmosomes and removal of blood from the liver. This step was followed by a second perfusion step with 120 ml Leibowitz 15 medium containing 25 mg collagenase for enzymatic separation of hepatocytes. Collection of hepatocytes was achieved through a centrifugation step at 270 rpm, followed by a second centrifugation using Percoll at 340mOsm/kg to eliminate dead hepatocytes. Percoll is composed of colloidal silica coated with polyvinylpyrrolidone and forms a density gradient upon high speed centrifugation. Its low viscosity, its compatibility with living cells and its impermeability into biological membranes helps to isolate dead, lighter cells from live, heavier cells. Cell viability was determined using the trypan blue exclusion method. Cells were plated at a density of $0.13x10^6$ cells/ml on fibronectin- coated 60 mm^2 petri dishes or 2- well chamber slides in DMEM

containing AdenoCre virus for 2.5hrs (see below). Uninfected control dishes received DMEM only for the same amount of time. Medium was changed twice to stop further infection of the virus and all cells were cultured in modified Chee's medium.

2.8.2 Tamoxifen in culture

Tamoxifen citrate was diluted in 50% ethanol to obtain a 5 mM solution. All other dilutions were performed in Chee's medium until a final concentration of 500 nM was reached. Medium was aspirated and the tamoxifen solution was then added to the cultures for a period of 24 hours. Aspiration of medium was followed by two washes with 1xPBS and replacement with Chee's medium only until cells were harvested.

2.8.3 AdenoCre in culture

AdenoCre virus was diluted in plating medium to obtain a multiplicity of infection (MOI) factor of 10. This infection medium was added to petri dishes or chamber slides and left in the incubator at 37°C and 5% CO_2 for 2.5 hours. Plates were then washed with modified Chee's medium twice and subsequently cultured in modified Chee's medium.

2.8.4 Thymidine incorporation

Dishes were rinsed with serum- free Glasgow- modified Eagle's medium and incubated with serum- free medium containing 1 μCi/ml ^{3}H- Thymidine at 37°C for 3 hrs. Cells were rinsed with PBS and lysed with 1% SDS at room temperature. 20% cold TCA was added and stored for 90 min at 4 °C to precipitate nucleic acid

polymers longer than 20 nucleotides and to separate radioactively labelled nucleotides from unincorporated label. All samples were filtered using 10% TCA. The filters were dried and then read in the scintillation counter Tri Carb 2100 TR (Packard) in Ultima Gold fluid (Packard Biosciences).

2.8.5 BrdU staining

For BrdU staining DNA replication is used to replace thymidine with BrdU in the DNA structure of dividing cells both in vitro and in vivo (Gage et al. 2000). Hepatocytes were incubated in 40μM BrdU for 6 hours at 37°C allowing BrdU incorporation. Cells were fixed in 80% ethanol at 4°C overnight and rinsed in PBS for 10 mins. All slides were incubated in 5M HCl for 45 mins on a rocker at room temperature and washed with PBS. Slides were then incubated in 1% H_2O_2 for 10 mins to block any intrinsic peroxidase activity and washed twice with PBS. Slides were covered in blocking solution for 10 mins at room temperature and incubated in anti- BrdU antibody diluted 1:100 with blocking solution for 1 hour. After a wash with PBS, slides were covered with rabbit anti- rat HRP diluted 1:100 with blocking solution for 30 mins at room temperature. Another wash with PBS was followed by incubation with DAB solution at room temperature, visualising the BrdU incorporation in each nucleus. Slides were rinsed in water, counterstained with 0.1% haematoxylin (w/v) and 0.1% light green (w/v) and mounted in cedarwood oil.

2.8.6 Feulgen staining

Slides were fixed overnight in Bouin's fixative at 4°C and then incubated in denaturing solution made of 5M HCl for 45 mins at room temperature. All slides were washed in water and stained with Schiff's reagent for 1 hour at room temperature. Slides were thoroughly washed in water until pink colour developed

and counterstained with 0.1% light green (w/v). All slides were mounted in cedarwood oil and stored at 4°C in the dark.

2.8.7 Comet assay

The comet assay is a single cell gel electrophoresis method that was introduced in 1984 by Ostling and Johanson to measure DNA damage in individual cells. This method was subsequently further developed by Singh et al. (1988) who used a more versatile alkaline based method to measure DNA strand breaks with high sensitivity. In summary, cells are embedded in agarose and nuclei are lysed to remove cellular protein. DNA unwinding is done under alkaline conditions and separated by gel electrophoresis. Finally, DNA is stained with a fluorescent dye to visualise the broken or damaged DNA that, during gel electrophoresis, migrated away from the nucleus. The extent of DNA liberated from the head of the comet is directly proportional to the DNA damage. Intact hepatocyte nuclei were prepared for the comet assay. $0.13x10^6$ cells were rinsed in ice- cold PBS, followed by a 5 min incubation of 1.4 ml swelling buffer to help hepatocytes detach from the fibronectin-coated slides. 140µl lysis buffer 1 was then added to the hepatocytes and cells were incubated on ice for 5 min under intermittent shaking. Aliquots of 2x700 µl were prepared per dish and centrifuged on a layer of 700 µl 0.6 M sucrose in TE buffer at 4˚C and 4000 rpm for 5 min. All pellets were gently dispensed in 100 µl PBS and 140 µl 1.5% low melting point agarose was added. By placing a coverslip over 70 µl of agarose and nuclei suspension on agarose- coated slides, a gel was formed at 4˚C. The extracted nuclei were then incubated in lysis buffer 2 for 5 min, followed by 3 washes in cold enzyme buffer. Half of the aliquots were incubated with formamidopyrimidine- DNA- glycosylase (Fpg) at 37˚C for 1 hour and the other half with buffer only. Alkaline unwinding in electrophoresis solution was done for 10 min and nuclei were subjected to electrophoresis at 300mA for 10 min. Samples were washed with neutralising buffer and stained with propidium iodide. All nuclei were analysed using a fluorescence microscope (Olympus) and the Komet software

(Kinetic Imaging Ltd., Liverpool). 50 nuclei per sample were analysed at random and the mean and standard deviation calculated.

2.8.8 Oil Red O stain on slides

Cytoplasmic lipids were stained red with Oil Red O to examine the amount of lipid accumulation in hepatocytes. Slides were incubated in 100% propylene glycol for 3x5 mins on a flatbed shaker (Stuart) at room temperature. Oil Red O stain was dissolved in 100% propylene glycol and filtered before use. Slides were incubated in Oil Red O solution for 1 hour on a flatbed shaker (Rotatest) at room temperature and subsequently washed in 85% propylene glycol for 5 mins. Slides were rinsed in DDW and cells were counterstained with 0.1% haematoxylin (w/v). Slides were mounted using glycerol.

2.8.9 DNA damaging agents

Three days after plating and infection, hepatocytes were challenged using three different DNA damaging agents. Glucose oxidase, an oxidative damage inducer, was given at 1, 5, 10, 50 and 100 μU in 1xHBSS per dish. Cells were incubated at 37°C for one hour, washed with PBS and fresh Chee's medium was added. For UVC irradiation, which induces lesions repaired by NER, medium was aspirated off all dishes and a small amount of PBS was added before irradiation. Cells were given 50 J/m^2, 20 J/m^2, 10 J/m^2, 5 J/m^2 and 2 J/m^2 of UVC irradiation using a UVGL-58 Miniregalight lamp (Ultra- Violet Prod. Inc.). Hepatocytes were incubated in 10 μg/ml, 5 μg/ml, 2 μg/ml and 1 μg/ml of Mitomycin C, an interstrand cross- link inducer, in Chee's medium for 24 hrs. Cells were washed with PBS and fresh Chee's medium was added.

3. Use of *Ercc1* floxed TTRCre mice to create a conditional, liver- specific knockout mouse model in vivo and in vitro

Ercc1 knockout mice die before weaning at 3 weeks of age (McWhir et al. 1993), making it difficult to characterise the liver phenotype and to determine the lesions responsible. We therefore decided to establish a liver- specific, conditional *Ercc1* knockout mouse to enable us to control the onset of *Ercc1*- deficiency in liver only. We decided to use a tamoxifen inducible Cre recombinase- loxP system as a similar system had already proven successful in our laboratory where a skin- specific *Ercc1* knockout was created (Doig et al. 2006).

Our Cre recombinase, with a mutated murine oestrogen receptor (MER) fused to both terminals was linked to the liver- specific transthyretin (TTR) promoter (Verrou et al. 1999, Tannour- Louet et al. 2002). The TTR gene sequence consists of 3 kb of regulatory sequence, exon 1, intron 1 and part of exon 2 with all potential ATG start codons in exon 1 and 2 being mutated (Figure 3).

A mutation in the oestrogen receptor at amino acid 525 leads to the replacement of a glycine with an arginine (Danielian et al. 1993). The mutated oestrogen receptor has lost its ability to bind to 17 β- oestradiol and can only be activated when the oestrogen receptor antagonist tamoxifen is present. Introduction of the transgene into mice results in liver- specific expression of Cre recombinase (Tannour-Louet et al. 2002).

In the cytoplasm, the chimeric Cre is complexed by the heat shock protein 90 (hsp90), leaving the chimeric Cre recombinase in an inactive state (Figure 4). Upon tamoxifen administration, the hsp90 is released from the Cre recombinase, resulting in a translocation of chimeric Cre into the nucleus. Once in the nucleus, Cre recombinase can detect the loxP sites and excise the *Ercc1* region between exons 3-5 (see Figure 4). This results in a loss of function for *Ercc1* in the liver.

3.1 Breeding of TTRCre *Ercc1* Flox animals

TTRCre mice were obtained from Dr M. Vasseur-Cognet (Tannour-Louet et al. 2002) and crossed onto animals that were heterozygous for *Ercc1* deficiency (*Ercc1* Wt/Null) (Figure 1). TTRCre *Ercc1* Wt/Null heterozygotes were then mated with *Ercc1* Flox/Flox animals. This cross resulted in TTRCre Ercc1 Flox/Null experimental animals and TTRCre *Ercc1* Flox/Wt animals which we used as controls.

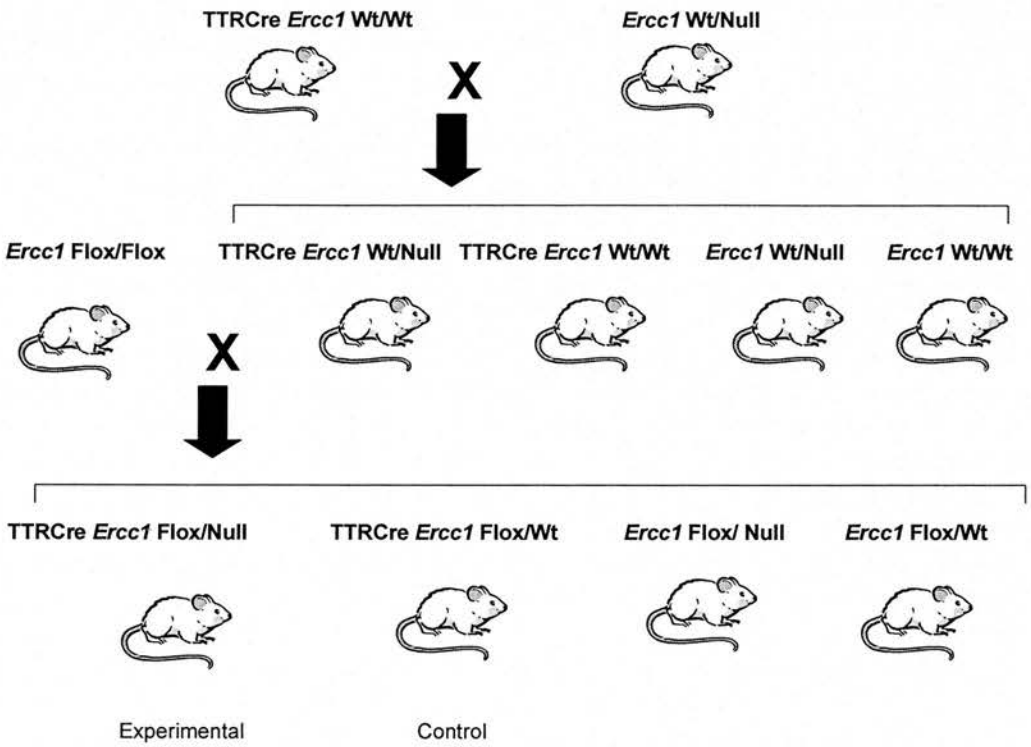

Figure 1: Breeding scheme for the production of TTRCre *Ercc1* Flox/Null and TTRCre *Ercc1*Flox/Wt mice. In both generations, the ratios of offspring are ¼:¼:¼:¼.

3.2 PCR assays for detection of TTRCre transgene, Ercc1 Null, Wt, recombined and Flox alleles

A PCR protocol for detection of the *Ercc1* knockout allele was set up (Figure 2). The *Ercc1* knockout was originally achieved by introducing a NEO cassette into exon 5 of the *Ercc1* gene (McWhir et al. 1993). Primers were located in the NEO cassette (M4956) and in exon 5 (035M) to give an 800 bp long product specific for the *Ercc1* knockout allele. The Flox allele was detected by placing one primer in exon 5 upstream of the 3' loxP site (432E) and another primer 3' of the loxP site in intron 5 (F25732). A 500 bp band indicates the Flox allele. In addition, a 1050 bp band for the Wt allele is detectable with the same primer pair (Figure 2). The difference in PCR product size of the Flox and Wt alleles results from the deletion of several hundred base pairs of intron 5 during loxP introduction, giving a shorter band for the Flox allele.

Recombination of the Flox *Ercc1* locus could be detected by placing primers immediately upstream of the 5' loxP site (F25731) and immediately downstream of the 3' loxP site (F25732) (Figure 2). No PCR product can be produced when the locus is not recombined as the primers are too far apart. Upon recombination, the exon 3-5 region is excised, the primers become located close to each other and a 250 bp band can be detected by PCR.

A PCR assay for detection of the TTRCre transgene in my animals was established. The primers were located in the Cre recombinase sequence (Cre) and the murine oestrogen receptor (Mer) sequence of the TTRCre transgene (Figure 3). The resulting PCR product was 1350 base pairs (bp) long. Figure 4 illustrates the TTRCre *Ercc1* floxed model and the recombination event itself in detail.

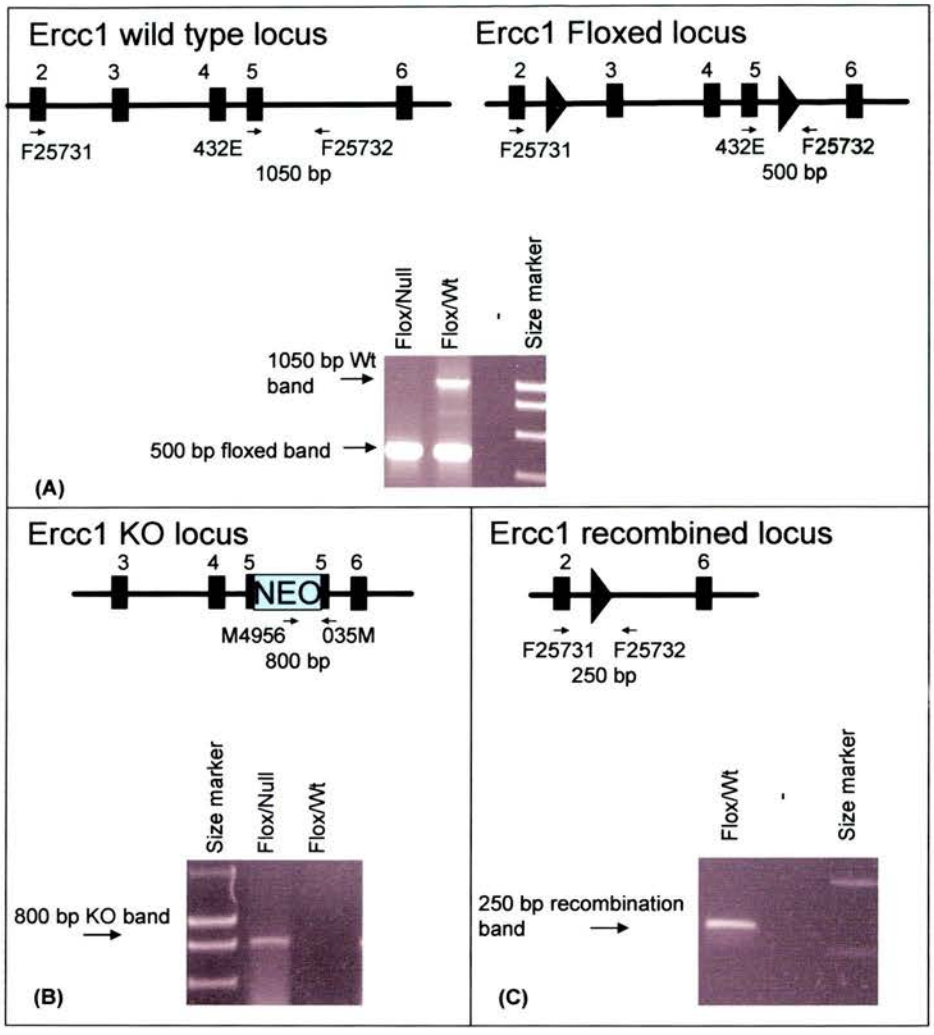

Figure 2: Schematic of the central region of the *Ercc1* Wt, Flox, Null and recombined loci. (A) *Ercc1* Wt and *Ercc1* Flox loci. Exons are numbered and shown as boxes. LoxP sites are marked as large arrow heads. Location of the primers is represented by small arrows and PCR band size is indicated. A gel with the PCR products for primers 432E and F25732 is shown for Flox/Null and Flox/Wt. The difference in size between Wt and Flox bands results from partial deletion of intron sequence during introduction of the loxP site. (B) *Ercc1* knockout (KO) locus. The NEO cassette was inserted into exon 5, leading to a disabled *Ercc1* allele. The PCR product for primers M4956 and 035M is shown for the *Ercc1* Flox/Null sample and a lack of product is shown for *Ercc1* Flox/Wt. (C) *Ercc1* recombined locus. Upon recombination of the Flox allele, the distance between primers F25731 and F25732 narrows so that a 250 bp product can be detected. A gel with the PCR product is shown for an *Ercc1* Flox/Wt sample.

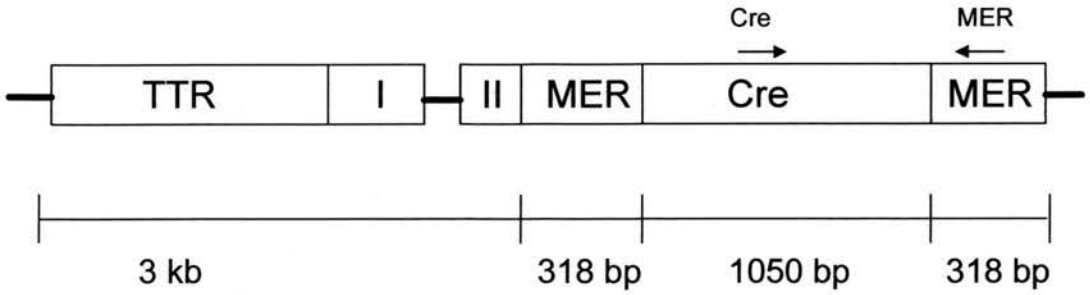

Expected PCR product: ~1350 bp

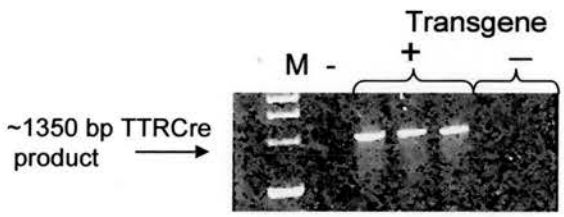

Figure 3: Schematic of the TTRCre transgene. Cre recombinase (Cre) is flanked by two ligand- binding domains of the murine oestrogen receptor (MER). A mutation at amino acid 525 (G525R) ensures that the MER receptor is only responsive to tamoxifen. Upstream of the MERCreMER construct, the 3 kb regulatory region containing the murine TTR promoter, exon 1 and intron 1 and most of exon 2 are used to drive liver specific transcription. Location of the primers is marked with small arrows and the band size indicated. A gel with the PCR products is shown for TTRCre and Wt livers.

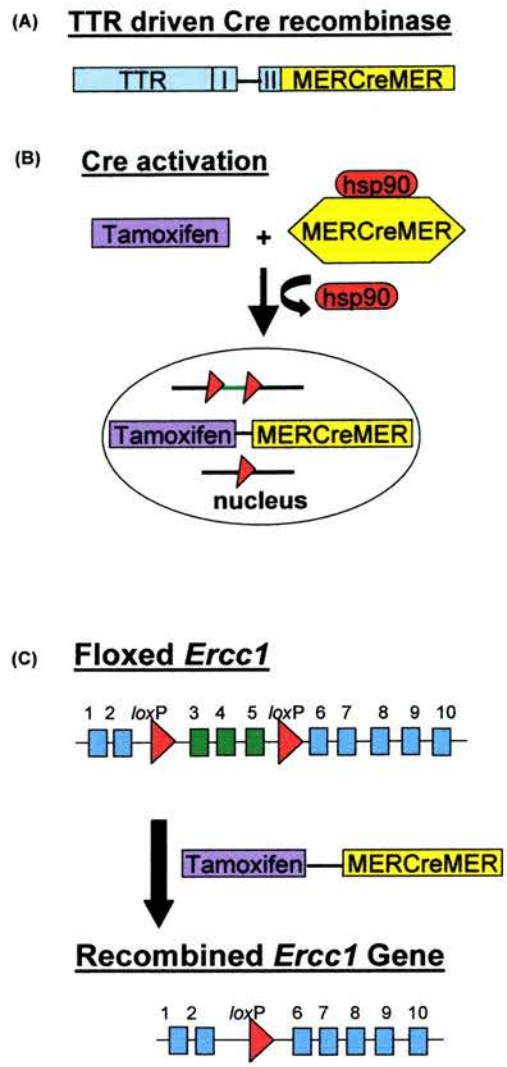

Figure 4: Schematic of Cre recombinase activation and the recombination event. (A) TTRCre transgene. (B) Cre recombinase activation upon tamoxifen administration. In the cytoplasm, chimeric Cre is complexed by the heat shock protein 90 (hsp90). In the presence of tamoxifen, the chimeric Cre is released from hsp90 and translocated into the nucleus where the Cre recombinase drives the recombination event upon recognition of loxP sites. (C) Schematic of the Flox and recombined *Ercc1* loci. Activation of Cre recombinase is initiated by tamoxifen administration. The Cre recombinase recognises the loxP sites and recombines the Flox *Ercc1* allele, leading to an excision of the *Ercc1* region spanning exons 3-5.

3.3 Establishment of primary hepatocyte cultures

I established a two- step perfusion protocol for primary hepatocyte cell culture to investigate the role of *Ercc1* in vitro. Yield of primary hepatocytes was improved from $1x10^6$ to $16.3x10^6$ by reducing the amount of collagenase used during the perfusion from 75 mg to 25 mg (Table 1, isolations 2 and 5). In addition, viability improved from 45% to 80%. I reduced the centrifugation speed from 600 rpm to 500 rpm as this seemed to be a milder treatment during hepatocyte isolation, although no clear effect could be seen on yield and viability. The perfusion time was increased from 8 min to 10 min and an improvement in yield and viability could be seen when comparing isolations 5 and 6 in Table 1. The effect of Percoll on the hepatocyte cultures was investigated. Without using Percoll during the second centrifugation step, the yield improved from $5.18x10^6$ to $12.5x10^6$, but the overall viability was compromised (isolations 3 and 4, Table 1). The effect of Percoll was further examined by subjecting Percoll treated and untreated hepatocyte populations to flow cytometry (Figure 5). Large amounts of apoptotic material and/or cell debris can be seen in isolations done without using Percoll when compared to Percoll treated isolations. Typically, a yield of $29x10^6$ and a viability of 88% were achieved by using 25 mg collagenase for 10 min, spinning the cells at 500 rpm and including the use of Percoll in the second spin. This protocol was used for establishment of subsequent cultures.

I went on to determine basic hepatocyte parameters of my Wt cultures looking at apoptosis, S-phase, development of tetraploidy and ^{3}H- thymidine incorporation from day 0 to day 9 (Table 2). S-phase was low initially with a peak of 4% at day 3 and a subsequent stabilisation to a rate of 2% in older cultures. Wt hepatocyte replication, as determined by ^{3}H- Thd incorporation, increased steadily from day 1 in culture with a peak at day 5 and subsequent lower levels in older cultures. In addition, cells showed low levels of apoptosis immediately after plating with a peak of 24% at day 3 and only slightly lower levels of 16-19% in older cultures. No change in polyploidy

was detected in any of the cultures over time. Thus, a basic hepatocyte cell culture system was established for use on *Ercc1* Flox/Wt and Flox/Null hepatocytes.

Table 1: Summary of the conditions used for hepatocyte isolation. + indicates the use of Percoll and – the absence of Percoll during the second spin. Best yield and viability were obtained using the conditions in isolation number 6.

Isolation (#)	Collagenase (mg)	Time of perfusion (min)	Percoll	Spin (rpm)	Yield	Viability (%)
1	75	8	+	600	$1x10^6$	29
2	75	8	+	500	$1x10^6$	45
3	50	8	+	500	$5.18x10^6$	80
4	50	8	-	500	$12.5x10^6$	48
5	25	8	+	500	$16.3x10^6$	80
6	25	10	+	500	$29.4x10^6$	88

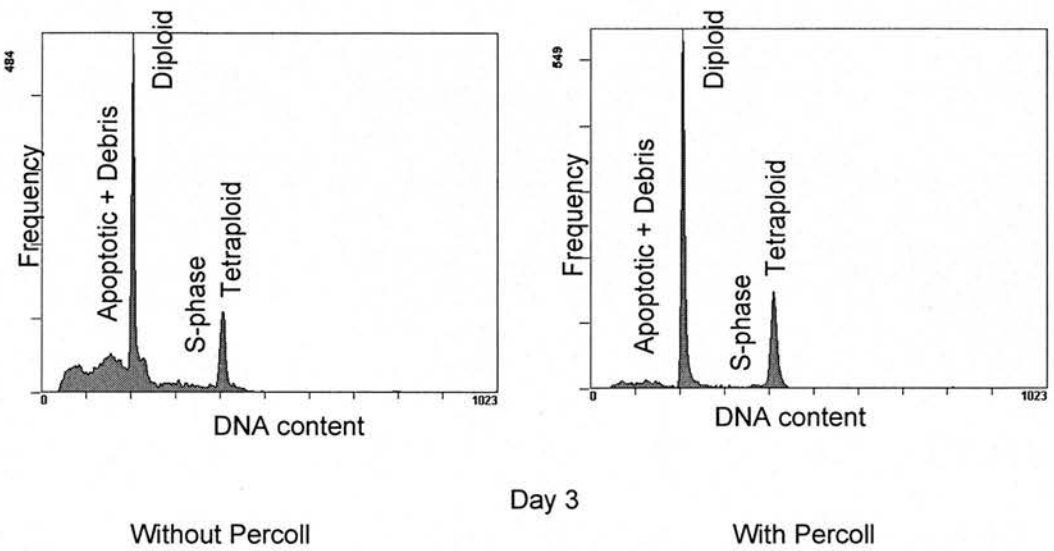

Figure 5: Flow cytometry profiles showing the effect of Percoll during hepatocyte isolation. Cell cultures were set up from isolations made with and without using Percoll. DNA content is shown at day 3 after plating. The different cell populations are labelled.

Table 2: Basic hepatocyte parameters obtained from wild type hepatocyte cultures over 9 days. Apoptosis, S-phase and tetraploidy values were obtained by flow cytometry. Apoptosis is shown as percentage of all cells. S-phase and tetraploidy are expressed as the percentage of all viable cells. Tritium labelled thymidine (^{3}H- Thd) incorporation was measured on three different dishes for each time point. The mean CPM (counts per minute) and SEM (standard error of the mean) are shown.

Parameters	Day 0	Day 1	Day 3	Day 5	Day 7	Day 9
Apoptosis (% of all cells)	0.5	15	24	19	16	17
S-phase (% of viable cells)	0.6	3	4	2	2	2
Tetraploidy (% of viable cells)	38	31	26	33	29	27
^{3}H-Thd (mean CPM + SEM)		5286 ± 218	12235 ± 377	35564 ± 2235	19050 ± 226	16572 ± 1435

3.4 Tamoxifen citrate treatment of primary hepatocyte cultures

Tamoxifen citrate was brought into solution by addition of absolute ethanol. All further dilutions were done with modified Chee's medium until a tamoxifen concentration of 500 nM was obtained. This solution was added to TTRCre *Ercc1* Flox/Null hepatocytes. Control dishes received Chee's medium only. DNA samples were taken 24, 48 and 72 hours after tamoxifen citrate addition. DNA content was matched by spectrophotometry and a semi- quantitative recombination PCR was performed. DNA from a cell line with 100% recombination was used for comparison. A faint band could be seen 48 hrs after tamoxifen treatment, but not at other time points (Figure 6). When a TTRCre transgene PCR was done on the same samples, all samples showed a strong transgenic band, indicating that the DNA was of sufficient quality. When I repeated this experiment using Flox/Wt and Flox/Null cultures, no recombination could be seen at any of the time points (data not shown). When higher doses of tamoxifen citrate were given to the cultures, hepatocytes showed high levels of cell death (data not shown). I was therefore unable to achieve high levels of recombination in vitro by tamoxifen administration to TTRCre *Ercc1* Flox/Null or Flox/Wt hepatocyte cultures.

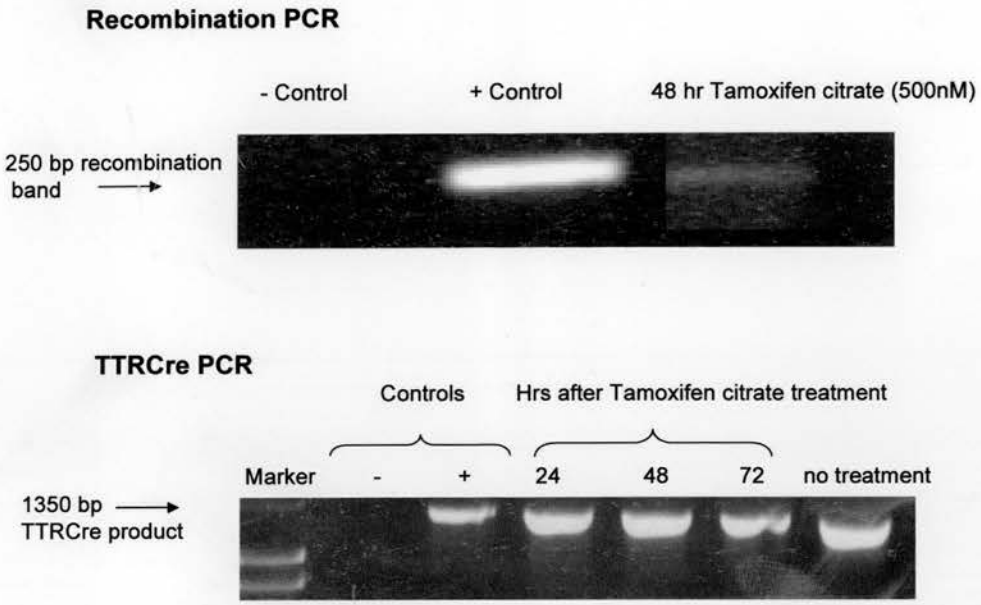

Figure 6: Recombination PCR on TTRCre *Ercc1* Flox/Null hepatocyte cultures. 500nM of tamoxifen citrate was added to hepatocyte cultures and DNA taken at 24, 48 and 72 hrs after tamoxifen addition. Recombination could only be detected at 48 hours. A control cell line with 100% recombination is shown for comparison. A TTRCre PCR was performed on all samples to determine DNA quality. Positive controls are indicated as + and negative controls as -. An untreated control hepatocyte culture is shown for comparison.

3.5 4- Hydroxytamoxifen (4-OHT) treatment in vivo

To test the TTRCre inducible system in combination with our Flox *Ercc1* gene as soon as possible, we mated TTRCre mice with *Ercc1* Flox/Null mice when the transgenics from France were still in the isolator. Initially, 4- hydroxytamoxifen was used for induction of recombination in vivo which was in accordance with Tannour-Louet et al. (2002). As a pilot experiment, 1 mg of 4-OHT was injected i.p. into each of two TTRCre *Ercc1*Flox/Null animals on two days, leaving 48 hours for recovery between injections. In addition, two *Ercc1* Flox/Null animals without theTTRCre transgene were treated in a similar manner and used as controls. DNA was extracted from liver, kidney and tail. DNA content of all samples was matched by spectrophotometry and a semi- quantitative recombination PCR was performed. A faint band could be detected in the liver of TTRCre *Ercc1* Flox/Null mice indicating low levels of recombination (Figure 7, only one pair of animals shown). In the absence of the TTRCre transgene, no recombination could be detected in the liver of *Ercc1* Flox/Null animals after 4-OHT treatment. We estimated the level of recombination in our TTRCre *Ercc1* Flox/Null livers by densitometry to be around 10% using a cell line with 100% recombination for comparison. The experiment was repeated giving 6 doses of tamoxifen to one male animal and 9 doses of tamoxifen to one female animal with an injection every second day. Again, low levels of recombination could be seen in the liver (data not shown). However, we judged the levels of recombination to be insufficient to generate high levels of *Ercc1*- deficient hepatocytes in vivo and decided to switch to tamoxifen citrate as inducer following recommendations of the French group. Tamoxifen citrate is easier to keep in solution and we hoped that it would enable us to achieve higher amounts of recombination in vivo and in vitro.

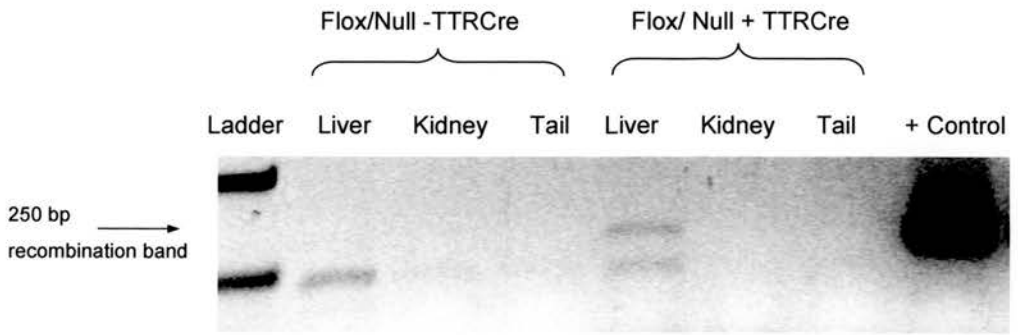

Figure 7: Recombination PCR on *Ercc1* Flox/Null mice with and without TTRCre transgene. Liver, kidney and tail samples were analysed. A sample with 100% recombination was used for comparison. In addition to the 250 bp recombination band, an unspecific band of 200 bp can be detected in liver, irrespective of the presence of the TTRCre transgene.

3.6 Tamoxifen citrate treatment of TTRCre *Ercc1* Flox/Wt and Flox/Null animals

Tamoxifen citrate injections were given to TTRCre Flox/Wt and Flox/Null animals of both genders. 1 course of tamoxifen citrate consisted of i.p. injections of 1 mg of tamoxifen citrate for 5 consecutive days.

After 1 and 2 courses of tamoxifen citrate and 5 days of recovery, I could detect low levels of recombination in Flox/Wt animals number 2, 3 and 4 (Table 3). The amounts of DNA were matched by spectrophotometry and recombination levels were detected by semi-quantitative PCR, using a cell line showing 100% recombination for comparison. The levels of recombination were estimated to be around 10-25% by densitometry with animal number 3 showing the highest levels of liver- specific recombination.

Table 3: Summary of levels of recombination and DNA content in TTRCre *Ercc1* Flox/Null and Flox/Wt mouse livers after tamoxifen citrate injections. One course of tamoxifen (tamox.) comprises of i.p. injections on five consecutive days. The time before sacrifice is shown, starting from the day of the first injection. Approximate levels of recombination (recomb.) were estimated via PCR using a cell line with 100% recombination for comparison. Recombination levels of samples 1 to 6 were further determined in the Southern blot shown in Figure 9. DNA content was determined by flow cytometry. A flow cytometry profile of samples 5 and 6 is shown in Figure 8. Amounts of ploidy and S-phase are given as the percentage of viable cells. Apoptosis levels are given as percentage of all cells.

Genotype	Sex	ID (#)	Recomb. (%)	Tamox. (# courses)	Time (to sacrifice)	2n (%)	4n (%)	8n (%)	Apoptosis (%)	S-phase (%)
*Ercc1*Flox/Null TTR	m	1	0	1	5 days	67.9	23.4	-	4.7	1.8
*Ercc1*Flox/Wt TTR	f	2	10	1	5 days	73.6	21.8	-	2.1	0.6
*Ercc1*Flox/Wt TTR	f	3	25	2	5 days	69.1	20.1	0.3	9.9	1.1
*Ercc1*Flox/Wt TTR	f	4	2	2	5 days	62.3	24.4	-	1.8	1.9
*Ercc1*Flox/Null TTR	m	5	0	2	3 weeks	34.4	39.3	20.4	11.6	1.7
*Ercc1*Flox/Wt TTR	m	6	0	2	3 weeks	58.2	30.6	2.6	5	1.2
*Ercc1*Flox/Null TTR	m	7	0	2	4 weeks	78.4	32.9	6.9	37	3.2
*Ercc1*Flox/Wt TTR	m	8	0	3	5 weeks	77.7	39.8	4.5	41.3	5
*Ercc1*Flox/Null TTR	m	9	0	2	6 weeks	56.8	37.8	3.3	7	1.4
*Ercc1*Flox/Null TTR	m	10	0	2	6 weeks	58.5	37.4	2.3	7.5	1.3
*Ercc1*Flox/Null TTR	m	11	0	2	6 weeks	54.1	35.8	8	6.7	1.4
*Ercc1*Flox/Wt TTR	m	12	0	2	6 weeks	63.8	33.5	-	4.6	0.5

When 2 courses of tamoxifen citrate were given to male animals of both genotypes and the recovery period extended to 3 weeks, high levels of ploidy and apoptosis were apparent by flow cytometry in TTRCre *Ercc1* Flox/Null animal number 5 when compared to the TTRCre *Ercc1* Flox/Wt control animal number 6 (Table 3 and Figure 8). The tetraploid peak consists of tetraploid nuclei in G1 phase and diploid nuclei in G2. Throughout this thesis, I refer to this peak as the tetraploid peak as the majority of nuclei will be tetraploid. Despite the changes in DNA content, no recombination could be detected by PCR in either animal (Table 3). No consistent genotype- dependend changes in polyploidy, apoptosis or S-phase were seen in any of the other animals given 1 or 2 courses of tamoxifen citrate.

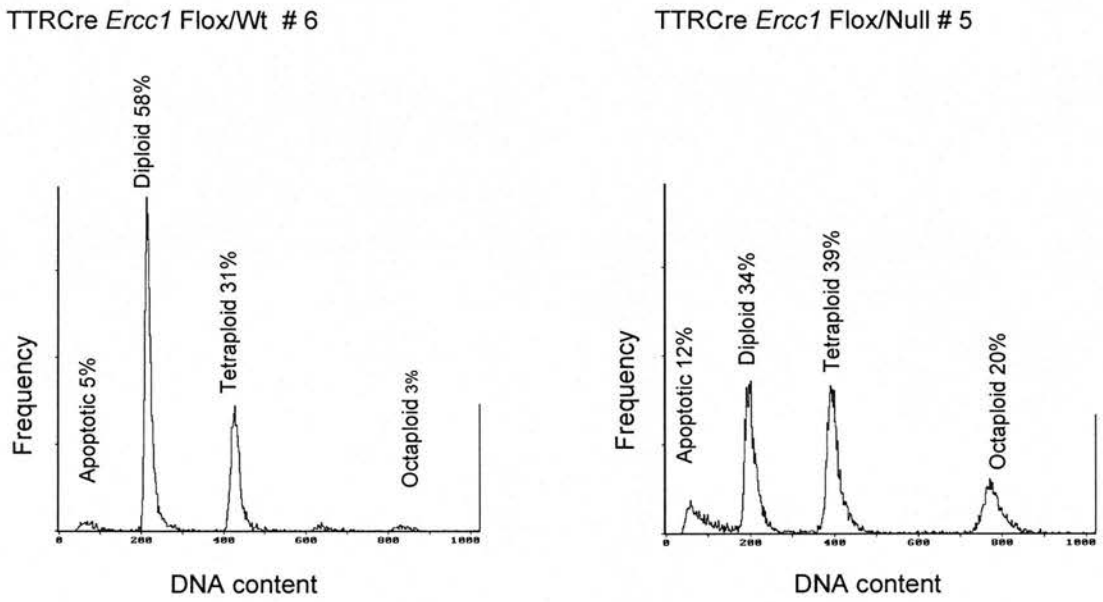

Figure 8: Flow cytometry profiles showing the DNA content of TTRCre *Ercc1* Flox/Null (# 5) and Flox/Wt (# 6) livers after two courses of tamoxifen citrate and three weeks recovery. The different cell fractions are labelled. Apoptosis is given as a percentage of the total amount of cells. Diploid, tetraploid and octaploid fractions are given as the percentage of viable cells.

I decided to allow longer recovery periods in the recently injected male animals and to extend the amount of tamoxifen citrate given from 2 to 3 courses in animal number 8 in order to increase the chance of development of polyploidy and high levels of recombination. However, I was unable to detect any recombination or polyploidy in male animals of either genotype, irrespective of treatment (Table 3).

Initially, we suspected a female bias towards success of recombination as only female animals had shown recombination of the liver (animals 2, 3 and 4 Table 3). We therefore injected males and females of both genotypes with several courses of tamoxifen citrate and varied the length of recovery as before. We were unsuccessful in seeing any recombination, higher levels of ploidy or apoptosis in livers of either gender (data not shown).

To determine recombination levels more accurately, a Southern blot was performed on animals number 1-6. A titration curve was created by spiking DNA from a cell line with 100% recombination with DNA from an *Ercc1* Flox/Flox liver in various dilutions (Figure 9). We were able to detect levels of recombination as low as 10% in our titration curve. In contrast, no recombination could be detected by Southern blotting in any of our samples. Therefore, the actual recombination levels of livers 2, 3 and 4 are below 10%, showing that our semi-quantitative PCR system leads to an over-estimation of the amounts of recombination in liver.

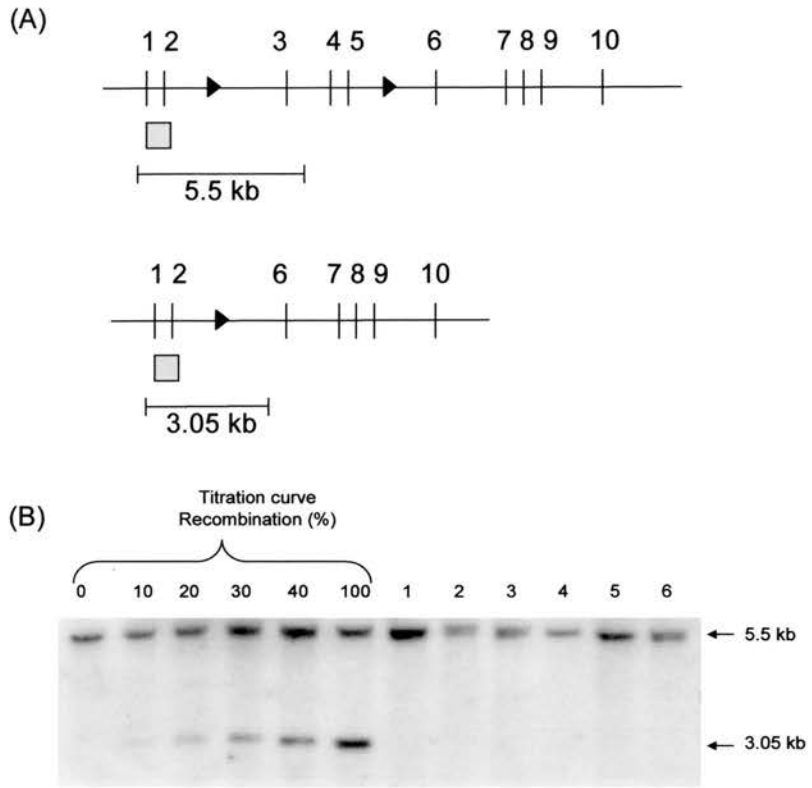

Figure 9: Liver specific recombination of the *Ercc1* Flox allele. (A) Schematic of *Ercc1* Flox and recombined alleles. All *Ercc1* exons are numbered and represented by a line. The loxP sites are shown as small arrow heads. The location of the probe is indicated by a grey box. The 5.5 kb fragment is produced from the Wt, Null and non- recombined Flox alleles (this region on the gene is identical in these three alleles) and the 3.05 kb fragment is from the recombined Flox allele. (B) Southern blot indicating the levels of recombination in TTRCre *Ercc1* Floxed/Null and Floxed/Wt livers after treatment with tamoxifen citrate and recovery. A titration curve was obtained by spiking varying amounts of DNA from a cell line showing 100% recombination into DNA from an *Ercc1* Floxed/Floxed liver. Lanes:

1) Floxed/Wt liver # 6, 2 courses of tamoxifen citrate and 3 weeks before sacrifice;

2) Floxed/Null liver # 5, 2 courses of tamoxifen citrate and 3 weeks before sacrifice;

3) Floxed/Wt liver # 3, 2 courses of tamoxifen citrate and 5 days before sacrifice;

4) Floxed/Wt liver # 4, 2 courses of tamoxifen citrate and 5 days before sacrifice;

5) Floxed/Wt liver # 2, 1 course of tamoxifen citrate and 5 days before sacrifice;

6) Floxed/Null liver # 1, 1 course of tamoxifen citrate and 5 days before sacrifice.

In conclusion, using 4- OHT or tamoxifen citrate to induce recombination in TTRCre *Ercc1* Flox/Wt or Flox/Null livers and hepatocytes, led to insufficient levels of recombination to induce *Ercc1*- deficiency. A phenotype, consisting of the typical polyploidisation of the liver seen in complete *Ercc1* knockout livers, was only seen occasionally, but no recombination could be seen in these animals. Consequently, because of the low levels of recombination observed and the irreproducible effects on the phenotype of the mice, we decided to use a different system to induce recombination in our *Ercc1* Flox animals.

3.7 Discussion

The establishment of hepatocyte primary cultures was a first step to ensure that in vitro experiments could be conducted on *Ercc1*- deficient hepatocytes. One issue with all primary cultures is the viability of cells. Primary hepatocytes do not survive for more than 2 weeks in culture (Mitaka 1998). My hepatocytes showed some apoptosis in culture shortly after isolation and cells did not survive beyond 10 days of culture, limiting experimental time. In addition, hepatocytes do not divide readily in culture and even upon stimulation with mitogens such as EGF and insulin, DNA synthesis is usually increased, but without subsequent cell division. It is estimated that hepatocytes undergo approximately one cycle of cell division in culture (Mitaka 1998). A way to improve cell division in hepatocytes is to co-culture hepatocytes with non-parenchymal cells such as Stellate and Kupfer cells. Tateno et al. (2000) have shown that large hepatocytes grow and form colonies when cultured with fractions of Kupfer and Stellate cells. However, the grade of hepatocyte maturity, the amount of granulation and the state of polyploidy all determine the ability for DNA synthesis and cell division of primary hepatocytes (Tateno et al. 2000). S-phase and growth potential have been shown to decrease with increased granularity, maturity and polyploidy in vivo (Tateno et al. 2000). Non- parenchymal cells in my hepatocyte cultures are mostly separated from my primary cells during the Percoll step. This could explain the shorter life-span of my primary hepatocyte cultures when compared to the literature. Another issue with hepatocyte culture is the maintenance

of the differentiated state in the liver. It is now widely accepted that hepatocyte differentiation is primarily controlled at the transcription level, emphasising the importance of transcription factor and protein synthesis (Mitaka 1998). There are two major ways to ensure hepatocyte maintenance, one being the addition of nicotinamide to improve hepatocyte survival and cell growth. In addition, nutrient-rich media containing high concentrations of amino acids and lower amounts of vitamins and trace metals help to stimulate protein synthesis and cell survival (Mitaka 1998). Our modified Chee's medium contains amino acids, vitamins and trace metals. It should therefore be suited to help with primary hepatocyte survival. In general, from our data on Wt hepatocyte cultures it seems that using ^{3}H- Thd incorporation as a measurement of proliferation is the better choice of method compared to flow cytometry, where only a slight increase in S-phase was observed in Wt hepatocyte cultures. In contrast, ^{3}H-Thd analysis showed much bigger range of DNA replication in culture. Maybe flow cytometry is not sensitive enough to pick up slight changes in S-phase in a whole liver or even cell culture system.

Tamoxifen is an anti-oestrogen with complex pharmacology and is known to lead to species and tissue specific responses upon administration (http://193.51.164.11/htdocs/monographs/vol66/tamoxifen.html 2005). Tamoxifen is readily absorbed and attains maximum plasma levels about 5 hours after administration in humans. The drug is extensively metabolised into N-desmethyltamoxifen and 4- hydroxytamoxifen (http://www.ncbi.nlm/nih.gov/books 2005). Both metabolites display a high affinity to the ER. Zhang et al. (1996) found that 4-OHT shows a 10-100x higher affinity to the hormone binding domain of MER than tamoxifen itself. We anticipated that using the metabolite 4-hydroxytamoxifen in our experimental setting should result in hepatocyte- specific Cre recombinase activation in vitro and in vivo. Similar protocols with the same TTRCre transgene have been used extensively, resulting in the desired recombination of different loci in animal models (Tannour- Louet et al. 2002, Wirth et al. 2003). However, in our animal model, 4-OHT was unable to induce high levels of recombination. We decided to switch to a more highly purified and concentrated form of tamoxifen,

tamoxifen citrate. Tamoxifen citrate is a nonsteroidal triphenylethylene derivative. It has been used in humans and is normally readily absorbed and metabolised in vivo. The change to tamoxifen citrate initially led to low, but sporadic levels of recombination in vitro and in vivo. None of those results could be repeated. The success of the system regarding recombination levels does not seem to be dependant on the form of tamoxifen used to induce Cre recombinase expression. The acute toxicity of tamoxifen in experimental animals is low, but long term treatment with tamoxifen is associated with onset of hepatocellular carcinoma in rats (Hirsimaki et al. 1993). A single dose of tamoxifen in rats produces DNA adducts in liver, with 10-15 fold differences compared to controls after six tamoxifen injections (Han and Liehr 1992). Suzme et al. (2001) showed that tamoxifen citrate doses of 10-20mg/kg resulted in high levels of ploidy. Levels of proliferation were estimated as a percentage of cells in S- phase using flow cytometry and remained the same when compared to untreated Wt animals. We could not detect an increase in ploidy in our animals when using tamoxifen on Flox/Wt animals after one or several courses of tamoxifen. Furthermore, changes in S-phase in our experimental animals could not be readily noted by flow cytometry which is in accordance to Suzme et al. (2001). This suggests that the doses of tamoxifen we are using do not have a significant, direct toxic effect on hepatocytes.

The route of tamoxifen administration and local levels of tamoxifen could be a contributing factor to the low levels of recombination that we see in our system in vivo. However, when using a cell culture system, where administration of the drug is not a limiting factor, recombination could only just be detected at a very low level. In fact, using 4-OHT did not give any successful recombination at all. When using tamoxifen citrate only low levels of recombination could be detected in vitro. It is therefore unlikely that the route of administration plays a major part in the failure to see recombination in our experimental settings.

The TTRCre construct consists of different parts which are all equally important for a functional transgene. One problem with our system could result from a dysfunction

of the murine oestrogen receptor (MER) part of the transgene, leading to a failure to respond to tamoxifen. However, the use of the mutated ER receptor has been widely tested in embryonic stem (ES) cells and mice. A mutated form of the human oestrogen receptor was first found by Fawell et al. (1990). They found that the oestrogen binding domain of the receptor is encoded by exon 7 and 8 in the conserved C-terminal region. Furthermore, a G to R mutation at amino acid 525 led to DNA binding with high affinity and dimerisation of the receptor without steroid binding. In contrast, tamoxifen was still able to induce a transcriptional response in this mutated receptor. In fact, it seems that the mutated form showed a higher DNA binding affinity compared to the Wt form of the receptor. The system was further developed by Feil et al. (1996) when Cre recombinase was fused to the mutated form of the human oestrogen receptor under the control of the CMV promoter. Murine ES cells and transgenic mice showed excision of the *tkneo* gene after a dose of 1 μM 4-OHT in vitro and 1 mg of 4-OHT i.p for 5 days in vivo in all tissues. As the expression of the CMV promoter varies in different tissues, recombination levels were found to vary from 40-50% in spleen, kidney and skin to 30% in liver.

The same G525R mutation was introduced into the murine oestrogen receptor (MER) by Zhang et al. (1996). The system was further exploited by fusing a single mutated MER to the Cre recombinase sequence in ES cells. A dose of 8-10 μM 4-OHT resulted in full recombination of the *lacZ* gene after 3-4 days in vitro. Higher doses of tamoxifen lead to toxicity in the cell cultures. This is in accordance with my own findings in hepatocyte cultures. The tamoxifen doses and the timing I used in vitro were similar to those used by Zhang et al. (1996), so that an insufficient concentration of tamoxifen or an insufficient incubation time can be excluded as a reason for the low levels of recombination seen in cultures after 48 hours. As the use of a single MER receptor showed moderate levels of background recombination after 8-10 weeks in culture, Zhang et al. (1996) fused a second MER to the other terminus of the Cre recombinase sequence. When tested in ES cells by staining for ß-galactosidase after *lacZ* expression, this new construct showed complete recombination after 48 hrs in one clone and after 72 hrs in another clone without

significant background in long term cultures (Verrou et al. 1999). The crystal structure for the Cre recombinase reveals a catalytic unit in the centre of the enzyme with the N- and C– termini being relatively free. Fusion of two receptors to either end should therefore not be a problem.

Three different groups subsequently reported on using the Cre recombinase system with the mutated human or mouse ER in combination with liver specific promoters. Levels of recombination seem to be varying in the different systems. Imai et al. (2000) reported 40-50% recombination of the *tkneo* gene in mouse liver carrying the transgene under the liver specific human α1- antitrypsin promoter after tamoxifen injections. Mosaic expression of Cre ERt was found by Imai et al. (2000) in about 40-50% of hepatocytes which correlated with mosaic transgene expression of the promoter. Mosaic recombination is a widely known problem with the Cre recombinase system (Ryding et al. 2001). This could be one contributing factor to why our system hardly shows any recombination at all. If the transgene is only expressed in a minority of the cells, then the overall effect after tamoxifen injection will be very small and could in fact be masked by the majority of normal hepatocytes. Another system used the liver specific albumin promoter and enhancer in combination with the α- fetoprotein enhancer to mimic the normal genomic organisation around a liver- specific gene (Kellendonk et al. 2000). Transgenic lines showed liver specific recombination of the glucocorticoid receptor after tamoxifen injections. A third group used the same albumin enhancer and promoter to excise the glucokinase gene after tamoxifen injections (Prostic and Magnusson 2000). 80% recombination was detected in 8 week old mice. However, it was noted that the recombination levels differed with time. 1 day old animals showed 40% recombination with a rise to 60% one week after birth and high levels after weaning. Clearly, the timing of recombination initiation is an important factor as expression of Cre recombinase may change with age. We are using young animals that are 6-8 weeks of age in which Cre recombinase expression is driven by the TTR promoter. It is possible that Cre recombinase is not expressed in our hepatocytes due to malfunction of the TTR promoter or mice being of the wrong age for maximal Cre

recombinase expression. The end point of the experiment might also play a role as the translocation of the Cre recombinase into the nucleus and subsequent recombination has been shown to take about 2-3 days after tamoxifen treatment (Metzger and Chambon 2001). We looked one day after tamoxifen treatment and up to 6 weeks after the treatment ended and could not find high levels of recombination as detected by PCR. In conclusion, although it seems that timing of recombination initiation and choice of promoter can lead to differences in recombination efficiency, I am confident that choosing the end point of the experiment was not a limiting factor in our case.

We decided to use a system with a transthyretin promoter driving liver specific Cre recombinase expression. Tannour- Louet et al. (2002) reported 50% recombination of the *Rosa* and *Ampk* genes using the TTRMERCreMER construct after 5 i.p. injections on consecutive days, with 80% recombination being detectable after multiple rounds of injections. This system was later used by Wirth et al. (2003) to delete the *Apc2* gene in liver, where 40% recombination was detected after one round of tamoxifen injections. The recombination we see in our system is below 10% as established by Southern blotting. This could depend on the location and accessibility of the loxP sites. Depending on how easily Cre recombinase can access the loxP sites, recombination efficiency should differ. The size of the deleted region might also play a role. The commonly used *lacZ* gene was excised using loxP sites that are only 950 bp apart. This amount of DNA should be more easily excised than a region spanning exon 3-5 of the *Ercc1* gene which consist of around 2.3 kB. However, Ryding et al. (2001) report that regions up to 2cM have been demonstrated to be excised in vivo. In addition, when using the Flox *Ercc1* alleles with a skin-specific Cre recombinase system, high levels of recombination are obtained regularly (Doig et al. 2006). This shows that the loxP sites in our *Ercc1* Flox cells are accessible and that the exon 3-5 region is not too big a region to be excised successfully.

It is possible that strain dependence is responsible for the low levels of recombination in our mice. Tannour-Louet et al. (2002) used a cross between

B6D2H and C57BL mice and Wirth et al. (2003) carried their experiments out in C57BL animals. Both groups found differences in recombination levels in liver when using the same TTRCre construct and tamoxifen regime. Our animals are on a mixed background derived from 129/Ola, C57BL and B6D2H and the genetic variation in our animals is therefore expected to be high. This could lead to complex interaction on a genomic level and explain the lack of recombination seen in our animals.

Although we first suspected a female bias toward successful recombination, we discarded that possibility after more extensive experimentation. After animals of both genders were exposed to different amounts of tamoxifen, we were still unable to detect anything other than low levels of recombination in our mouse livers and hepatocytes regardless of gender. Furthermore, no such gender bias is reported in the literature using a similar tamoxifen inducible Cre recombinase system in mice. The only report on gender specificity is based on skin specificity of Cre recombinase being transferred through the father rather than the mother (Ramirez et al. 2004). When females were carrying the skin specific transgene, recombination in all organs could be detected. Ramirez et al. (2004) suggested that Cre expression in late stage oocytes and persistence into the developing embryo was responsible for the recombination detected. This pattern could not be detected in our mice as recombination, if it occurred, was always liver specific.

Another possibility might be that *Ercc1* is so essential in the liver, that *Ercc1* deficient cells have a survival disadvantage. This could be especially true after tamoxifen injections, as tamoxifen has been shown to have an effect on liver, producing DNA adducts after one injection only (Han and Liehr 1992). This in combination with the defect in NER and other major repair pathways due to *Ercc1*-deficiency might be an explanation for the lack of recombination seen in our animals and hepatocytes. As shown previously, *Ercc1*- deficient animals die of liver failure at three weeks of age (McWhir et al. 1993). We did detect higher levels of apoptosis by Flow cytometry in *Ercc1* Flox/Null liver after 2 courses of tamoxifen compared to Flox/Wt injected animals (Figure 8). However, no recombination could be detected

in either of those animals. These findings could be taken to support the view that *Ercc1*- deficiency is incompatible with hepatocyte survival when further challenged with tamoxifen. However, if this was the case we would only expect it to apply to *Ercc1* Flox/Null animals, where high levels of recombination could lead to *Ercc1*-deficient hepatocytes. High levels of recombination in *Ercc1* Flox/Wt animals would produce hepatocytes with 50% of the normal levels of ERCC1 protein. This should not affect viability since *Ercc1* Wt/Null heterozygotes have normal livers and viability and high levels of recombination were not seen in either genotype.

One obvious explanation for the lack of recombination is that the TTRCre transgene is not expressed in our mice. We tried to address this issue by using Northern and Western blotting. Patterns of TTRCre transgene expression on the mRNA and protein level were inconsitent using either approach in TTRCre *Ercc1* Flox/Wt and Flox/Null animals. In addition, the results obtained were irreproducible and were therefore not included in this thesis. We can not exclude the possibility that a lack of TTRCre expression is responsible for the results obtained in this chapter. However, as only low and irreproducible levels of recombination were detected in vivo or in vitro with no consistent biological effects, we decided to switch to an approach using the loxP system in combination with an AdenoCre virus.

4. Conditional Ercc1 knockout approach using AdenoCre virus in vitro

After extensive investigation of a liver specific, tamoxifen inducible conditional knockout system using TTRCre mice, we needed another way of inducing recombination in our mice in vivo and in hepatocytes in vitro. One relatively easy way of achieving recombination of loxP sites is the use of a virus which delivers the Cre recombinase. We chose to use an Adenovirus that was derived from a human type 5, replication deficient vector with an integrated Cre recombinase from P1 (Anton and Graham 1995). The human CMV promoter, an immediate-early promoter, drives Cre recombinase expression. It has been shown that Cre recombinase is expressed in replication permissive 293 cells and non-permissive minimal residual cancer cells (MRC) cells (Anton and Graham 1995). In general, AdenoCre integrates rarely into the eukaryotic genome making it ideal for in vitro and in vivo long- term use. The AdenoCre virus was tested in murine primary hepatocyte cultures, where recombination of the Rb locus could be detected 24 hours after infection (Prost et al. 2001). In addition, Rb protein levels were undetectable 48 hours after the infection (Prost et al. 2001). Furthermore, no chromosomal abnormalities, cell death or p53 stabilisation could be detected in those cultures. However, addition of AdenoCre virus led to an increase in proliferation as measured by BrdU incorporation 48 hrs after infection. In addition, hepatocytes displayed a shortened G1 and hastened into S-phase (Prost et al. 2001). We felt that the properties of the virus along with an easy route of administration in vitro via addition to the culture medium made this approach suitable to achieve recombination of the *Ercc1* loxP sites in hepatocytes.

4.1 Detection of recombination levels via PCR and Southern blotting

For all experiments, *Ercc1* Flox/Null and Flox/Wt hepatocyte cultures were set up and infected with AdenoCre virus. In addition, uninfected Flox/Null cultures were used as controls for effect of virus.

Recombination levels were assessed in all cultures 24, 48 and 72 hrs after infection. A semi-quantitative recombination PCR was conducted on infected Flox/Wt cultures. DNA was matched by spectrophotometry and a cell line with 100% recombination was used for comparison. Strong bands were seen by PCR in all lanes, with an increase in band intensity from 24 hours after AdenoCre infection up to 72 hours post- infection (Figure 10 (A)). For further quantification of recombination in AdenoCre infected Flox/Wt cultures, a Southern blot was performed. A titration curve showing 100, 75, 50, 10 and 0 % recombination was achieved by spiking DNA from a cell line with 100% recombination with DNA from a Flox/Flox liver. All amounts of DNA were matched by spectrophotometry. Only a faint Wt band could be detected in our hepatocyte samples 24, 48 and 72 hours after AdenoCre infection, probably pointing to a certain amount of DNA degradation which would have a greater effect on the larger Wt band (Figure 10 (B)). The Southern blot indicates that recombination levels in AdenoCre infected Flox/Wt samples are very high from 24 hours after infection onwards (Figure 10 (B)). This shows that in vitro deletion of the floxed locus is achieved at an early stage after AdenoCre infection.

(A)

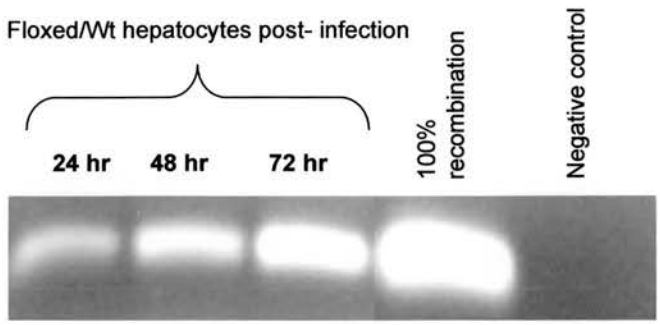

(B)

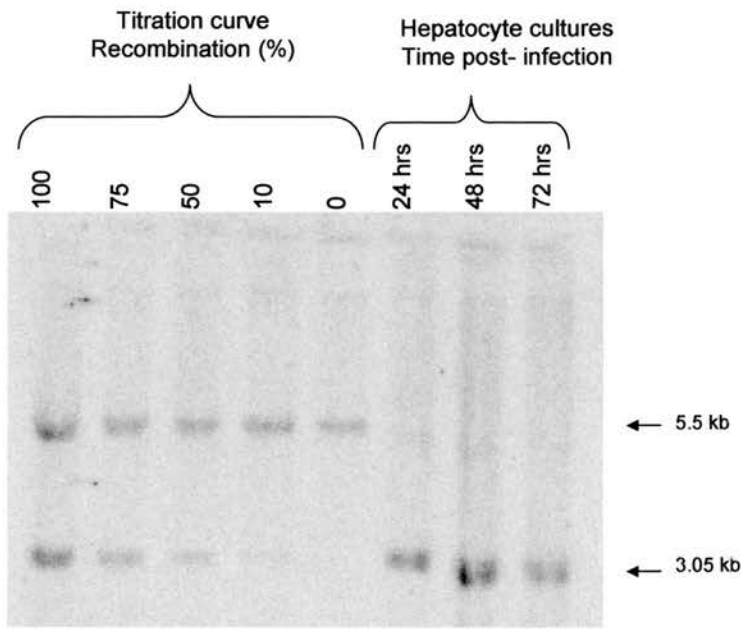

Figure 10: Recombination levels in hepatocyte cell cultures 24, 48 and 72 hours after AdenoCre virus infection. (A) Recombination PCR gel showing PCR products from Flox/Wt hepatocytes and from a cell line with 100% recombination for comparison. The amounts of DNA were matched by spectrophotometry. The negative control contained water only. (B) Southern blot showing recombination in AdenoCre infected Flox/Wt hepatocyte cultures. DNA amounts were matched by spectrophotometry. A titration curve was obtained by spiking DNA from a cell line with 100% recombination with Flox/Flox liver DNA. Samples were taken 24, 48 and 72 hours after AdenoCre infection and show high levels of recombination.

4.2 Determination of protein levels via western blotting

ERCC1 protein levels were determined in Flox/Null hepatocyte cultures 24, 48 and 72 hours after AdenoCre infection using western blotting. *Ercc1* Wt/Wt, Null/Null livers and an uninfected Flox/Null hepatocyte sample were used as controls. ERCC1 protein was visible as a 33 kDa band in our western blot in Wt liver and in the uninfected Flox/Null control (Figure 11). In addition, a complete lack of protein could be seen in *Ercc1*- deficient liver. A reduction of ERCC1 protein levels was visible in Flox/Null hepatocytes 48 hours after AdenoCre infection, with a complete lack of the protein 72 hrs after infection. A cross- reacting band was detected in all lanes, irrespective of genotype or treatment. In conclusion, the recombination of the *Ercc1* locus in Flox/Null mice led to ERCC1 protein levels being reduced with a complete lack of the protein after 3 days in culture. Our cell culture system could now be used to further determine the consequences of *Ercc1*- deficiency in hepatocytes in vitro.

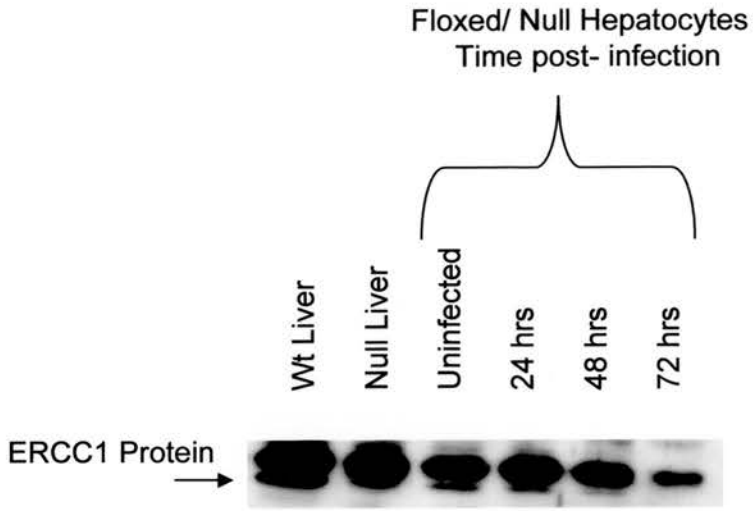

Figure 11: Western blot determining ERCC1 protein levels after AdenoCre virus infection. Flox/Null hepatocyte cultures are shown 24, 48 and 72 hours after infection. Protein content of one uninfected Flox/Null culture is shown for comparison. The positive control represents Wt ERCC1 liver and the negative control represents ERCC1- deficient liver. A non- specific cross reacting band can be seen just above the 33 kDa ERCC1 protein band in all lanes irrespective of genotype and is used as loading control. Amounts of protein were matched, but with the 72 hour time point being slightly underloaded.

4.3 Feulgen staining to assess the amount of apoptotic, necrotic and normal cells in culture

Feulgen staining was performed to distinguish between apoptotic, necrotic and normal cells in AdenoCre infected Flox/Wt and Flox/Null and in uninfected Flox/Null hepatocyte cultures (Figure 12).

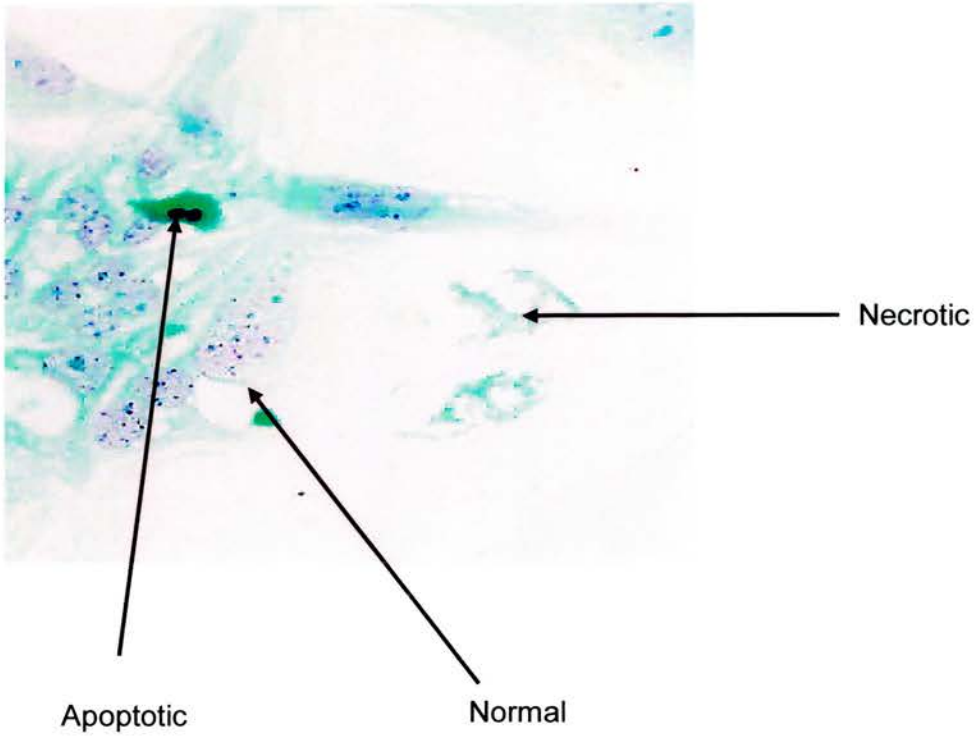

Figure 12: Apoptotic, necrotic and normal hepatocytes in AdenoCre virus infected Flox/Null cultures. Hepatocytes were Feulgen stained and a picture taken with a 20x objective. Arrows point to the different types of cell which are labelled accordingly.

500 cells were counted in duplicate cultures 1, 2, 5 and 7 days after AdenoCre infection. The mean frequency from two independent experiments is given along with the standard error of the mean (Figure 13). There was a trend towards an increase in the frequency of necrotic cells with increased time in culture, but this was not correlated with genotype or viral infection. One day after AdenoCre infection no differences in the frequency of apoptotic cells between samples could be detected. However, from day 2 onwards, the levels of apoptosis rose and were higher in infected Flox/Null cultures compared to infected Flox/Wt and uninfected Flox/Null (Figure 13). The p values below are for the null hypothesis that there was no difference between levels of apoptosis in infected Flox/Null and infected Flox/Wt or uninfected Flox/Null cultures by a χ^2 test.

Day 1: Infected Flox/Null 5.1 %; infected Flox/Wt 5.8 % ($p= 0.92$); uninfected Flox/Null 3.8 % ($p= 0.19$)

Day 2: Infected Flox/Null 9.8 %; infected Flox/Wt 5 % ($p= 0.0008$); uninfected Flox/Null 3.3 % ($p= 0.00002$)

Day 5: Infected Flox/Null 23 %; infected Flox/Wt 6.6 % ($p< 0.000001$); uninfected Flox/Null 11.8 % ($p< 0.000001$)

Day 7: Infected Flox/Null 34.3 %; infected Flox/Wt 9 % ($p< 0.000001$); uninfected Flox/Null 9.1 % ($p< 0.000001$)

At 7 days post- infection 34.3 % of cells in infected Flox/Null cultures were apoptotic, more than 3- fold higher than in corresponding infected Flox/Wt and uninfected Flox/Null cultures. In conclusion, levels of apoptosis increased with time in culture from 2 days to 7 days post- infection in Flox/Null hepatocytes and were significantly higher than in infected Flox/Wt and uninfected Flox/Null cultures.

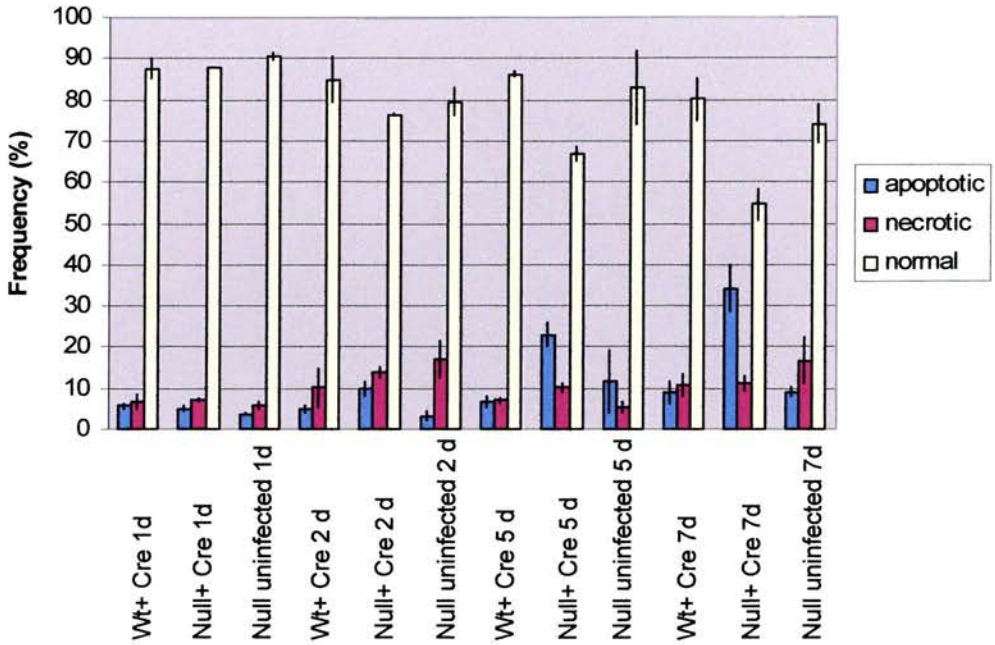

Figure 13: Apoptotic and necrotic cell death in AdenoCre virus infected hepatocyte cultures. Infected *Ercc1* Flox/Wt, Flox/Null and uninfected Flox/Null hepatocyte cultures were scored 1, 2, 5 and 7 days after infection. For each culture 500 Feulgen stained cells were counted in two separate chambers. Data shown represent the mean of two different experiments. The SEM is indicated with error bars. All values are expressed as percentage of counted cells.

4.4 Identification of DNA content via flow cytometry

DNA content was measured using flow cytometry at different time points after infection and in different experiments. Apoptosis levels, S-phase as well as ploidy changes were monitored. All results are summarised in Table 4. Uninfected Flox/Null and Flox/Wt hepatocytes showed low levels of S-phase and apoptosis before plating. Diploid, tetraploid and a small population of octaploid cells could be detected in both genotypes before plating (Table 4 group 6 and 9). However, after plating and AdenoCre infection, the amount of cells in S-phase and undergoing apoptosis increased independent of time point. Feulgen staining detected significantly increased levels of apoptosis in infected Flox/Null hepatocyte cultures compared to the two controls. While a similar elevation was observed by flow cytometry in some experimental groups (7 and 8), this was not a consistent overall finding. Viral infection, irrespective of genotype, resulted in an increase in levels of S-phase in some groups (2, 3, 8, 11, 12), but again this was not a consistent finding. No clear difference in ploidy status could be observed between infected Flox/Null cultures and both controls over time. This differs from the higher ploidy seen in the livers of *Ercc1*- deficient animals compared to controls (McWhir et al. 1993).

Table 4: DNA content of AdenoCre infected hepatocyte cell cultures as determined by flow cytometry. Flox/Wt, Flox/Null and uninfected (uninf.) Flox/Null hepatocyte cultures are shown before plating and 2, 3, 4, 5 and 7 days after infection. Apoptosis is displayed as percent of all cells. Ploidy status and S-phase are shown as percent of viable cells. Data from 4 different experiments are shown.

Exp. (#)	Group (#)	Sample	Time (days)	2n (%)	4n (%)	8n (%)	16n (%)	Apoptosis (%)	S-phase (%)
1	1	Flox/Wt+Cre	2	32.8	30.4	3.4		14.5	13.3
		Flox/Null+Cre	2	32.8	23.9	3.8		11.4	17.2
	2	Flox/Wt+Cre	3	23.8	27	2.9		20.1	17.5
		Flox/Null+Cre	3	25.6	28.2	5.2		15.4	15.7
		Flox/Null uninf.	3	42	32	1.5		13.5	8.4
	3	Flox/Wt+Cre	7	11.9	29.4	16.1		13.8	13.9
		Flox/Null+Cre	7	12.2	20.6	16.2	3.5	13.8	13.8
		Flox/Null uninf.	7	38	41.9	1.7		7.2	7.7
2	4	Flox/Wt+Cre	2	40	33.2	4.4		7.3	8.6
		Flox/Null+Cre	2	21.9	21.2	8.4		32.8	12.8
	5	Flox/Wt+Cre	5	25.6	37.9	9.3		6.8	10.1
		Flox/Null+Cre	5	14.7	19.7	11.1		23	16.5
		Flox/Null uninf.	5	17.2	26.4	7.4		25	13.4
3	6	Flox/Wt+Cre	0	46.5	38.7	11.8		0.1	1
		Flox/Null+Cre	0	51.6	27.3	8.6		0.1	1.3
	7	Flox/Wt+Cre	2	24.5	36	10.5		3	10.2
		Flox/Null+Cre	2	27.9	31.5	8.5		10.4	13.5
		Flox/Null uninf.	2	30.8	33.7	13.1		4.6	10.5
	8	Flox/Wt+Cre	5	12.6	22.6	17		3.5	17.9
		Flox/Null+Cre	5	15.7	12.5	7		14.6	24.8
		Flox/Null uninf.	5	18.9	40.6	12.1		3	12.2
4	9	Flox/Wt+Cre	0	45.6	15.4	12.8		0.3	3.6
		Flox/Null+Cre	0	38.1	34.6	8.7		1.1	2.3
	10	Flox/Wt+Cre	2	54.5	30.1	2.4		1.3	6.4
		Flox/Null+Cre	2	32.9	43.3	6.9		1.3	5.8
		Flox/Null uninf.	2	35.1	37.9	5		1.7	7.8
	11	Flox/Wt+Cre	3	41.2	25.2	2.8		2.9	16.1
		Flox/Null+Cre	3	26.6	27.2	4.8		3.2	16.4
		Flox/Null uninf.	3	32	36.1	6.9		1.7	8.1
	12	Flox/Wt+Cre	4	36.8	38.9	6.2		1.6	9.9
		Flox/Null+Cre	4	29.8	40.2	7.5		2.4	14.1
		Flox/Null uninf.	4	44.6	42.7	2.9		1.3	5.8
	13	Flox/Wt+Cre	5	28.6	36.8	7.6		2.3	9.6
		Flox/Null+Cre	5	26.5	33.5	7.6		2.4	13.5
		Flox/Null uninf.	5	25.9	24.5	3.7		3.7	21.5
	14	Flox/Wt+Cre	7	25.7	42.8	11.1		1.2	7.5
		Flox/Null+Cre	7	30.7	32.8	7.4		3.2	13.2
		Flox/Null uninf.	7	34.9	39.4	5.7		2	8.6

4.5 Frequencies of mono- and binucleate cells in vitro

Binucleation is a normal part of liver development with reduced levels of binucleation being apparent in *Ercc1*- deficient liver (Nunez et al. 2000). The ratio of mononucleate and binucleate cells was assessed in all AdenoCre infected Flox/Null and Flox/Wt cultures and in uninfected Flox/Null hepatocytes. Cells were stained and 500 cells were counted in duplicate cultures 2, 5 and 7 days after infection. No difference in the mononucleate to binucleate ratio could be seen between the three cultures. Around 80% of hepatocytes were already binucleate after 2 days in culture (Figure 14). The amount of binucleate cells did not change with time in culture in any of the genotypes. This differs from the lower frequencies of binucleate cells observed in *Ercc1*- deficient livers when compared to Wt littermates (Nunez et al. 2000).

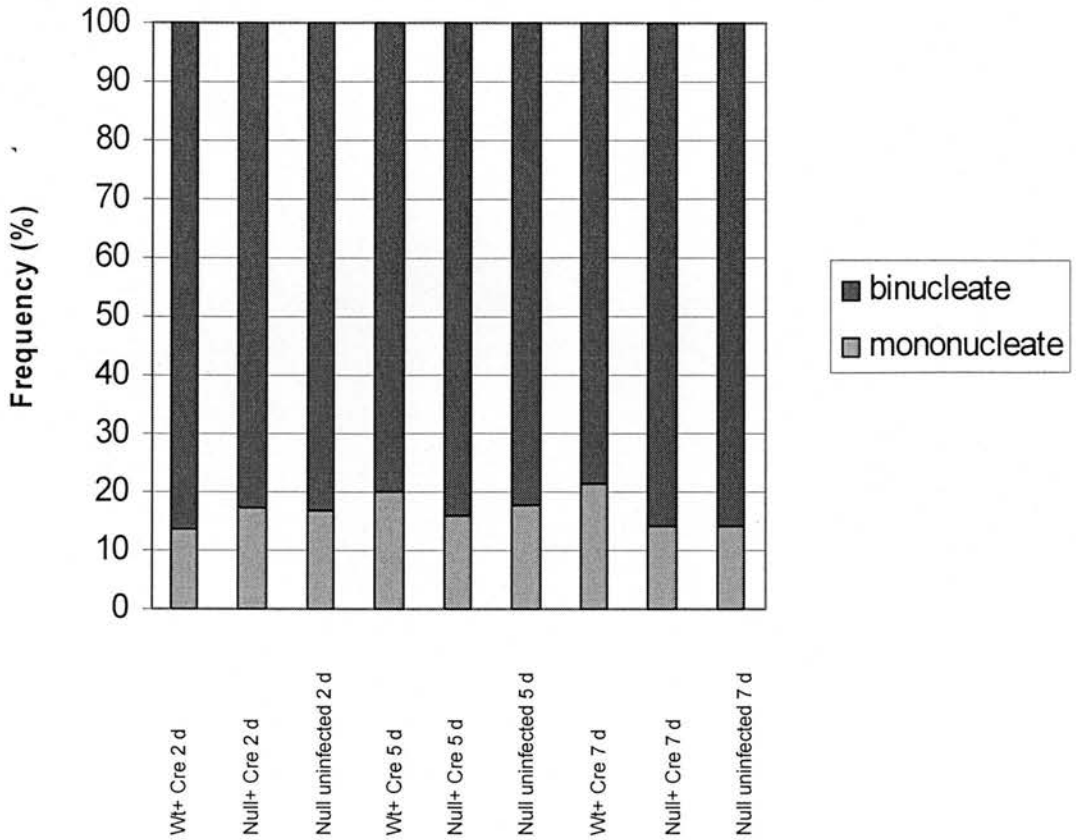

Figure 14: Frequency of binucleate and mononucleate cells in infected hepatocyte cultures. Hepatocytes were scored 2, 5 and 7 days (d) after plating. 1000 cells of AdenoCre infected Flox/Wt, Flox/Null and uninfected Flox/Null cultures were counted for each genotype.

4.6 Measurement of ^{3}H- Thymidine incorporation to determine replication potential

To estimate the amount of replication in our Flox/Null and Flox/Wt cultures ^{3}H-Thymidine (^{3}H- Thd) incorporation was measured 1, 2, 3, 4 and 5 days after AdenoCre infection in duplicate cultures. In addition, ^{3}H-Thymidine incorporation was determined in uninfected Flox/Null cultures at the same time points. Lower levels of replication were apparent in uninfected Flox/Null cultures at all time points (Figure 15). Infected Flox/Wt cultures showed a peak of ^{3}H-Thymidine incorporation 3- 4 days after infection. Levels of incorporation were lower at the equivalent stage in infected Flox/Null cultures, but the high level of variability for each genotype meant that this difference was not significant.

Furthermore, BrdU incorporation was measured in culture using immunohistochemistry. The uninfected Flox/Null cultures always showed few labelled nuclei compared to the infected Flox/Null and Flox/Wt cultures which had similar staining frequencies. No clear difference in amount of stained nuclei could be established between the two infected genotypes (data not shown).

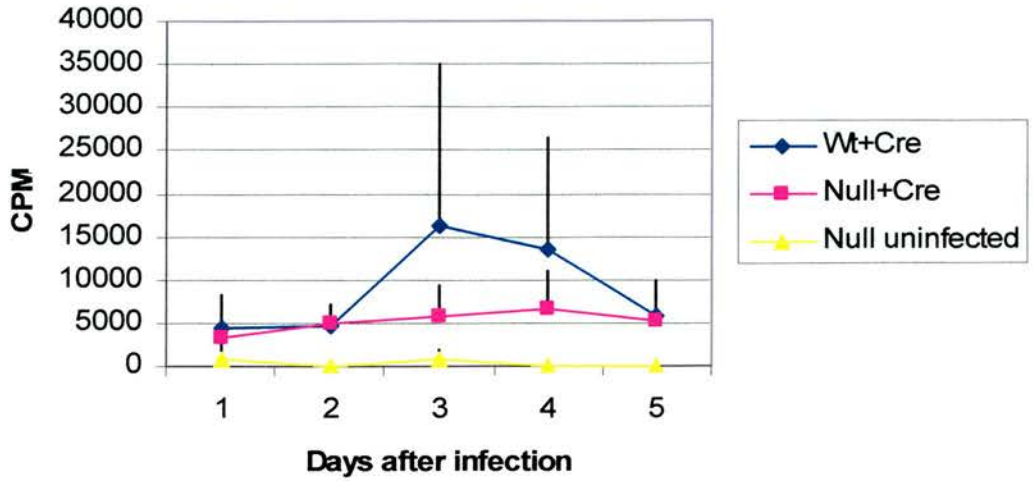

Figure 15: ^{3}H-Thymidine incorporation in AdenoCre infected hepatocyte cultures.

^{3}H-Thymidine incorporation was measured as counts per minute (CPM) in infected Flox/Wt, Flox/Null and uninfected Flox/Null hepatocyte cultures 1, 2, 3, 4 and 5 days after infection. All samples were counted three times. Data shown represent the mean of three different experiments. The SEM is given for all data points.

4.7 Assessment of oxidative damage in vitro using the comet assay

The comet assay is an assay primarily examining the levels of oxidative lesions and DNA strand breaks (Wheelhouse et al. 2003). DNA migration is measured as a function of size and number of broken ends of DNA which is expressed as the Olive tail moment. The amounts of oxidative damage and strand breaks were assessed in AdenoCre infected Flox/Wt and Flox/Null cultures 1 day after infection (Figure 16). Infected Flox/Null hepatocytes exhibited a mean and standard deviation of 23.6 % ± 13.6 tail DNA compared to 29.7% ± 17.6 in Flox/Wt without addition of enzyme. A paired t-test revealed a just significant difference between AdenoCre infected Flox/Wt and Flox/Null cultures ($p=0.049$), indicating, counterintuitively, more accumulation of damage in infected Flox/Wt compared to Flox/Null hepatocyte cultures. The enzyme formamidopyrimidine- DNA- glycosylase (Fpg) is known to recognise and process a variety of oxidative DNA adducts, leading to strand breaks which can then be detected in the comet assay. When Fpg was added to both preparations, infected Flox/Null hepatocytes showed a mean and standard deviation of 31.2% ± 13.5 tail DNA and Flox/Wt cells a mean and standard deviation of 28.9% ± 19 of tail DNA. No significant difference could be detected between the two genotypes after treatment with enzyme when a paired t-test was performed ($p= 0.48$). Comparison of genotypes at later time points did not reveal a difference between the genotypes (data not shown). In conclusion, there was no evidence for elevated levels of oxidative DNA damage in infected Flox/Null cultures.

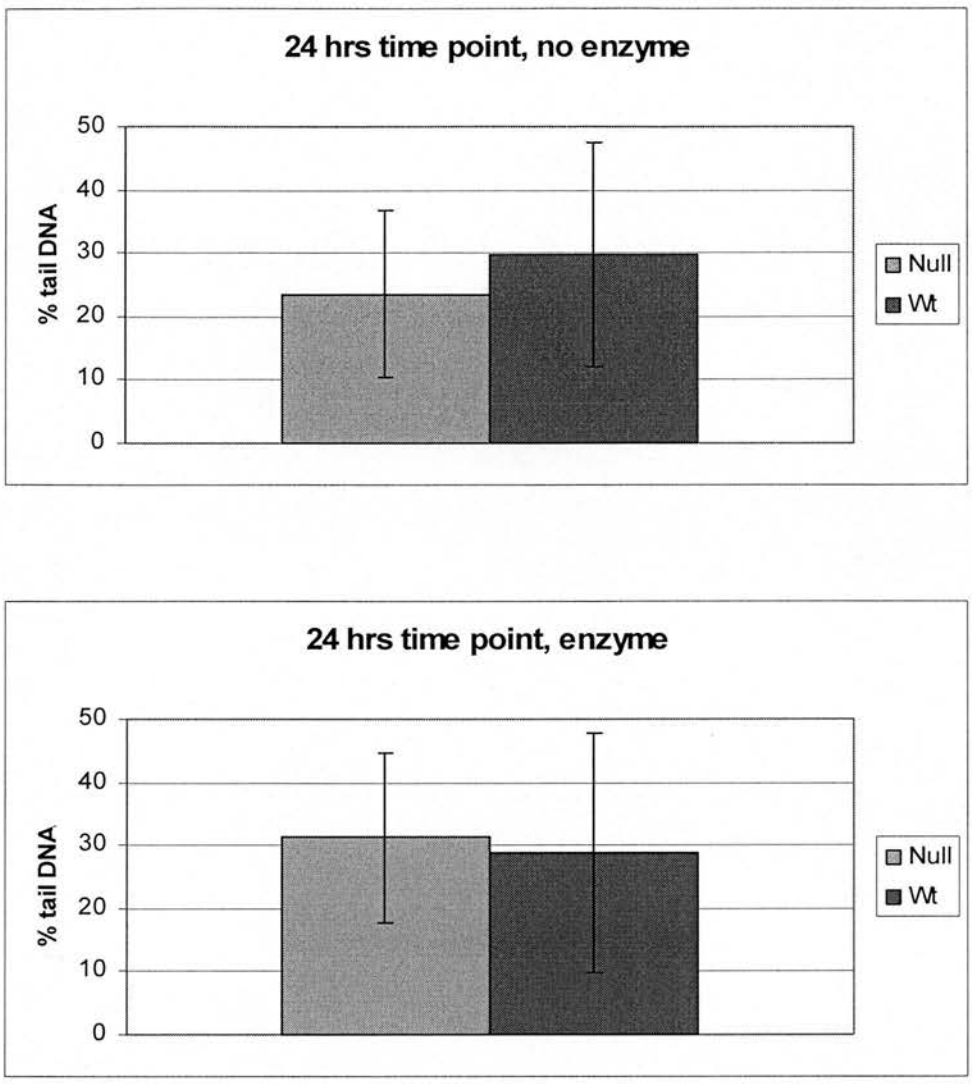

Figure 16: Comet analysis in AdenoCre infected hepatocyte cultures. The percentage of tail DNA in infected *Ercc1* Flox/Wt and Flox/Null hepatocyte cultures was scored 24 hours after infection. Data shown represent both genotypes with and without addition of the Fpg enzyme. The mean of 50 counted comets is given. The standard deviation is indicated by error bars.

4.8 Oil Red O stain to visualise lipid accumulation in hepatocyte cultures

AdenoCre infected Flox/Null and Flox/Wt and uninfected Flox/Null hepatocytes were stained with Oil Red O for lipid detection 5, 7 and 9 days after infection.

Lipid accumulation increased gradually in *Ercc1*- deficient cultures from day 5 after infection with higher levels at days 7 and 9. Much lower levels of lipid were detected in both control cultures and then only from day 7 onwards (Figure 17). When the pattern of lipid accumulation in primary hepatocyte cultures was examined at higher power, it was observed that AdenoCre infected Flox/Null cultures contained many microvesicles accumulating throughout the cytoplasm compared with fewer microvesicles in both controls (Figure 18).

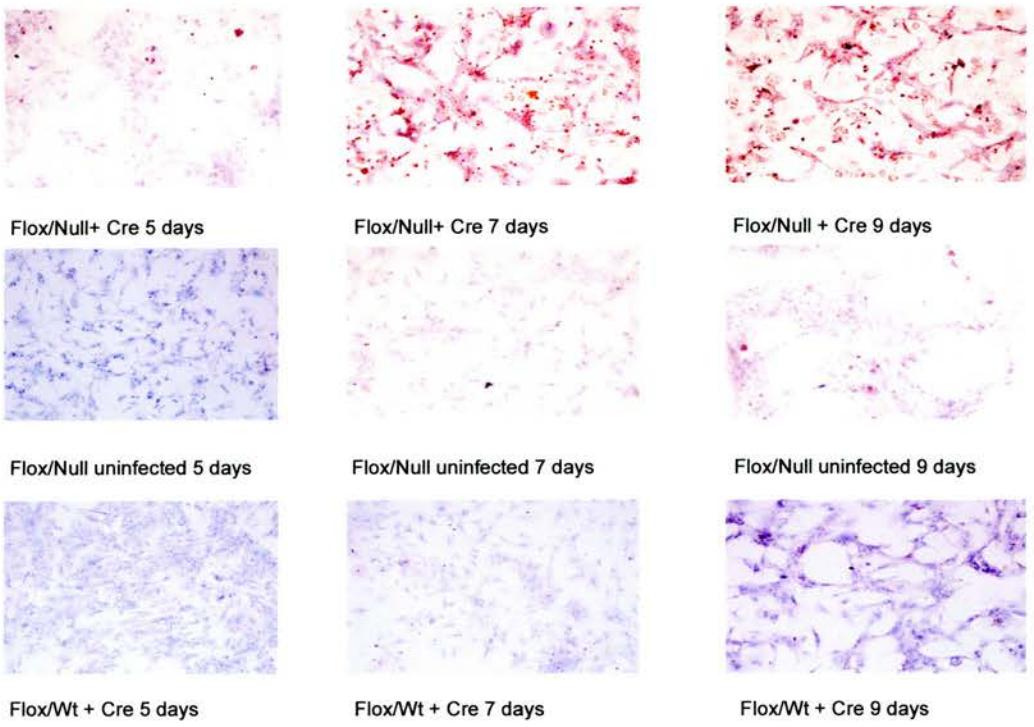

Figure 17: Lipid accumulation in AdenoCre infected hepatocyte cultures. Infected *Ercc1* Flox/Wt, Flox/Null and uninfected Flox/Null hepatocyte cultures were stained with Oil Red O 5, 7 and 9 days after plating. Images taken with a 10x objective show the amount of lipid accumulation overall. Lipid vesicles are stained in red and cytoplasm and nuclei are stained in blue. Round apoptotic cells stain intensely red.

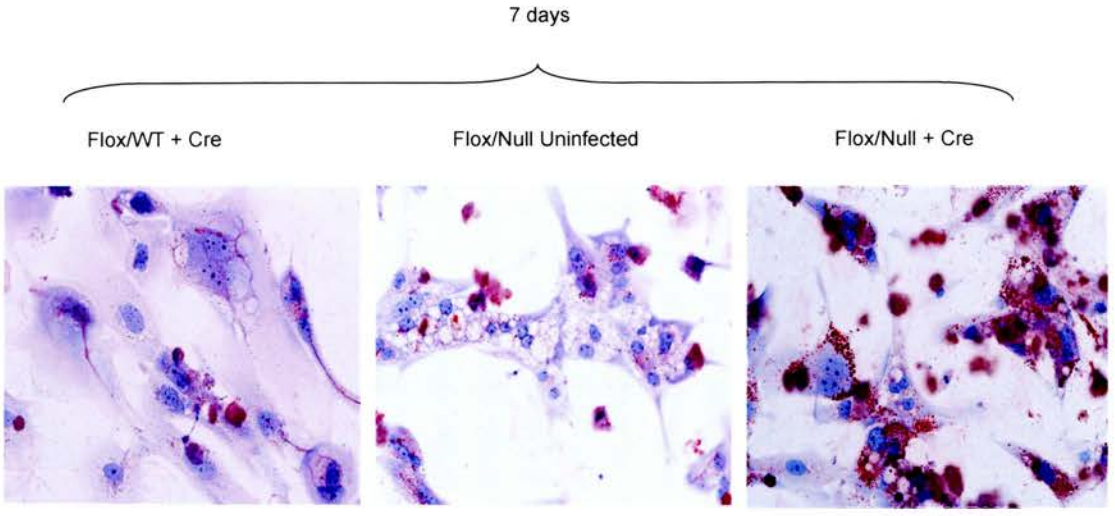

Figure 18: Detail of lipid accumulation in AdenoCre infected hepatocytes. Infected *Ercc1* Flox/Wt, Flox/Null and uninfected Flox/Null hepatocyte cultures were stained with Oil Red O 7 days after plating. The 40x objective highlights the small droplets of lipid accumulated in infected Flox/Null cultures. Lipid vesicles are stained in red and cytoplasm and nuclei are stained in blue. Round apoptotic cells stain intensely red.

4.9 Feulgen staining to assess apoptotic, necrotic and normal cells after UV irradiation, Glucose oxidase and Mitomycin C treatment

AdenoCre infected Flox/Wt and Flox/Null and uninfected Flox/Null hepatocyte cultures were challenged with UVC, Glucose oxidase and Mitomycin C to examine their impact on cell status. 3 days after infection, cells were challenged with different doses of the damaging agents and Feulgen staining was performed 2 days later. 500 cells were counted in duplicate cultures. The mean and standard error of the mean of two different experiments is shown for UVC (Figure 19) and Glucose oxidase (Figure 20). A single experiment for Mitomycin C exposure is shown in Figure 21.

UVC irradiation- induced DNA damage is repaired by the nucleotide excision repair pathway which is abrogated in infected Flox/Null cultures. In infected Flox/Null cultures, apoptosis increased with UV dose and, at all doses, levels of apoptosis were significantly higher in infected Flox/Null cultures when compared to the two controls (Figure 19). The p values below are for the null hypothesis that there was no difference between levels of apoptosis in infected Flox/Null and infected Flox/Wt or uninfected Flox/Null cultures by a χ^2 test.

$2J/m^2$: infected Flox/Null 4.5 %; infected Flox/Wt 1.7 % ($p< 0.000001$); uninfected Flox/Null 3.3 % ($p= 0.00005$)

$10J/m^2$: infected Flox/Null 11.2 %; infected Flox/Wt 6 % ($p= 0.0059$); uninfected Flox/Null 4.1 % ($p= 0.0011$)

$20J/m^2$: infected Flox/Null 21.8 %; infected Flox/Wt 4.8 % ($p< 0.000001$); uninfected Flox/Null 7.2 % ($p< 0.000001$)

$50J/m^2$: infected Flox/Null 66.5 %; infected Flox/Wt 15.5 % ($p< 0.000001$); uninfected Flox/Null 39.6 % ($p< 0.000001$)

Levels of necrosis were low for all samples. At $20J/m^2$ 21.8 % of cells in infected Flox/Null cultures were apoptotic, more than 3- fold higher than in corresponding infected Flox/Wt and uninfected Flox/Null cultures. In conclusion, significantly higher levels of UV- induced apoptosis were observed in infected Flox/Null hepatocyte cultures when compared to controls.

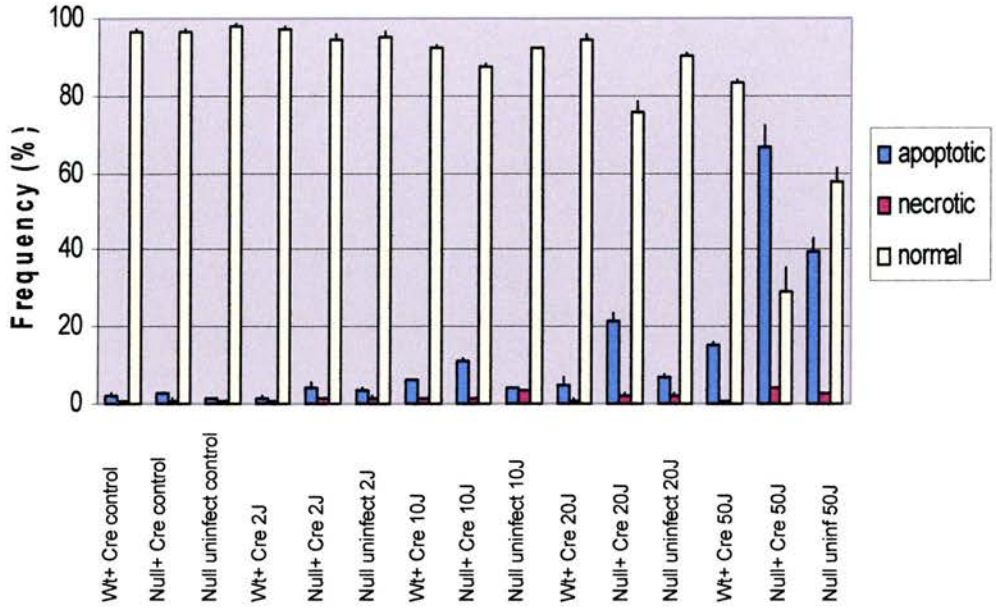

Figure 19: Apoptotic and necrotic cell death in AdenoCre virus infected hepatocyte cultures after UVC. Infected *Ercc1* Flox/Wt, Flox/Null and uninfected Flox/Null hepatocyte cultures were scored 2 days after UVC irradiation. The doses of UVC varied from 2 J/m^2 to 50 J/m^2. Non- irradiated controls are shown for all genotypes. For each culture 500 cells were Feulgen stained and counted in two separate chambers. Data shown represent the mean of two different experiments. The SEM is indicated with error bars.

Glucose oxidase is a potent oxidative damage inducer. Some forms of oxidative DNA damage are repaired by the nucleotide excision repair pathway which is abrogated in infected Flox/Null cultures. Infected, untreated Flox/Null hepatocytes showed higher levels of apoptosis when compared to infected, untreated Flox/Wt ($p=0.00004$) and uninfected, untreated Flox/Null cultures ($p=0.02$). This is in accordance with our previous findings examining spontaneous levels of apoptosis in *Ercc1*- deficient cultures when compared to controls. In infected Flox/Null cultures, apoptosis increased with GO dose and, at low doses, levels of apoptosis were significantly higher in infected Flox/Null cultures when compared to the two controls (Figure 20). The p values below are for the null hypothesis that there was no difference between levels of apoptosis in infected Flox/Null and infected Flox/Wt or uninfected Flox/Null cultures by a χ^2 test.

1μU GO: infected Flox/Null 11.7 %; Flox/Wt 1.2 % ($p< 0.000001$); uninfected Flox/Null 3.9 % ($p= 0.000002$)

5 μU GO: infected Flox/Null 15 %; Flox/Wt 1.6 % ($p< 0.000001$); uninfected Flox/Null 8.1 % ($p= 0.00052$)

10μU GO: infected Flox/Null 18.2 %; Flox/Wt 2.6 % ($p< 0.000001$); uninfected Flox/Null 10.2 % ($p= 0.00028$)

50 μU GO: infected Flox/Null 23.5 %; Flox/Wt 5.3 % ($p< 0.000001$); uninfected Flox/Null 17 % ($p= 0.015$)

100 μU GO: infected Flox/Null 28.7 %; Flox/Wt 18.1 % ($p= 0.00012$); uninfected Flox/Null 22.7 % ($p=0.086$)

Levels of necrosis were low in all samples. At a dose of 1 μU GO 11.7% of infected Flox/Null hepatocytes were apoptotic, 3- fold higher than in corresponding infected Flox/Wt and uninfected Flox/Null cultures. In conclusion, at low levels of GO, significantly higher levels of GO- induced apoptosis could be detected in infected Flox/Null hepatocyte cultures when compared to controls.

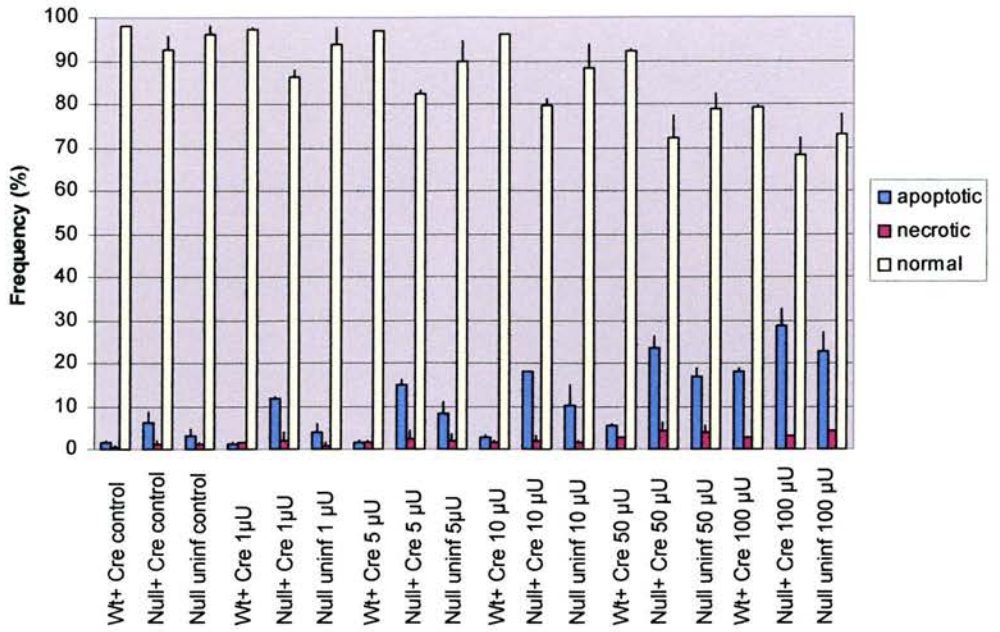

Figure 20: Apoptotic and necrotic cell death in AdenoCre virus infected hepatocyte cultures after Glucose oxidase exposure. Infected *Ercc1* Flox/Wt, Flox/Null and uninfected Flox/Null hepatocyte cultures were scored 2 days after treatment with GO. The doses given varied from 1µU to 100 µU. Untreated controls are shown for all genotypes. For each culture 500 cells were Feulgen stained and counted in two separate chambers. Data shown represent the mean of two different experiments. The SEM is indicated with error bars.

Ercc1 is involved in the repair of interstrand cros- links. A wide range of doses of Mitomycin C (MMC), an interstrand cross- link inducer, was tested on hepatocyte cultures, but no difference in MMC- induced cell death was detected (Figure 21). At doses above 1 μg Mitomycin C, all hepatocytes showed 5-10% of necrosis, independent of genotype or treatment. Doses higher than 10 μg resulted in high amounts of cell death in all genotypes (data not shown).

We further tried to characterise the impact of all three damaging agents by determining the DNA content of all cultures by flow cytometry. No significant difference in ploidy could be observed after exposure to the different DNA damaging agents and between the different genotypes (data not shown).

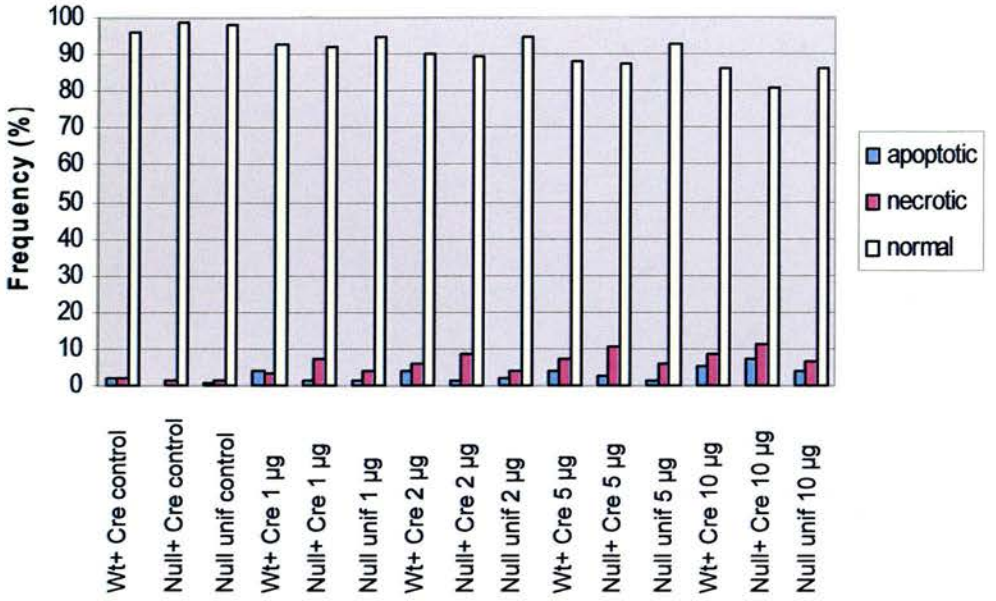

Figure 21: Apoptotic and necrotic cell death in AdenoCre virus infected hepatocyte cultures after Mitomycin C exposure. Infected *Ercc1* Flox/Wt, Flox/Null and uninfected Flox/Null hepatocyte cultures were scored 2 days after treatment with MMC. The doses of Mitomycin C varied from 1 µg to 10 µg. Untreated controls are shown for all genotypes. For each culture 1000 cells were Feulgen stained and counted in two separate chambers.

4.10 Oil Red O stain to visualise lipid accumulation after UV irradiation

Previously, we had observed lipid accumulation only in old, infected Flox/Null cultures. However, when hepatocytes were treated with $10J/m^2$ of UVC, we noticed a change in lipid accumulation pattern in all cultures. Therefore, AdenoCre infected Flox/Null and Flox/Wt and uninfected Flox/Null hepatocytes were stained with Oil Red O 5 and 7 days after infection, which equated to 2 and 4 days after UVC irradiation. Non- irradiated cultures of all genotypes were used for comparison. Exposure to UVC led to accumulation of lipids in all genotypes 5 days after infection (Figure 22). Lipid accumulation in Flox/Null uninfected cultures and in infected Flox/Wt hepatocyte cultures was subsequently reduced 7 days after infection. As most infected Flox/Null hepatocytes had undergone apoptosis, I was unable to stain those cells at the same time point. Control dishes showed lipid accumulation in older, infected Flox/Null hepatocytes only as seen previously. In conclusion, it seems that lipid accumulation in hepatocytes is a consequence of DNA damage and disappears with time when functional DNA repair mechanisms are present.

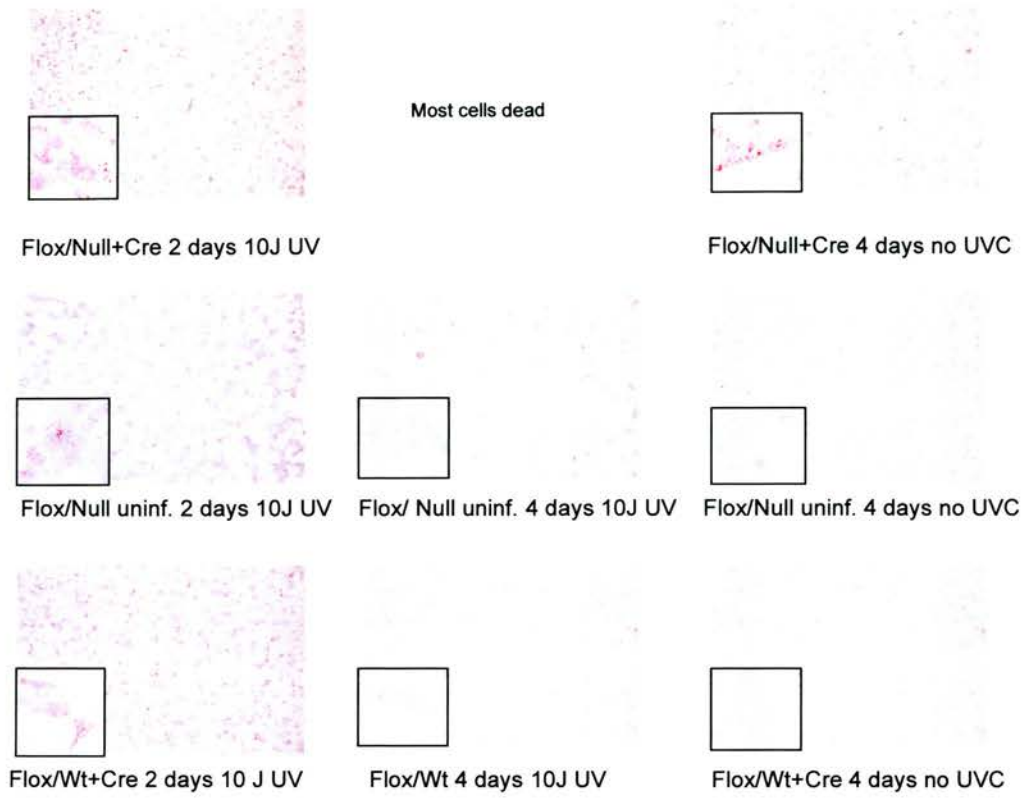

Figure 22: Lipid accumulation in AdenoCre infected, UVC- irradiated hepatocyte cultures. Infected *Ercc1* Flox/Wt, Flox/Null and uninfected Flox/Null hepatocyte cultures were stained with Oil Red O. 2 and 4 days after 10 J/m^2 UVC. Non- irradiated controls are shown for all genotypes 4 days after irradiation. The objective used was 10x with an inset picture taken with a 40x objective showing the pattern of lipid stain in more detail. No picture was obtained for AdenoCre infected Flox/Null cultures 4 days after UVC as the majority of cells were dead.

4.11 Discussion

Most hepatocytes contain polyploid nuclei, in which recombination can be efficiently induced by the AdenoCre virus without leading to any major abnormalities in the hepatocyte cultures. However, Addison et al. (1997) have shown that the human CMV promoter is less effective in murine cells when compared to its effect on human cells. Given the recombination efficiency observed by Prost et al. (2001) in floxed *Rb* mouse hepatocytes along with the rapid disappearance of protein, using this AdenoCre virus to induce recombination of the floxed *Ercc1* locus should be achieved easily. In fact, when recombination efficiency was determined in vitro, recombination could be readily detected 24 hours after AdenoCre infection, with the amount of recombination being around 90%. Using the human CMV promoter did not lead to any complications with recombination efficiency in our system. Furthermore, ERCC1 protein could no longer be detected 72 hours after AdenoCre infection, proving that recombination of the loxP sites in *Ercc1* Flox/Null and Flox/Wt hepatocytes does result in downregulation of ERCC1 protein.

To investigate basic parameters of *Ercc1*- deficiency in AdenoCre infected hepatocyte cell cultures, replication potential was examined at different time points after AdenoCre administration. In vivo, hepatocytes do not replicate unless stimulated by hepatic toxins such as carbon tetrachloride where a peak of DNA synthesis can be observed 60 hours after insult (Bellamy et al. 1997). In *Ercc1*-deficient liver, an indication of lower BrdU incorporation was detected when compared to Wt, although this finding was not statistically significant (Nunez et al. 2000). In vitro, however, replication is less rare as the perfusion itself seems to trigger DNA synthesis in cultured hepatocytes forcing the cells from a quiescent stage into proliferation (Bellamy et al. 1997). I found that uninfected *Ercc1* Flox/Null hepatocyte cultures showed very low levels of ^{3}H- Thd incorporation overall, indicating low levels of replication. In contrast, in infected *Ercc1* Flox/Null

and Flox/Wt hepatocytes cultures higher levels of ^{3}H- Thd incorporation were detected. No difference between the infected genotypes was established, indicating that the addition of AdenoCre virus rather than the perfusion event is responsible for triggering replication in my cell culture system. These findings are further supported by the fact that uninfected Flox/Null hepatocytes did not stain for BrdU whilst *Ercc1* Flox/Null and Flox/Wt cultures showed high amounts of BrdU stain after AdenoCre infection. The stain intensities varied from nucleus to nucleus, but not between genotypes. In accordance with my findings, when BrdU incorporation and ^{3}H-Thd incorporation was measured in mouse liver at different time points after toxic insult, no difference in labelling index or intensity of stain could be noted, leading to the conclusion that both methods are interchangeable (Lanier et al. 1989,

Eldridge et al.1990). In conclusion, there was no evidence that replication was affected in infected Flox/Null cultures compared to the infected Flox/Wt controls.

Binucleation is a normal feature of liver development, leading to a majority of binucleate cells with age (Sheahan et al. 2004). Binucleation in *Ercc1*- deficient liver has, however, been demonstrated to be inhibited (Nunez et al. 2000). This finding could not be confirmed in cultures as most hepatocytes were already binucleate 2 days after plating. The rapid binucleation in vitro could be a result of cell fusion or DNA replication without cytokinesis. The perfusion process itself and culture methods could encourage binucleation and diminish the difference between *Ercc1*-deficient cells and Wt hepatocytes. In addition, Mossin et al. (1994) have shown that the addition of growth hormones such as EGF can induce binucleation in vitro. Nunez et al. (2000) studied binucleation in 2-3 week old *Ercc1*- deficient animals. In contrast, animals used for cell culture experiments were 6-8 weeks old. As binucleation is a feature of older livers, high amounts of binucleate hepatocyte nuclei in vitro when compared to in vivo results could be explained by the discrepancy in age between animals used.

Polyploidisation is a general physiological process seen in all cell types in mammals, insects and plants (Comai 2005). By providing duplicated genes, polyploidisation

might fuel long- term diversification and evolutionary success. It is thought to be a protective mechanism against deleterious recessive mutations when a bottleneck population is apparent and is also thought to be a response to immediate DNA damage when repair is impaired (Comai 2005, Mc Whir et al. 1993). In hepatocytes polyploidisation is part of the normal maturation process and is associated with late foetal development (Gupta 2000). Mature hepatocytes display higher levels of ploidy, increasing cell size and accumulation of lipofuscin and other lipid peroxidation products (Gupta 2000). In addition, p21 accumulation has been noted in senescent hepatocytes (Sigal et al. 1999). This hypertrophic change could be mimicked in vitro when the appropriate growth hormones were added to the cultures (Gupta 2000). In general, external stimuli seem to induce polyploidisation. Mossin et al. (1994) noted that an increase in ploidy is correlated with a decrease in proliferation in vitro independent of mitogenic stimuli.

These findings have been confirmed in vivo, where diseased liver is associated with a decrease in DNA synthesis and an increase in the polyploid hepatocyte fraction (Gupta 2000). It is generally hypothesised that polyploidy arises when DNA synthesis is completed without cell division or cytokinesis (Gupta 2000). In fact, Guidotti et al. (2003) showed that binucleation is an intermediate step to higher ploidy status in vitro. When primary rat hepatocyte cultures were examined, it was established that about 20% of diploid, binucleate cells aborted cytokinesis after progression through S-phase to form tetraploid, mononucleate cells.

Polyploidisation is one of the most striking features of *Ercc1*- deficient liver. Before dying of liver failure at the age of 3 weeks, *Ercc1*- deficient mice have equivalent levels of polyploidy to that normally seen only in 2 year old, normal adults (McWhir et al. 1993). This polyploidy could not be observed in infected *Ercc1* Flox/Null when compared to infected Flox/Wt hepatocytes. One of the factors responsible might be the limited survival rate in culture not leaving enough time to establish octaploidy in primary hepatocytes. Another reason for similar levels of polyploidy in AdenoCre infected Flox/Null and Flox/Wt hepatocytes could be the addition of virus and the

subsequent stimulation of replication in all cultures. The artificial culture environment might also be responsible for the absence of polyploidy in AdenoCre infected Flox/Null hepatocytes, not providing all essential stimuli needed for polyploidisation. In conclusion, a polyploid phenotype similar to that seen in *Ercc1*-deficient liver in vivo could not be established in in vitro hepatocyte cultures.

Apoptosis and cell proliferation are closely linked events in hepatocytes with many apoptotic factors being involved in cell cycle and division (Kanzler and Galle 2000). The liver is an organ with low cell turnover where 1-5 cells/ 10 000 cells undergo apoptosis at any given time point (Kanzler and Galle 2000). There are two main pathways of apoptosis, one being the extrinsic pathway which is initiated by ligand binding to a death receptor and a direct activation of caspase 8 and 3. The intrinsic pathway can also be stimulated through activation of death receptors, but it does need the involvement of mitochondrial cytochrome c release in order to cleave and activate caspase 3 (Li et al. 2003). Fas and TNF-α receptors mediate apoptosis in hepatocytes using similar but not identical pathways. Fas mediated apoptosis leads to a quick response which does not necessarily involve mitochondrial activation (Hatani et al. 2000). It is also the most common type of apoptotic induction in hepatocytes which express high levels of receptor, but not ligand (Guicciardi and Gores 2005). In contrast, TNF– α mediated apoptosis requires mitochondrial permeability transition and is therefore generally the slower pathway (Guicciardi and Gores 2005). In both cases, NFκB activation has been shown to protect primary murine hepatocytes from apoptosis (Hatano et al. 2000).

Generally, it seems that repair instead of apoptosis is favoured in murine hepatocytes. This hypothesis is supported by the fact that NER levels in murine hepatocytes are comparable to those in human fibroblasts with all other murine organs showing a much lower rate of NER (Prost et al. 1998). Even when *Irf*, a gene thought be involved in DNA damage repair, is absent from hepatocytes, no difference in apoptosis is noticed when compared to Wt cells, both spontaneously and after UV irradiation. In contrast, *Ercc1*- deficient hepatocyte cultures show

higher levels of apoptosis when compared to controls using the Feulgen method. The addition of AdenoCre virus cannot be responsible for the higher apoptosis levels seen in *Ercc1*- deficient cultures, as infected Flox/Wt cultures showed low levels of apoptosis even over a longer period in culture. The results obtained by Feulgen staining could not be repeated when flow cytometry was used to assess DNA content and apoptosis. This discrepancy could be explained by the fact that the assay used for flow cytometry is primarily designed to visualise differences in ploidy, which might not be sensitive enough to pick up the apoptotic cell fraction in our cultures. A separate stain could have been used to look at apoptosis levels by flow cytometry. Also, fragile hepatocyte nuclei do not tolerate flow cytometry well. Nuclear fragmentation during preparation could make it harder to detect increased levels of apoptosis associated with *Ercc1* deficiency. However, we felt confident that the Feulgen stain method was powerful enough to reveal differences in normal apoptotic and necrotic cell fractions in vitro. In conclusion, apoptosis is uncommon in hepatocytes so the defect caused by *Ercc1*- deficiency must be severe given that a strong apoptotic response is triggered. Therefore, *Ercc1* seems to play a crucial role in murine liver and hepatocytes seem to be unable to survive without *Ercc1* in prolonged in vitro culture.

The possibility of oxidative DNA damage contributing to the induction of apoptosis in *Ercc1*- deficient hepatocytes was further explored using the comet method. When we compared the Olive tail moment of AdenoCre infected Flox/Null and Flox/Wt hepatocyte cultures 24 hours after infection a slight difference between the genotypes could be established. One of the reasons for the, counterintuitively, higher amount of DNA strand breaks in Flox/Wt hepatocytes could be due to the isolation procedure which has been shown to lead to additional DNA damage (Wheelhouse et al. 2003). When DNA strand breaks were also introduced at oxidative lesion sites by using the enzyme Fpg, no difference in Olive tail moment was observed between genotypes. The lack of more DNA damage in infected Flox/Null hepatocytes could be due to ERCC1 protein still being present in sufficient concentration to deal with DNA repair at 24 hours after infection. However, even at later time points, when the levels

of ERCC1 protein had decayed, no differences between AdenoCre infected Flox/Null and Flox/Wt cultures could be found. The overall amount of spontaneous oxidative damage and strand breaks in our cultures might not be high enough to reveal a difference in Olive tail moment between genotypes. Alternatively, other repair pathways such as BER and error- prone post- replication repair (PRR) could be responsible for dealing with the lesions caused in culture, masking the lack of NER. However, when considering the increased, spontaneous levels of apoptosis in *Ercc1*-deficient hepatocytes, the likelihood of other repair pathways efficiently dealing with the lesions caused by a defect in NER is low.

To further strengthen the hypothesis that *Ercc1* is crucial to hepatocyte survival and to examine the lesions that may be responsible for the phenotype seen in *Ercc1*-deficient liver, experiments were conducted using UVC which induces DNA damage repaired by the NER pathway, Glucose oxidase which induces oxidative DNA damage and Mitomycin C which is responsible for the formation of interstrand cross-links. The main DNA adducts after UVC irradiation are cyclobutanepyrimidine dimers and (6-4) photoproducts (Dunkern et al. 2001). In *Ercc1*- deficient Chinese hamster ovary (CHO) cells, apoptosis can be detected 24 hours after irradiation with a dose- dependent increase of apoptosis up to 85% at 20 J/m^2. Necrosis levels were low and peaked at about 15% throughout time in culture (Dunkern et al. 2001). In the same experiment, activation of caspase- 8, 3 and 9 was demonstrated as early as 10 hours after UVC. *Bcl 2*, an anti- apoptotic factor, was subjected to more rapid degradation after UVC, increasing the likelihood for *Ercc1*- deficient CHO to undergo apoptosis as a result of unrepaired DNA damage (Dunkern et al. 2001). In addition, UVC- induced apoptosis has been demonstrated to be higher in *Ercc1*-deficient, immortalised murine fibroblasts (Melton et al. 1998). This is in accordance with my findings that UVC induces high levels of apoptosis in *Ercc1*- deficient hepatocyte cultures. UV- induced apoptosis in *Ercc1*- deficient cultures suggests that a malfunction of NER is responsible for the induction of apoptosis and that a lack of *Ercc1* leads to a survival disadvantage of hepatocytes in culture after UVC-irradiation. When Dunkern et al. (2001) treated CHO cells with ionising radiation,

no such increase in apoptosis could be found, showing that *Ercc1*- deficient CHO cells are not generally sensitised to DNA damaging agents, but react specifically to UVC. Of course, UV- induced DNA damage is not responsible for the phenotype in *Ercc1*- deficient liver. However, some forms of oxidative DNA damage are repaired by NER and elevated levels of oxidative DNA damage in *Ercc1*- deficient liver could be contributing to the phenotype.

In primary hepatocytes, mild sensitivity to oxidative damage could also be demonstrated when low doses of Glucose oxidase were given, leading to a stronger apoptotic response in *Ercc1*- deficient hepatocytes when compared to controls. Glucose oxidase, an enzyme oxidising glucose, is responsible for production of hydrogen peroxide during the oxidation process (Mueller et al. 2001). In our cell culture system a constant production of hydrogen peroxide induces oxidative damage in hepatocytes. Accumulation of oxidative DNA damage has several severe consequences for the hepatocytes. After induction of a wide range of oxidative stress, mutations and replication fork blockage has been observed, along with increased microsatellite instability and changes in intracellular signalling due to altered gene expression after reactive oxygen species (ROS) production (Cooke et al. 2003). Therefore, multiple repair pathways have evolved to deal with oxidative lesions, the most prominent of which is BER with its main substrate being 8-oxo-guanine (Cooke et al. 2003). However, oxidative damage triggers a moderate, apoptotic response when *Ercc1* is absent in culture. It has been suggested that oxidative damage in the liver contributes to the premature polyploidy observed in vivo (Mc Whir et al. 1993). This suggestion is supported by the elevated levels of 8-oxo-G levels observed in *Ercc1* knockout liver (Selfridge et al. 2001) and by my observations of greater sensitivity to glucose oxidase in *Ercc1*- deficient hepatocytes in vitro.The absence of a more drastic response in hepatocyte cultures can be explained by the rapid degradation of hydrogen peroxide by hepatic catalases and glutathione peroxidase, protecting the primary hepatocytes from extensive damage (Mueller et al. 2001). When higher doses of Glucose oxidase were added to the cultures, extensive cell death could be observed in all cultures independent of genotype. This could be

explained by an imbalance of hydrogen peroxide concentration compared to catalase and glutathione peroxidase activity, leading to an overall toxicity in vitro and cell death.

In vitro, both NER and oxidative damage repair properties of *Ercc1* seem to play a role in hepatocyte maintenance. A combination of DNA lesions arising due to different roles of *Ercc1* could contribute to the premature ploidy seen in vivo and the extensive apoptotic response in vitro. In addition, the lack of development of polyploidy which could protect *Ercc1*- deficient hepatocytes from apoptosis is not apparent in our cell culture system, possibly exposing those hepatocytes to higher amounts of cellular stress and increasing the likelihood of apoptotic cell death.

Psoralen inter- strand cross links (ICL) in yeast are dealt with by several repair pathways: The error- free pathway involves NER in which NER proteins induce DSB around the lesion upon replication to be repaired by homologous recombination (HR). On the other hand, the error- prone post- replication repair (PRR) pathway ensures the bypass of the lesion (Saffran et al. 2004). Mitomycin C (MMC) induces ICL, leading to a block of the replication fork and DSB. By linking two sister chromosomes together, MMC interferes with the ability of the chromosomes to separate during cell division. In addition, pyrimidine dimers and tandem base substitutions can be observed upon MMC administration (Nohmi and Masumura 2005). As a result of the complexity of the lesion and the inability of chromosomes to segregate during cell division, inter- strand cross links are known to be very cytotoxic and rodent cells have been shown to be hypersensitive to ICL. (Lan et al. 2004). Mitomycin C exposure has been shown to result in higher levels of apoptosis of *Ercc1*- deficient Chinese hamster ovary cells and immortalised embryonic mouse fibroblasts when compared to Wt cells (McWhir et al. 1993, Melton et al. 1998) probably acting through caspase 8 activation (Dunkern et al. 2001). Interestingly, immortalised embryonic mouse fibroblasts seemed to be less sensitive to Mitomycin C than CHO cells, suggesting that there might be a second pathway in the mouse to deal with interstrand cross-links. This is in accordance with my findings that

Mitomycin C does not readily induce apoptosis in primary, *Ercc1*- deficient hepatocytes. Another possible explanation could also be lack of cell division in my hepatocyte cultures. As mentioned above, the cytotoxicity of MMC results from cross linking two sister chromosomes which lose the ability to separate during cell division. If cell division is low or lacking in hepatocyte cultures, exposure to MMC would have no effect on hepatocyte survival.

In general, lower levels of apoptosis could be seen in control untreated cultures during the DNA damaging experiments at 5 days after plating when compared to the original estimation of spontaneous apoptosis in cultures at the same time point. Levels of apoptosis were found to be around 23 % in infected *Ercc1* Flox/Null hepatocyte cultures at day 5 after plating. Infected *Ercc1* Flox/Null control cultures in the DNA damaging experiments at the same time point showed 3-7 % of apoptosis. This discrepancy could be explained by a different batch of virus that was used to assess spontaneous apoptosis and when cultures were challenged with DNA damaging agents.

One of the more striking features of our *Ercc1*- deficient hepatocyte cultures is the accumulation of microvesicular lipids in older cultures. Lipid accumulation is generally a sign of diseased liver and occurs rapidly after insult. A progression from microvesicles to the formation of macrovesicles is usually noticed with time (D. Harrison, personal communication). Lipid accumulation is a sign of insufficient hepatic mitochondrial β- oxidation of free fatty acids, leading to a conversion of excess fat to, for example, triglycerides which are stored in the cytoplasm (Patrick 2002). Mitochondrial β- oxidation produces reactive oxygen species as part of the normal metabolism in mitochondria. ROS can in turn initiate lipid peroxidation of stored triglycerides in the cytoplasm (Patrick 2004). The production of reactive aldehydes such as 4- hydroxynoneal or malondialdehyde can lead to damage in mtDNA and nuclear DNA (Fromenty et al. 2004). Another reason for cytoplasmic lipid accumulation can be found when lipogenesis is increased or when microsomal cytochrome P450A ω - oxidation is impaired (Videla et al. 2004). Lipid

accumulation and mitochondrial dysfunction have been shown to lead to apoptosis or necrosis, depending on the energy status of the cell (Fromenty et al. 2004). My findings of lipid accumulation in liver point to a malfunction of mitochondria caused by *Ercc1*- deficiency. In addition, the increased levels of apoptosis in *Ercc1*-deficient cells might be partly responsible for the high amounts of lipids observed in these cultures. No direct involvement of NER in mitochondrial DNA repair has been found in mammalian cells or yeast to date with BER mechanisms being operational in mitochondria instead (Larsen et al. 2005). However, DNA damage that arises in the nucleus in a situation of absent NER could lead to alterations in nuclear gene expression and cause a disruption of mitochondrial lipid metabolism indirectly.

Lipid accumulation in all cell culture dishes independent of genotype was apparent after UVC irradiation, showing that accumulated DNA damage in the liver can lead to a malfunction of lipid oxidation pathways (D. Harrison, personal communication). In general, lipid accumulation is known to be a feature of diseased liver and is common in models of alcoholic liver injury (Deaciuc et al. 2000). It seems that in control dishes, where DNA repair is functional, normal lipid oxidation can take place once the DNA damage is repaired and lipids no longer accumulate. In *Ercc1*-deficient liver lipid accumulation persists as a result of unrepaired DNA damage in the hepatocytes.

In conclusion, *Ercc1*- deficient primary hepatocyte cultures helped to further characterise *Ercc1*- deficiency in liver. We observed that absence of NER led to high rates of apoptosis in hepatocytes. In addition, it was established that the DNA lesions most likely to be found in *Ercc1*- deficient liver and implicated with the phenotype observed is oxidative DNA damage. A possible disruption of lipid metabolism, as indicated by hepatic lipid accumulation, could further contribute to damage in hepatocytes and liver failure in *Ercc1*- deficient animals in vivo. The liver phenotype in *Ercc1*- deficiency was further tested using AdenoCre virus in *Ercc1* Flox/Null and Flox/Wt animals.

5. Conditional *Ercc1* knockout approach using AdenoCre virus in vivo

5.1 Determination of recombination via PCR and Southern blotting

Six week old *Ercc1* Flox/Null and Flox/Wt animals were i.v. injected with $1x10^9$ or $4x10^9$ pfu of AdenoCre virus to determine short term consequences of *Ercc1*-deficiency in vivo. Animals of each group consisted of littermates and were sacrificed 1 and 3 weeks after virus injection. DNA was prepared from liver. All amounts of DNA were matched and samples were subjected to a semi- quantitative recombination PCR using a tissue sample with 200% recombination for comparison. A faint 250 bp recombined band could be detected in all liver samples. The *Ercc1* Flox/Wt sample receiving $4x10^9$ AdenoCre virus showed the highest amount of recombination 3 weeks after injection with levels being estimated at around 25% (Figure 23, ID # 14 in Table 5).

Southern blotting was performed on samples receiving $1x10^9$ pfu AdenoCre virus 1 and 3 weeks after infection to determine the amounts of recombination more accurately. A titration curve was obtained by spiking varying amounts of DNA from a cell line showing 100% recombination into DNA from an *Ercc1* Flox/Flox liver. The 3.3 kb recombined band could be detected in samples showing down to 25% recombination in the titration curve, indicating the lower level of sensitivity for this blot. In the infected *Ercc1* Flox/Null and Flox/Wt samples, no recombined band could be detected 1 or 3 weeks after infection. This result suggests that recombination levels after AdenoCre infection in our *Ercc1*Flox/Null and Flox/Wt livers are below 25%.

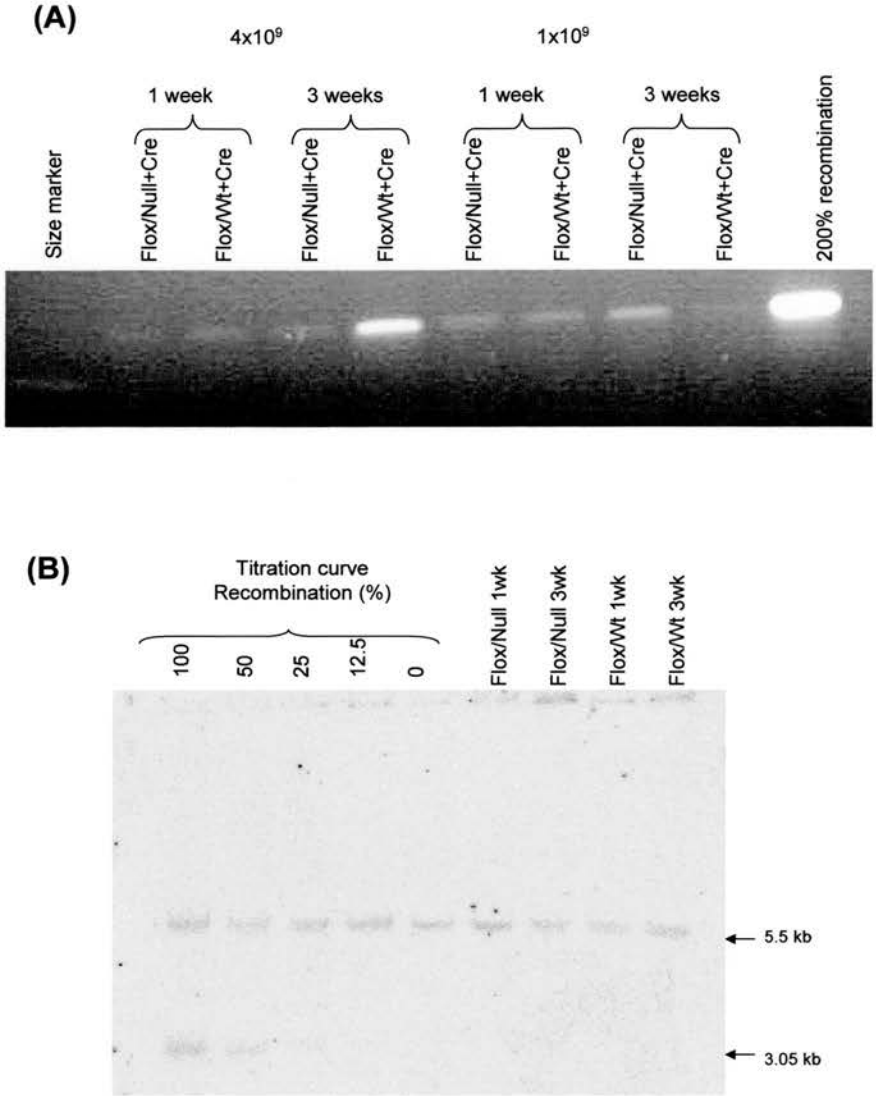

Figure 23: Liver specific recombination of the *Ercc1* floxed allele after AdenoCre virus administration. (A) Semi- quantitative PCR showing a 250 bp recombined band in *Ercc1* Flox/Null and Flox/Wt liver 1 and 3 weeks after i.v. AdenoCre administration. Virus concentrations varied from $1x10^9$ to $4x\ 10^9$ pfu per animal. An *Ercc1* Flox/Flox tissue sample showing 200% recombination (two floxed alleles, each with 100% recombination) was used for comparison. All DNA was matched by spectrophotometry. (B) Southern blot indicating the levels of recombination in *Ercc1* Flox/Null and Flox/Wt livers after AdenoCre virus administration. A titration curve was obtained by spiking varying amounts of DNA from a cell line showing 100% recombination into DNA from an *Ercc1* Flox/Flox liver. *Ercc1* Flox/Null and Flox/Wt livers show no recombined band 1 and 3 weeks after AdenoCre infection.

5.2 Characterisation of the liver phenotype after AdenoCre virus injection using histology

H&E slides were prepared from *Ercc1* Flox/Null and Flox/Wt liver samples after administration of $4x10^9$ pfu AdenoCre virus 3 weeks after infection. Large, polyploid hepatocyte nuclei could be detected in all samples independent of genotype following a random distribution throughout the liver (Figure 24). We anticipated a possible accumulation of polyploid nuclei around sinusoids in *Ercc1* Flox/Null liver as sinusoids are likely to be one of the main routes of entry for the virus. No such pattern of polyploidisation could be detected.

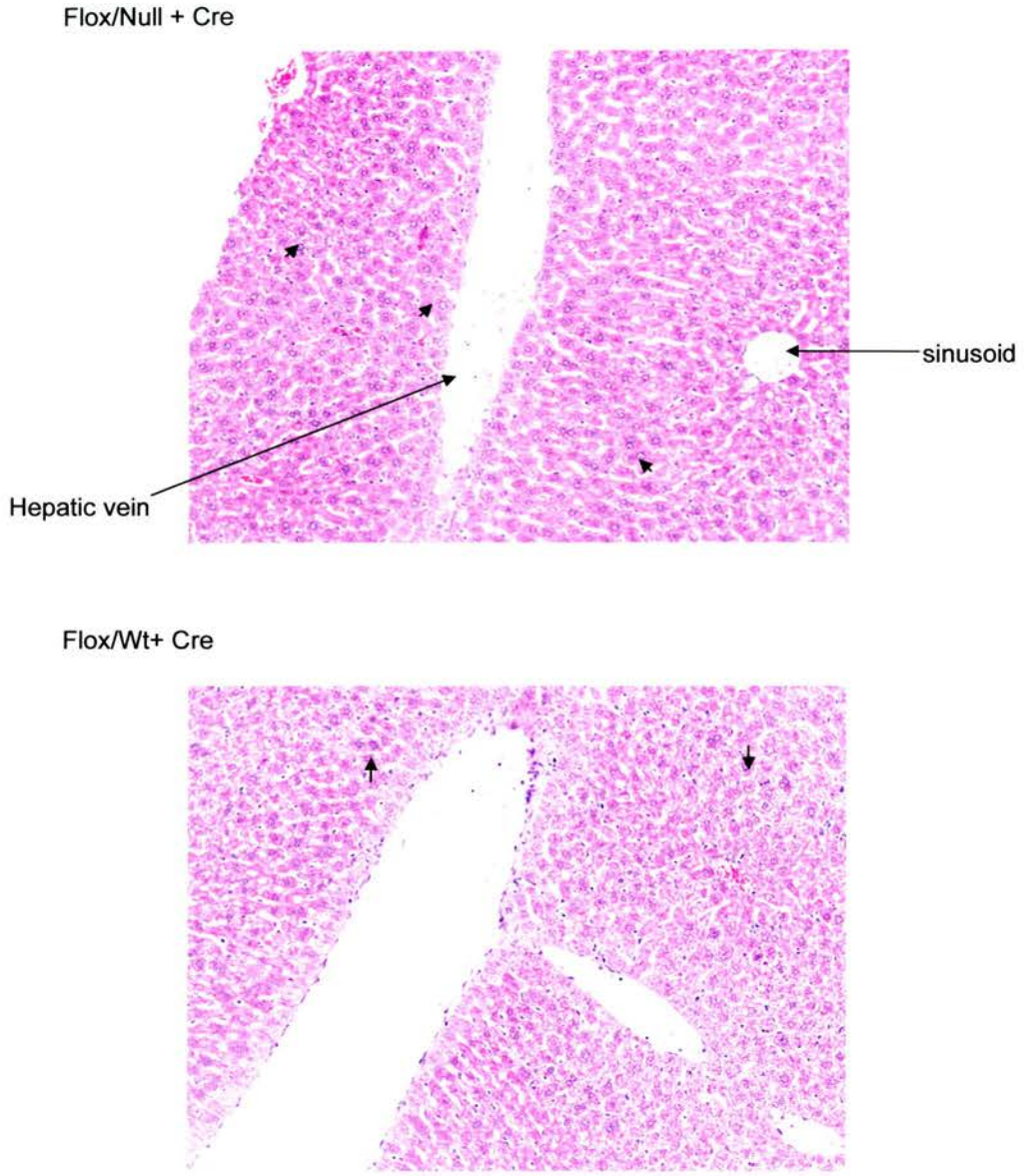

Figure 24: Histology of AdenoCre virus infected *Ercc1* Flox/Null and Flox/Wt livers. Liver sections were taken 3 weeks after i.v. infection with $4x10^9$ pfu AdenoCre virus. Sections were H&E stained and pictures taken with a 10x objective. Hepatic veins and sinusoids are labelled accordingly. Black arrow heads indicate large hepatocyte nuclei in all slides.

5.3 Determination of DNA content after AdenoCre virus injection using flow cytometry

Flow cytometry was used to determine the DNA content of $1x10^9$ pfu AdenoCre infected *Ercc1* Flox/Wt samples 24 and 72 hours after injection (Table 5, ID #1 and 2). No clear difference in any of the parameters measured could be detected in infected samples when compared to an uninfected littermate Flox/Wt control (ID #3). $1x10^9$ and $4x10^9$ pfu AdenoCre infected *Ercc1* Flox/Null and Flox/Wt samples, which were used for recombination determination by PCR, were subjected to flow cytometry 1 and 3 weeks after infection. One week after infection, *Ercc1* Flox/Null samples showed higher levels of polyploidy (8n) when compared to the Flox/Wt livers, independent of the total amount of virus given (Table 5, ID # 4 compared to 5; 10 compared to 11). Higher levels of ploidy were also detected in *Ercc1* Flox/Null livers 3 weeks after administration of $4x10^9$ pfu AdenoCre virus when compared to the infected Flox/Wt control (Table 5, ID # 14 compared to 15). A rise in octaploidy could also be detected in $1x10^9$ pfu AdenoCre injected Flox/Null livers 3 weeks after injection when compared to 1 week after injection (Table 5, ID # 5 compared to 8). However, the total amounts of polyploidy were smaller in *Ercc1* Flox/Null livers when compared to Flox/Wt controls 3 weeks after $1x10^9$ AdenoCre administration (Table 5, ID # 7 compared to 8). Levels of polyploidy were low in uninfected Flox/Wt control and Flox/Null control littermates (Table 5, ID # 6, 9, 12, 13). In conclusion, in three out of four pair wise comparisons the level of polyploidy (8n) was more than 2- fold higher in infected *Ercc1* Flox/Null livers than in Flox/Wt controls. The low levels of polyploidy in uninfected *Ercc1* Flox/Wt (ID # 6, 12, Table 5) and uninfected Flox/Null (ID # 9, 13, Table 5) livers indicate that the increased ploidy in infected *Ercc1* Flox/Null livers is a consequence of viral infection and partial loss of *Ercc1*.

Apoptosis levels were low in general with sample Flox/Wt # 14 showing the highest amount of apoptosis. This same sample also displayed the highest amount of recombination as detected by PCR. Levels of S-phase were also low, with no clear relationship with genotype, viral infection or time after infection.

Table 5: DNA content of *Ercc1* Flox/Null and Flox/Wt livers after AdenoCre virus administration. Virus was given at $1x10^9$ and $4x10^9$ pfu. Control animals were littermates that did not receive virus. Animals were sacrificed as indicated by the time after AdenoCre infection. Age is given at the time of sacrifice. Apoptosis is given as a percentage of the total amount of cells. Diploid, tetraploid, octaploid and S-phase fractions are given as the percentage of viable cells. Individual samples are given ID numbers.

Genotype	ID	Age	Virus conc.	Time (after injection)	2n	4n	8n	Apoptosis	S-phase
	(#)	(weeks)	(pfu)		(%)	(%)	(%)	(%)	(%)
Flox/Wt	1	7	$1x10^9$	24hrs	53.2	35.8	1.5	1.4	2.3
Flox/Wt	2	7	$1x10^9$	72hrs	61.1	34	0.6	1.1	1.4
Flox/Wt	3	7	0	72hrs	52.1	38.1	0.9	1.1	1.8
Flox/Wt	4	7	$1x10^9$	1 week	53.7	36	1.5	1.1	1.5
Flox/Null	5	7	$1x10^9$	1 week	49.7	41.2	5.2	0.7	0.9
Flox/Wt	6	7	0	1 week	58.9	34	2.5	0.8	1.4
Flox/Wt	7	9	$1x10^9$	3 weeks	44.8	38	11.5	1.2	1.3
Flox/Null	8	9	$1x10^9$	3 weeks	49.7	35.8	8.4	0.8	1.8
Flox/Null	9	9	0	3 weeks	58.8	32	2.8	0.7	1
Flox/Wt	10	7	$4x10^9$	1 week	69	20.6	0.8	1.1	2.9
Flox/Null	11	7	$4x10^9$	1 week	47.8	30.4	12.5	0.9	3
Flox/Wt	12	7	0	1 week	61	29.7	1.3	0.8	1.3
Flox/Null	13	7	0	1 week	58.3	29.6	2.7	0.7	0.7
Flox/Wt	14	9	$4x10^9$	3 weeks	61.5	25.3	3.8	3.2	0.9
Flox/Null	15	9	$4x10^9$	3 weeks	53.7	33	7.5	1.4	1.8

5.4 Lipid accumulation visualised by Oil Red O staining

Liver sections of 6 week old *Ercc1* Flox/Null and Flox/Wt animals injected with $4x10^9$ pfu virus were taken 1 and 3 weeks after injection. Cryosections were cut and then stained for lipids using Oil Red O. Pictures were taken with a 40 x objectives. *Ercc1* Flox/Null livers showed a large number of cytoplasmic macrovesicles containing lipids when compared to Flox/Wt livers which only showed very small amounts of microvesicular lipid accumulation in the cytoplasm 1 week after virus infection (Figure 25). Small amounts of lipid accumulation persisted 3 weeks after AdenoCre injection in Flox/Null livers and to a lesser extent in Flox/Wt livers (Figure 25). In conclusion, cytoplasmic lipid accumulation is initially induced in *Ercc1* Flox/Null livers, disappearing with time after infection.

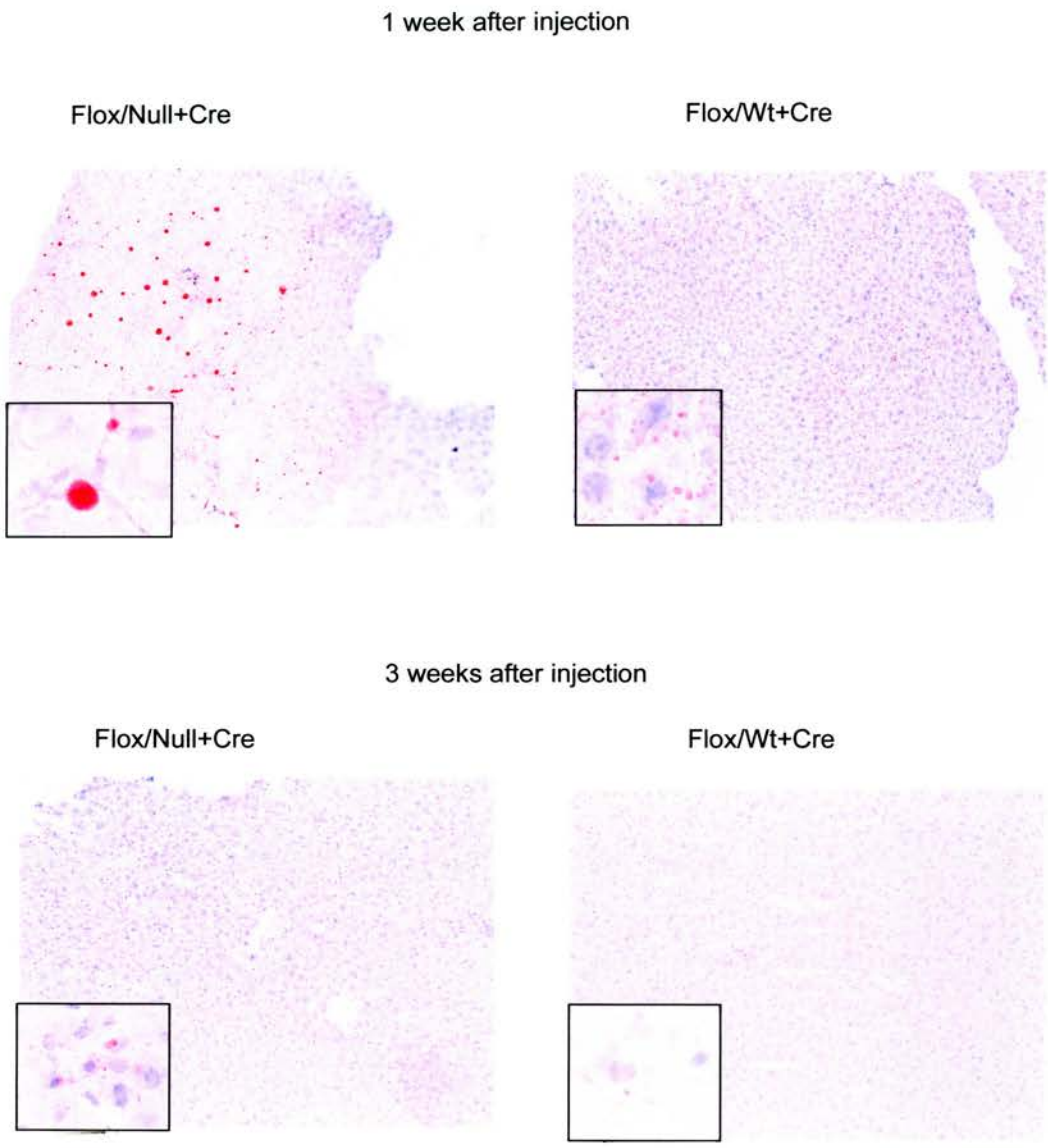

Figure 25: Lipid accumulation in AdenoCre infected liver. *Ercc1* Flox/Null and Flox/Wt livers were taken 1 and 3 weeks after infection with $4x10^9$ pfu AdenoCre and stained with Oil Red O. The objective used for the pictures is 20x with an inset picture taken with a 40x objective. Lipids and apoptotic cells are stained in red and hepatocytes and nuclei are stained in blue.

5.5 Induction and characterisation of necrosis using carbon tetrachloride (CCl_4)

We reasoned that a greater difference between AdenoCre infected *Ercc1* Flox/Null and Flox/Wt livers might be apparent if the livers were stimulated to replicate. Liver does not readily replicate unless hepatocytes are challenged by damaging agents. To stimulate replication in the liver, we decided to use CCl_4 which induces necrosis of the liver and subsequent recovery. Necrosis of *Ercc1* Flox/Wt liver and subsequent regeneration was induced in 6 week old animals. At a single dose of 51 mg/ml, which corresponds to 51 μg per g of mouse, CCl_4 and 1 day after injection necrotic islands could be detected around hepatic sinusoids when stained with H&E (Figure 26). Signs of necrosis with small nuclei and lighter stain remained around sinusoids 5 days after CCl_4. Complete regeneration of the liver had occurred 7 days after injection with hepatocytes showing normal sized nuclei throughout. The amount of necrosis in CCl_4 treated livers was further determined using the Olympus DP software. Nine littermates were injected with 51 mg/ml CCl_4 and sacrificed 1, 5 and 7 days after injection and amounts of necrosis were estimated. One day after CCl_4 treatment, 25% of liver tissue was classified as necrotic, decreasing to around 15% 5 days after injection with no necrosis being apparent at day 7 (Figure 27).

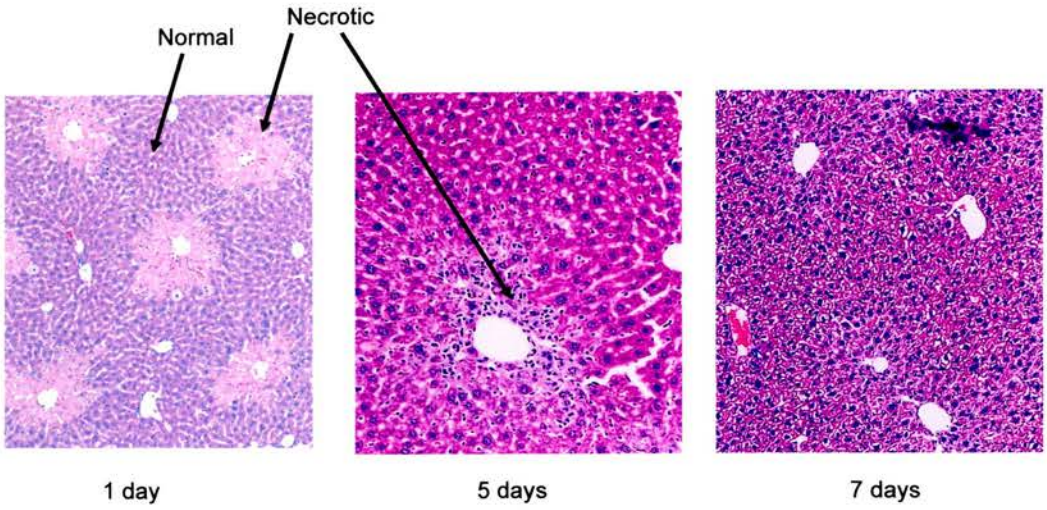

Figure 26: Histology of carbon tetrachloride (CCl_4) treated *Ercc1* Flox/Wt livers. Animals were sacrificed 1, 5 and 7 days after i.p. injection with 51 mg/ml CCl_4. Sections were stained for H&E and pictures taken with a 40x objective. Necrotic and normal hepatocytes are indicated by arrows with necrotic cells showing a light pink stain compared to darker normal hepatocytes.

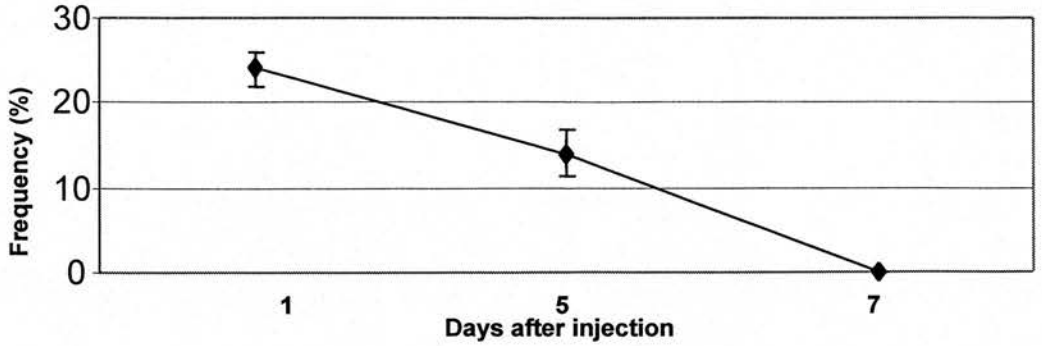

Figure 27: Levels of necrosis in *Ercc1* Flox/Wt livers after CCl_4 treatment. Animals were sacrificed 1, 5 and 7 days after i.p. injection with 51 mg/ml CCl_4. Sections were stained for H&E and pictures taken with a 10x objective. The amount of necrosis was estimated for each slide using the Olympus DP software.The mean of three different mouse livers is shown for each time point. The SEM is indicated with error bars.

Flow cytometry was further used to characterise DNA content of liver samples after 23, 51 and 102 mg/ml CCl_4 was given to the animals. Those doses corresponded to 23 μg per g of mouse, 51 μg per g of mouse and102 μg per g of mouse. Different time points after injection were chosen as time of sacrifice. A dose of 23 mg/ml of CCl_4 led to an increase in octaploidy in all treated *Ercc1* Flox/Wt livers when compared to uninjected Flox/Wt littermates (Table 6, ID # 16- 23). The highest amounts of polyploidy in these samples could be noted 3 and 5 days after treatment (Table 6, ID # 18 and 20). Apoptosis and S-phase levels were low in all samples.

Ercc1 Flox/Null animals were treated with 51mg/ml CCl_4 to determine the effect of an increased dose of agent on a different genotype. 2 and 3 days after 51mg/ml CCl_4 administration an increase in octaploidy was seen in treated animals when compared to an untreated littermate control (Table 6, ID # 25 and 27 compared to 26). A high level of apoptosis was seen in an *Ercc1* Flox/Null liver 1 day after 51 mg/ml CCl_4 when compared to an uninjected control (Table 6, ID # 24 compared to 26). This level decreased with time. Levels of S-phase were increased 2 days after 51 mg/ml CCl_4 treatment when compared to an untreated control (Table 6, ID # 25 compared to 26).

We decided to increase the dose of CCl_4 to 102 mg/ml in an attempt to see a more pronounced effect on replication. Levels of octaploidy were increased in most treated *Ercc1* Flox/Null and Flox/Wt livers when compared to an untreated Flox/Wt littermate (Table 6, ID # 28- 33 compared to 34). In addition, CCl_4 treated Flox/Null samples showed higher amounts of ploidy when compared to CCl_4 treated Flox/Wt samples 2 and 3 days after injection. An increase in apoptosis could be detected in injected samples in the same experiment when compared to the uninjected control (Table 6, ID # 28-33 compared to 34). An increase in S-phase could be noted in all livers after 102 mg/ml CCl_4 with *Ercc1* Flox/Null liver # 31 displaying up to 5 % of cells in S-phase.

Table 6: DNA content of *Ercc1* Flox/Null and Flox/Wt livers after CCl_4 administration. A single dose of CCl_4 was given i.p. at 23, 51 and 102 mg/ml. Control animals were littermates that did not receive CCl_4. Animals were sacrificed as indicated at the time after CCl_4 administration. Apoptosis is given as a percentage of the total amount of cells. Diploid, tetraploid, octaploid and S-phase fractions are given as the percentage of viable cells. All samples are labelled with individual ID numbers.

Genotype	ID (#)	CCl_4 treatment (mg/ml)	Time (days)	2n (%)	4n (%)	8n (%)	Apoptosis (%)	S-phase (%)
Flox/Wt	16	23	1	62	29	4.5	0.7	1.3
Flox/Wt	17	0	1	58	29.7	2.7	0.8	2
Flox/Wt	18	23	3	59.7	24	10.4	1.3	2
Flox/Wt	19	0	3	56.4	32.6	3.7	1.1	1.5
Flox/Wt	20	23	5	57.3	29.6	8	0.9	1.6
Flox/Wt	21	0	5	58.9	34	2.5	0.9	1.4
Flox/Wt	22	23	7	51.7	38.6	5.1	0.8	1.1
Flox/Wt	23	0	7	52.9	36	4.1	0.8	1.7
Flox/Null	24	51	1	64.5	23.9	0	5.2	3.1
Flox/Null	25	51	2	66	21.4	3	1.5	4.9
Flox/Null	26	0	2	74.5	17.3	2	1.7	3
Flox/Null	27	51	3	55	31.5	5.3	2.1	2.5
Flox/Wt	28	102	1	63.8	22.7	4.5	2.6	2.6
Flox/Null	29	102	1	60.7	28	3.1	1.2	2.1
Flox/Wt	30	102	2	58.6	31.4	1.8	2.6	3.1
Flox/Null	31	102	2	59.5	26	4.1	0.9	5.1
Flox/Wt	32	102	3	64.9	16.7	9.4	1.3	3.6
Flox/Null	33	102	3	54.5	25.7	12.4	0.7	2.6
Flox/Wt	34	0	3	69	24	2.7	0.6	1.8

In summary, carbon tetrachloride stimulates necrosis from day 1 after injection with liver regeneration being completed 7 days after injection. A general increase in ploidy was apparent in treated samples when compared to untreated controls. Irrespective of genotype, small increases in S-phase could be noted after higher doses of CCl_4. Overall, the highest amounts of octaploidy and apoptosis were detected in injected Flox/Null livers.

Additional pilot studies using multiple injections of 51 mg/ml CCl_4 showed sufficient induction of replication without harming the animals on a long term basis (results not shown). We therefore decided to use 51mg/ml CCl_4 to induce liver regeneration and replication in our short term study of *Ercc1* deficiency in an attempt to exaggerate the possible consequences of *Ercc1* loss in the liver.

5.6 Short term consequences of AdenoCre infection and carbon tetrachloride injections

Previously, AdenoCre infection resulted in higher levels of octaploidy in *Ercc1* Flox/Null compared to Flox/Wt livers. We now wished to investigate whether this difference could be exacerbated by CCl_4 treatment. 6 week old animals received $1x10^9$ or $4x10^9$ pfu AdenoCre virus followed by 51 mg/ml CCl_4 once weekly. An untreated littermate was used as control. For characterisation *Ercc1* Flox/Null and Flox/Wt livers were subjected to flow cytometry. High levels of octaploidy were apparent in all samples when compared to an uninjected control littermate with *Ercc1* Flox/Null sample # 38 displaying up to 22% of octaploidy (Table 7). When $1x10^9$ virus was given, treatment with CCl_4 resulted in higher levels of octaploidy in Flox/Null livers when compared to treated Flox/Wt livers 1 week after AdenoCre virus injection (Table 7, ID # 35 compared to 36). In addition, one week after virus injection higher levels of apoptosis and S-phase were seen in *Ercc1* Flox/Null compared to the Flox/Wt animal. These differences were not noticed 3 weeks after injection with $1x10^9$ pfu.

Table 7: DNA content of *Ercc1* Flox/Null and Flox/Wt livers after AdenoCre virus infection and CCl_4 administration. AdenoCre virus was given i.v. at a pfu of $1x10^9$ and $4x10^9$. CCl_4 was given i.p. at 51 mg/ml weekly. One control animal was a littermate that did not receive virus or CCl_4. Animals were sacrificed as indicated at the time after AdenoCre administration, leaving 6 days of recovery after the last CCl_4 injection. Age is given at the time of sacrifice. Apoptosis is given as a percentage of the total amount of cells. Diploid, tetraploid, octaploid and S-phase fractions are given as the percentage of viable cells.

Genotype	ID (#)	Age (weeks)	Virus conc. (pfu)	CCl_4 (mg/ml)	Time (weeks)	2n (%)	4n (%)	8n (%)	Apoptosis (%)	S-phase (%)
Flox/Wt	35	7	$1x10^9$	51	1	50.9	38.5	6.9	0	1.6
Flox/Null	36	7	$1x10^9$	51	1	46.1	30.7	14.3	3.1	2.7
Flox/Wt	6	7	0	0	1	58.9	34	2.5	0.8	1.4
Flox/Wt	37	9	$1x10^9$	51	3	47.5	24.5	19.7	1.2	1.3
Flox/Null	38	9	$1x10^9$	51	3	46	23.6	22.4	0.8	1.8
Flox/Null	9	9	0	0	3	58.8	32	2.8	0.7	1
Flox/Wt	39	7	$4x10^9$	51	1	51.5	29.8	8.3	2.2	3
Flox/Null	40	7	$4x10^9$	51	1	57.3	27.2	7.6	1.1	2.9
Flox/Wt	12	7	0	0	1	61	29.7	1.3	0.8	1.3
Flox/Null	13	7	0	0	1	58.3	29.6	2.7	0.7	0.7
Flox/Wt	41	7	0	0	1	61	29.7	1.3	0.7	1.3
Flox/Wt	42	9	$4x10^9$	51	3	59.1	27.3	10.9	0.9	0.5
Flox/Null	43	9	$4x10^9$	51	3	60.8	22.8	9.1	1.4	2.5

Use of CCl_4 at a virus concentration of $4x10^9$ pfu did not lead to a clear difference in octaploidy between treated *Ercc1* Flox/Null and Flox/Wt animals (Table 7, ID # 39, 40, 42, 43). Similarly, there were no clear genotype differences when levels of apoptosis and S-phase were compared.

In conclusion, the polyploidy in regenerating liver induced by CCl_4 treatment reduced rather than increased the ploidy differences observed following AdenoCre infection of *Ercc1* Flox/Null and Flox/Wt livers.

5.7 Diethyl nitrosamine (DEN) induction of liver cancer in *Ercc1* Flox/Wt mice

A pilot liver cancer induction experiment was conducted prior to designing an experiment to investigate the effect of loss of *Ercc1* on susceptibility to liver cancer. One male *Ercc1* Flox/Wt mouse was injected with 1 μg/g body weight (BW) DEN i.p. at 14 days of age. The animal was regularly examined for signs of discomfort and sacrificed at 39 weeks of age. A picture was taken of the whole liver and H& E sections were taken from tumour nodules and surrounding normal tissue. Figure 28 shows several tumour nodules accumulating throughout the liver. 19 small and 2 larger nodules were sampled in total. Histology of the tumours revealed that the nodules consisted of hepatocellular adenomas (Dr. David Brownstein, personal communication, data not shown).

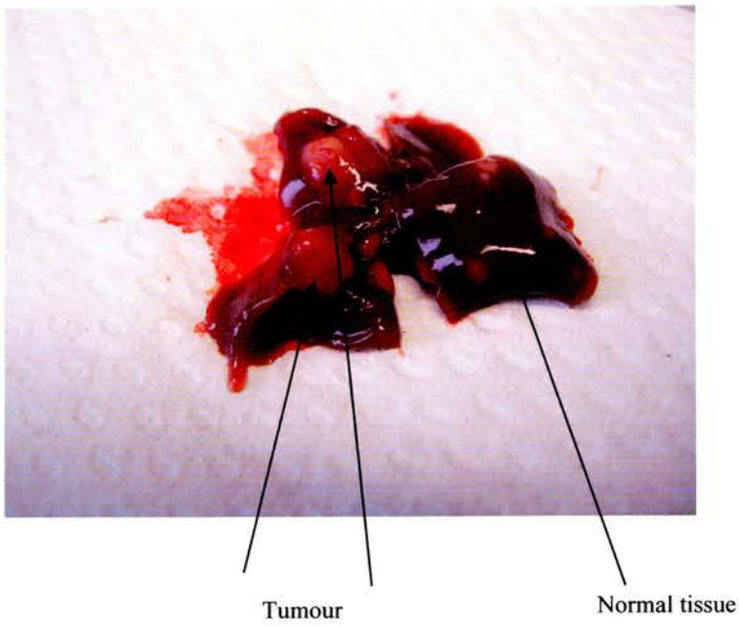

Figure 28: Liver of Flox/Wt mouse 37 weeks after diethyl nitrosamine (DEN) injection. 8 µg DEN was i.p. injected into a 2 week old male animal. Healthy liver tissue is intensely red. White nodules comprise tumours of different size and pathology.

5.8 Discussion

AdenoCre virus was i.v. injected into *Ercc1* Flox/Null and Flox/Wt animals to determine short term consequences of *Ercc1*- deficiency in vivo. Low levels of recombination were detected in all liver samples by PCR 1 and 3 weeks after AdenoCre infection using two different titers of virus. To quantify the levels of recombination, a Southern blot was performed including a titration curve. The lower limit of detection was 25%. No recombination in AdenoCre injected samples was detected by Southern blotting, indicating that the level of recombination was below 25%. The route of administration could be one reason for the low levels of recombination seen in the liver. The virus is delivered by i.v. injection with no liver specific receptor being targeted. Akagi et al. (1997) and Wang et al. (1996) reported recombination levels to be around 50% in liver after i.v. injection of AdenoCre virus with lower levels of recombination being found in spleen and all other tissues. After $1x10^9$ pfu AdenoCre virus infection, 80% of hepatocytes showed recombination of the *lacZ* locus (Akagi et al. 1997). Therefore, the route of administration and the concentration of virus used in our study should be sufficient. However, 90% of the viral DNA was lost 60 days after injection, indicating extensive liver regeneration after AdenoCre injection leading to an elimination of infected hepatocytes. Akagi et al. (1997) suspected an increase in β- galactosidase activity, triggered by recombination of the *lacZ* locus, rather than the virus itself as being responsible for the extensive immune response observed. Stec et al. (1999) also found an inflammatory response after injection of AdenoCre virus which was indicated by an enlargement of the spleen. Although the immune system was clearly activated, it did not affect the study results. An activation of the immune system and a clearance of virally infected recombined hepatocytes could be responsible for the low levels of recombination seen in our animals. In addition, *Ercc1*- deficient hepatocytes might be more prone to undergoing apoptosis in the liver as indicated by the high levels of apoptotic cells in *Ercc1*- deficient hepatocyte cultures in vitro. Interestingly, the *Ercc1* Flox/Wt liver sample showing the highest amounts of recombination after

$4x10^9$ AdenoCre infection also showed the highest amounts of apoptosis, indicating that there might be a link between amounts of viral infection and rate of elimination of virally infected hepatocytes.

Clusters of infected hepatocytes were noticed by Stec et al. (1999), but no such patterns were seen when liver sections were assessed for clusters of polyploid hepatocytes around sinusoids. Polyploidy is, of course, only an indirect indicator of viral activity and a lack of polyploid clustering need not mean that viral infection is evenly distributed in the liver.

Although only low levels of recombination could be detected in *Ercc1* Flox/Null and Flox/Wt animals after AdenoCre infection, a biological response in the form of increased levels of polyploidy and cytoplasmic lipid accumulation in some of the livers could be noted when liver samples were subjected to flow cytometry and Oil Red O staining. Development of premature polyploidy is one of the hallmarks of *Ercc1*- deficiency and was seen in 6 week old, infected Flox/Null animals 1 week after viral infection when compared to infected Flox/Wt littermates. In the same experiment, levels of polyploidy in Flox/Null livers continued to be higher compared to Flox/Wt livers at 3 weeks after $4x10^9$ pfu AdenoCre virus. Although ploidy increased in $1x10^9$ pfu AdenoCre infected Flox/Null liver 3 weeks after infection when compared to the earlier time point, slightly higher levels of ploidy were observed in the Flox/Wt control. The addition of AdenoCre virus, which stimulates replication in *Ercc1* Flox/Null and Flox/Wt cultures in vitro, cannot explain the higher amounts of polyploidy seen in all *Ercc1* Flox/Null livers at 1 week after the infection as infected Flox/Wt littermates show lower levels of ploidy at this time point. It also cannot be explained by a higher spontaneous level of polyploidy in infected Flox/Null compared to Flox/Wt livers. Instead, *Ercc1*- deficiency, induced by AdenoCre mediated recombination, could be responsible for the increased levels of ploidy in the liver of 6 week old animals. *Ercc1*- deficient animals are thought to undergo premature ageing with ploidy levels in 3 week old animals corresponding to those of 2 year old Wt animals (McWhir et al. 1993). In normal liver diploid

hepatocytes are the predominant cell type at birth displaying high amounts of S-phase. An increase in ploidy and a decrease in mitotic activity occurs after weaning and continues throughout life (Torres et al. 1999). In the adult liver, hepatocytes are quiescent but remain with the capacity to re- enter the cell cycle upon toxic insult (Gupta 2000). This replicative senescence in liver is thought to prolong life span as telomerase activity is less apparent in mammals after birth, rendering the chromosome telomeres prone to shortening after cell division (Anantharaju et al. 2002). Polyploidy in the liver, which is exposed to high levels of endotoxins, could be seen as a protective mechanism where hepatocytes develop multiple copies of the same gene without undergoing cell division. Partial *Ercc1*- deficiency as observed in AdenoCre infected *Ercc1* Flox/Null livers led to elevated levels of ploidy indicating that normal levels of ERCC1 are required for normal liver function. This early response in our male animals could be mediated by testosterone and 3, 5, 3'-triiodothyronine which have both been shown to help induce polyploidy in rats (Torres et al. 1999). The lower levels of polyploidy observed in $1x10^9$ pfu AdenoCre infected Flox/Null liver 3 weeks after infection could be caused by clearance of the lower levels of infected hepatocytes with time. In conclusion, higher levels of ploidy were observed in 6 week old AdenoCre infected Flox/Null livers when compared to infected Flox/Wt mimicking the premature polyploidy seen in complete *Ercc1*-deficient liver.

Lipid accumulation is a phenotypic characteristic of ageing liver and is associated with a rise in mtDNA mutations and deletions (Anantharaju et al. 2002). Mitochondria are the main source of cellular ROS and at the same time are the main target for ROS. A decrease in activity of hepatic anti- ROS defence mechanisms such as Mn- superoxide dismutase (SOD) might be responsible for the accumulation of oxidative mtDNA damage with age leading to a malfunction of mitochondrial pathways (Anantharaju et al. 2002). Higher amounts of macrovesicular lipids could be noted in 6 week old AdenoCre infected *Ercc1* Flox/Null liver 1 week after infection when compared to injected Flox/Wt controls. This lipid accumulation disappeared 3 weeks after infection in all Flox/Null samples. Clustered lipid

accumulation might take place in *Ercc1* Flox/Null hepatocytes that have undergone AdenoCre mediated recombination. Localised *Ercc1* deficiency in those hepatocytes might lead to cell clearance, which could explain the loss of accumulated, cytoplasmic lipid in *Ercc1* Flox/Null hepatocytes 3 weeks after AdenoCre infection. The early lipid accumulation could be caused by mitochondrial malfunction in the *Ercc1*- deficient hepatocyte population in the liver. Lipid peroxidation, caused by increased levels of ROS, can destroy the mitochondrial membrane, reducing its functionality. As lipids that are taken up from the blood are subjected to mitochondrial β- oxidation, a reduced capacity of mitochondrial function can lead to excess fat being stored in the cytoplasm (Patrick 2004). Although no evidence for direct involvement of *Ercc1* in the mitochondria exists (O'Neil and Melton, unpublished data), nuclear DNA mutations resulting from *Ercc1* deficiency could lead to a decrease in supply of nuclear encoded proteins needed to maintain mitochondrial function. Therefore, *Ercc1*- deficiency could indirectly lead to mitochondrial malfunction and lipid accumulation. The decrease in accumulated lipid in Flox/Null livers 3 weeks after infection could be explained by a partial clearance of *Ercc1*- deficient hepatocytes. Lipid accumulation as a consequence of mitochondrial membrane disruption has been found by Dirkx et al. (2005). A liver specific elimination of peroxisomes was achieved using the Cre loxP system, leading to an alteration in mitochondrial membrane structure and an accumulation of lipid vesicles in the cytoplasm. It would be interesting to determine the mitochondrial membrane potential in our Flox/Null AdenoCre infected livers to further strengthen the hypothesis that the accumulation of lipid observed is linked to a malfunction of mitochondrial pathways. In general, *Ercc1* Flox/Null livers with increased levels of polyploidy also showed higher amounts of lipid accumulation compared to *Ercc1* Flox/Null livers with a lesser response to the AdenoCre virus, indicating that lipid accumulation might be an early and more subtle response to loss of ERCC1 than polyploidisation.

Carbon tetrachloride is a liver damaging agent known to cause necrosis of the liver. CCl_4 requires metabolic activation in the liver and has been shown to act by

damaging lipid containing cellular components such as mitochondria, the endoplasmatic reticulum and the Golgi apparatus (Weber et al. 2003). Haloalkylation, impairment of lipid metabolism and lipid peroxidation is initiated by the radical, metabolically active form of CCl_4. Lipid accumulation and cell death occur in several stages after dosing (Weber et al. 2003). Necrosis is first seen 5-6 hours after CCl_4 treatment, leading to central zone necrosis after 12 hours and to massive necrosis 24-48 hours after injection with CCl_4 (Weber et al. 2003). High amounts of necrotic cell death were observed 1 day after injection with CCl_4. This is in accordance with the literature. Signs of necrosis were still apparent 5 days after insult with a complete recovery 7 days after treatment with CCl_4. Animals subjected to partial hepatectomy (PH) are able to replace the loss of liver mass within 1 week (Gupta 2000). PH leads to hepatocytes re- entering the cell cycle in a synchronised manner with a peak of DNA synthesis 36-40 hours after PH (Taub 2004). As a result of the liver mass replacement, hepatocytes become more polyploid and binuclear, limiting further regeneration. CCl_4 induces injury to the liver leading to the activation of similar molecular mechanisms as PH. However, hepatocytes are known to enter the cell cycle in a non- synchronised manner after CCl_4 injections (Taub 2004).

The capacity of the liver to recover from toxic insult results from its ability to re-enter the cell cycle and replace damaged hepatocytes (Seglen et al. 1997). Small, stem cell like hepatocytes are also thought to play a role during liver regeneration giving rise to a pool of diploid cells that can easily divide after insult (Mitaka et al. 1998). Cell cycle re-entry and subsequent liver regeneration is thought to be mediated in 2 different steps. Firstly, liver mass is replaced to its original size. Secondly, the reformation of the normal liver architecture can then be undertaken (Taub 2004). There are 2 main pathways regulating the restoration of the liver mass, one being the cytokine dependent pathway and the other being the growth factor dependent pathway. Cytokine IL- 6 is a key effector of liver regeneration and, upon binding to its receptor, activates the MAPK pathway, crucial to hepatocyte proliferation, and PI3K signalling, ensuring cell survival (Taub 2004). The growth factor mediated pathway promotes DNA replication during liver regeneration using

the hepatic growth factor (HGF)- Met pathway. DNA replication is induced by HGF binding to its receptor Met and then activating the PI3K and the MAPK-ERK pathway (Taub 2004). Stellate cells induce connexin-32 and keratin-8 production approximately 4 days after PH, helping to maintain the liver architecture by supplying extracellular matrix to the newly formed hepatocyte clusters. The termination of liver regeneration is regulated via a feed-back loop where cytokine suppressors are upregulated upon cytokine induction. In addition, maintenance of liver function during regeneration is ensured by upregulation of gluconeogenesis, supplying the organism with sufficient energy (Taub 2004). Cell cycle re- entry in our animals could be observed by measuring elevated levels of S-phase initially after treatment with 51 mg/ml and after 102 mg/ml of CCl_4 as detected by flow cytometry, although this increase was not as large as we had anticipated.

In addition to necrosis, higher levels of apoptosis were observed by flow cytometry when 51 mg/ml and 102 mg/ml of CCl_4 were given. Depending on the energy status of the cell and the damage caused by CCl_4, the cellular response can differ between apoptosis and necrosis (Schulze- Bergkamen 2006). High levels of ATP favour an apoptotic response in hepatocytes whereas depletion of ATP during mitochondrial membrane transition favours necrosis. In addition, ROS can activate lysosomal proteases which, at a low concentration, will cleave caspases and lead to apoptotic cell death. In contrast, high amounts of lysosomal proteases can induce a necrotic response (Schulze- Bergkamen 2006). This shows that different cell death patterns can co-exist in liver. Overall, CCl_4 treatment results in clearly increased polyploidy with small increases in S-phase and apoptotic cells, but no clear difference between the response in *Ercc1* Flox/Null and Flox/Wt livers.

The combination of AdenoCre virus and treatment with CCl_4 in vivo led to higher levels of ploidy in *Ercc1* Flox/Null livers compared to Flox/Wt samples when $1x10^9$ pfu virus was given. This difference was apparent 1 week after viral infection and treatment with CCl_4, but not after 3 weeks. In addition, no difference in ploidy status between the two genotypes could be observed when animals were treated with $4x10^9$

pfu AdenoCre and CCl_4. Furthermore, elevated levels of S-phase were found to be independent of genotype or virus titer in all treated livers. It seems that the increased polyploidy in both genotypes resulting from CCl_4 treatment is masking the small increase in ploidy observed as a result of *Ercc1* deficiency induced in *Ercc1* Flox/Null livers by AdenoCre infection. This model could therefore not be used to investigate short term consequences of *Ercc1*- deficiency.

Diethyl nitrosamine (DEN) is a known inducer of liver cancer acting through DNA adduct formation and oxidative DNA damage (Loft et al. 1998). A close correlation between elevated levels of 8-oxo-G and formation of liver tumours after DEN administration has been shown in rat liver (Loft et al. 1998). In addition, around 26 weeks after DEN exposure, using similar amounts of carcinogen to ourselves, Wt male rats displayed high amounts of adenomas with lower tumour frequency being apparent in female rat livers (Ischiwaka et al. 2001). Kalinina et al. (2003) found an increase in adenomas in Wt mice 25 weeks after 1μg/g BW DEN was given with hepatocellular carcinoma (HCC) appearing at around 42 weeks of age. We found a high tumour burden in *Ercc1* Wt liver 39 weeks after exposure to DEN. These tumours were classed as hepatocellular adenomas, showing that hepatocytes rather than other cell types undergo DEN induced changes. Lim (2002) describes and characterises a liver cancer model where DEN was used to initiate mutational damage to hepatocytes followed by weekly injections of Nodularin or Thioacetamide (TTA), which are similar in action to CCl_4, over a 10 week period to promote tumour formation by stimulating replication and cell division. Fixation of further mutations then led to hepatocellular carcinoma in rat livers 20 weeks after DEN treatment (Lim 2002). DEN induced p53 protein activation in liver during the initiation step, but no mutations in *p53* could be found during the first weeks after DEN injection. Exposure to TTA after DEN injections led to a loss of Rb function caused by an overexpresssion of gankyrin, which has been shown to accelerate the degradation of Rb (Lim 2002). In addition, although initially p16 expression was not altered after TTA treatment, hypermethylation of the promoter DNA led to an inactivation of p16 at later stages during TTA promotion. TGFβ receptors were found to be upregulated

in hepatocytes during the regeneration of the liver after DEN/TTA treatment (Lim 2002). In addition, non- parenchymal cells upregulated TGFβ expression, initially preventing uncontrolled hepatocyte proliferation and promoting apoptosis. However, during analysis of the HCC tissue a loss of TGFβ receptors was apparent in the tumours, explaining the gradual loss of response to TGFβ expression with time.

In skin of *Ercc1*- deficient mice, UVB- induced tumours were apparent in animals 8-17 weeks after three irradiations per week, with Wt animals not developing tumours when subjected to the same regime (Doig et al. 2006). Coordinated overexpression of *ERCC1* and *XPC* has been found to take place in hepatocellular carcinomas when compared to non-tumour tissue along with an increase of NER activity (Fautrel et al. 2005). This induction of *ERCC1* overexpression and increased activity of NER has been linked to EGF- stimulated proliferation in hepatocytes in tumour and normal livers via the MAPK pathway (Andrieux et al. 2006). In addition, ovarian, gastric and colon cancers are known to overexpress *ERCC1*, leading to a resistance to chemotherapeutic drugs. Thus, a lack as well as overexpression of *ERCC1* seem to have consequences during tumour development. A clear association with *ERCC1* deregulation and cancers has been established and it would be of interest to assess the long- term consequences of *Ercc1*- deficiency in liver. Our AdenoCre based mouse model using *Ercc1* Flox/Null and Flox/Wt animals is suited to address this issue, although my data indicate that there is uncertainty about the long term viability of *Ercc1*- deficient hepatocytes. In fact, a similar protocol to that of Lim (2002) could be used in a cancer study to determine the effect of partial *Ercc1*- deficiency in the liver. Unfortunately, limited time did not permit the inclusion of this study in my thesis.

6. Changes in the liver of complete *Ercc1* knockout mice

Originally, we set out to characterise the liver phenotype caused by *Ercc1* deficiency in a conditional, liver- specific knockout mouse model. However, one of the most striking features of *Ercc1* loss in the liver, premature polyploidy, was difficult to replicate in our conditional knockout system in vitro and in vivo. We therefore resumed examining our original *Ercc1* Null animals in more detail. Premature polyploidy has been previously characterised by nuclear size change (Chipchase et al. 2003). We hoped that flow cytometry could further help to examine the development of polyploidy in *Ercc1* Null and Wt animals of different age. In addition, we wanted to examine whether the lipid accumulation seen in older *Ercc1*-deficient hepatocyte cultures, after UV in vitro and in AdenoCre infected livers 1 week after infection was also apparent in our complete *Ercc1* knockout animals. In our conditional hepatocyte culture system it was indicated that both loss of NER function and of oxidative repair pathways led to decreased survival in *Ercc1*-deficient hepatocyte cultures. We set out to examine the lesions responsible for the premature polyploidy in our *Ercc1* Null livers in vivo in more detail. In addition, expression changes of selected genes were studied to help understand the changes in *Ercc1*- deficient livers on a molecular level.

6.1 Histology of *Ercc1* Null and Wt livers

Liver samples from 20 day old littermates were taken and processed for histology. H&E slides were prepared and pictures taken with a 40x objective. Large, polyploid nuclei were visible in *Ercc1* Null livers at 20 days of age with smaller nuclei persisting throughout the liver (Figure 29). *Ercc1* Wt nuclei showed few enlarged, polyploid nuclei. In conclusion, *Ercc1* Null livers contain polyploid nuclei at 20 days of age which is in accordance with previous findings (McWhir et al. 1993). We used flow cytometry to characterise the development of polyploidy in *Ercc1* Null and Wt livers in more detail.

Ercc1 Null Liver # 19

Ercc1 Wt Liver # 19

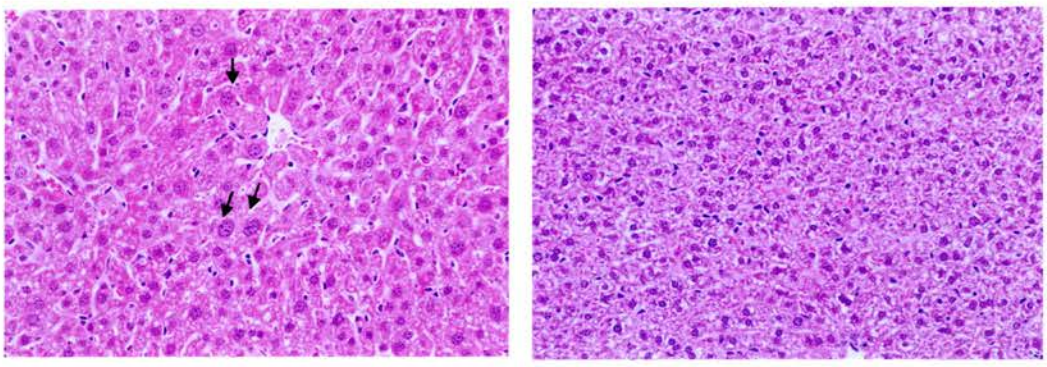

Figure 29: Histology of *Ercc1*- deficient and Wt liver. Liver sections were taken from littermate pair # 19 at 20 days after birth. All sections were H&E stained and pictures taken with a 40 x objective. Large hepatocyte nuclei in the Null sample are labelled with small black arrows.

6.2 Determination of DNA content in *Ercc1* Null and Wt livers by flow cytometry

Flow cytometry was used to analyse DNA content of *Ercc1* Null and Wt livers of different age. The individual ID numbers of littermate pairs are given in Table 8. The same samples were subjected to multiple analyses in this study. The amount of apoptosis is given as percent of all cells and the ploidy and S-phase data are expressed as percent of all viable cells. *Ercc1* Null animals displayed higher amounts of ploidy in the liver when compared to Wt littermates, even at a young age (Table 8). However, the difference in ploidy between *Ercc1* Null and Wt livers became more pronounced with age as visualised in a typical flow profile of livers of 20 day old animals (Figure 30). This increased polyploidy is in accordance with previous results obtained by McWhir et al. (1993), although no 16n hepatocyte population could be detected towards the maximum life span of the animals as previously described. Instead tetraploidy was 2 to 3- fold increased in *Ercc1* Null animals when compared to Wt littermates from the age of 12 days onwards. Animals were grouped into 3 different age categories to analyse the onset of polyploidisation in more detail. *Ercc1* Null livers showed no significant difference when compared to Wt littermates using a paired, two- tailed Student's t- test at the age of 1-5 days ($p= 0.2$ for 4n, $p= 0.16$ for 8n) (Table 9). However, *Ercc1* Null livers aged 10- 14 days showed significantly higher amounts of tetraploidy when compared to Wt littermate controls ($p= 0.03$, Table 9). The increased levels of octaploidy were borderline significant in *Ercc1*- deficient livers when compared to Wt control livers ($p= 0.057$, Table 9). Increases in both tetra- and octaploidy in *Ercc1* Null livers were significant when compared to Wt littermate controls in 19-21 day old animals ($p= 0.000004$ for 4n, $p= 0.0002$ for 8n, Table 9). Figure 31 summarises the increases in tetra- and octaploidy in *Ercc1* Null livers in the different age groups and shows typical levels of ploidy for age matched littermate controls.

Table 8: DNA content of *Ercc1*- deficient and Wt livers determined by flow cytometry. Data from littermates of different age are shown for both genotypes. The age is given in days after birth. Apoptosis is displayed as percentage of all cells. Ploidy status and S-phase are shown in percent of viable cells.

Genotype	Age (days)	Littermate Pairs (ID#)	2n (%)	4n (%)	8n (%)	S-phase (%)	Apoptotic (%)
Null	1	20	66.1	9.4	2.9	19.1	2.9
Wt	1	20	70.3	10.5	0.2	17.3	0.8
Null	1	21	67.9	13.5	0.4	16.3	0.6
Wt	1	21	70.3	8.7	0.2	18.9	1.6
Null	4	11	73.9	12.5	0.6	10.8	0.5
Wt	4	11	63.4	13.7	0.4	15.8	0.4
Null	4	12	68.6	17.1	1.2	9.2	0.8
Wt	4	12	72.1	11.5	0.3	13.2	0.7
Null	5	29	75.7	8.5	0.5	14.1	0.7
Wt	5	29	80.9	5.4	0.3	12.8	0.3
Null	10	13	85.8	8.3	0.6	2.2	1.9
Wt	10	13	84.7	6.0	0.2	6.5	0.9
Null	10	14	75.8	15.6	1.1	4.4	1.0
Wt	10	14	83.6	6.5	0.1	7.9	0.6
Null	12	27	71.1	18.0	2.9	4.9	0.2
Wt	12	27	86.3	5.9	0.3	5.7	0.2
Null	14	15	73.8	17.3	2.0	3.1	1.4
Wt	14	15	89.2	6.1	0.3	2.6	0.4
Null	19	17	61.0	25.3	5.9	1.5	0.8
Wt	19	17	75.4	10.6	0.5	2.1	0.4
Null	19	23	79.5	16.2	2.1	0.9	0.2
Wt	19	23	92.5	4.7	0.1	2.3	0.1
Null	19	24	76.4	17.0	2.7	1.6	0.3
Wt	19	24	90.2	7.9	0.2	1.0	0.3
Null	20	19	72.6	17.9	3.7	4.1	0.6
Wt	20	19	88.2	7.3	0.4	2.4	0.5
Null	20	25	69.7	20.7	4.2	2.1	1.1
Wt	20	25	85.6	11.0	0.4	1.5	0.6
Null	21	22	70.1	20.6	4.0	1.4	1.1
Wt	21	22	81.5	8.5	0.4	1.9	0.4
Null	21	26	70.4	21.2	4.5	1.3	0.2
Wt	21	26	88.8	8.1	0.0	1.1	0.2

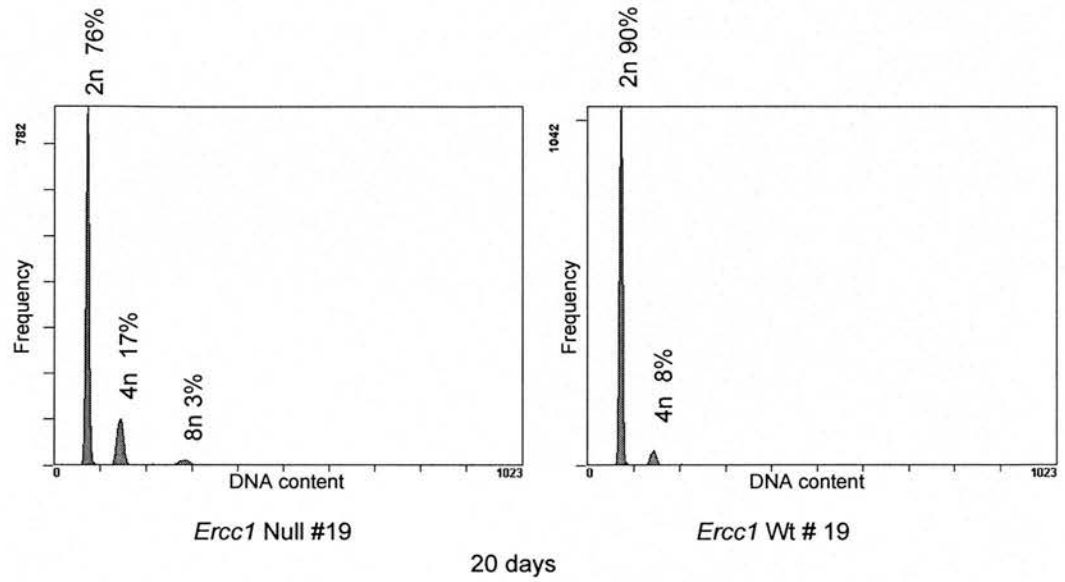

Figure 30: Flow cytometry profile showing the DNA content of 20 day old *Ercc1*- deficient and Wt liver (pair # 19). The different cell fractions are labelled. Diploid, tetraploid and octaploid fractions are given as the percentage of viable cells.

Table 9: Statistical analysis of DNA content of *Ercc1*- deficient and Wt livers in different age groups. Animals were divided into 3 different age groups, 1-5, 10-14 and 19-21 days after birth. The mean and the SEM is given for each group and genotype. A two- tailed, paired Student's t- test was performed and the p value is given for the null hypothesis that there is no difference between genotypes.

Genotype	Age (days)	2n (Mean ± SEM)	p value (2n)	4n (Mean ± SEM)	p value (4n)	8n (Mean ± SEM)	p value (8n)	S-phase (Mean ± SEM)	p value (S-phase)	Apoptotic (Mean ± SEM)	p value (Apoptosis)
Null	1-5	70.43 ± 1.9	0.75	12.18 ± 1.5	0.20	1.11 ± 0.5	0.160	13.89 ± 1.8	0.29	1.08 ± 0.5	0.56
Wt	1-5	71.4 ± 2.8		9.95 ± 1.4		0.29 ± 0.04		15.6 ± 1.2		0.75 ± 0.2	
Null	10-14	76.65 ± 3.2	0.098	14.8 ± 2.2	0.03	1.64 ± 0.5	0.057	3.65 ± 0.6	0.17	1.13 ± 0.4	0.1
Wt	10-14	85.95 ± 1.2		6.09 ± 0.1		0.22 ± 0.04		5.68 ± 1.1		0.54 ± 0.1	
Null	19-21	71.37 ± 2.2	0.000002	19.82 ± 1.2	0.000004	3.87 ± 0.5	0.0002	1.83 ± 0.4	0.83	0.61 ± 0.1	0.054
Wt	19-21	86.03 ± 2.2		8.29 ± 0.8		0.28 ± 0.1		1.74 ± 0.2		0.35 ± 0.1	
Null	1-21									0.9 ± 0.2	0.046
Wt	1-21									0.5 ± 0.1	

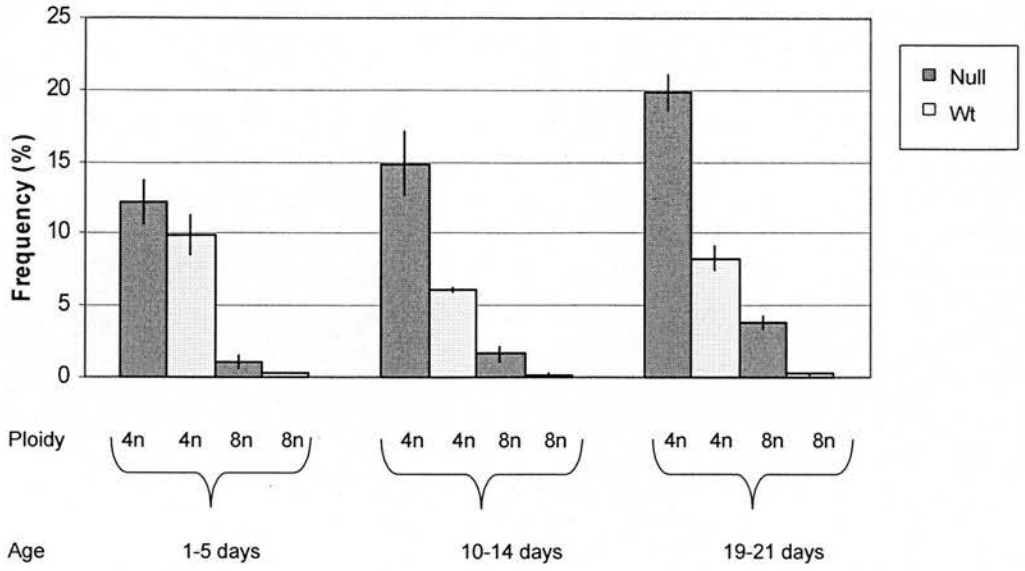

Figure 31: Development of tetra- and octaploidy in *Ercc1*- deficient and Wt livers in different age groups. Animals were divided into 3 different age groups, ranging from 1-5, 10-14 and 19-21 days after birth. The mean and the SEM is given for each group and genotype.

Levels of S-phase seemed to be high in all young animals, decreasing with age (Table 9). Significant levels of haematopoiesis still occur in livers of young animals. When levels of S-phase in *Ercc1* Null and Wt livers were compared between the 3 age groups, no significant difference was noted between the genotypes (Table 9). When *Ercc1* Null and Wt livers were grouped according to age, a slight difference in apoptosis levels between genotypes became apparent (Table 9). 1-5 day and 10-14 day old livers displayed no significant difference in levels of apoptosis in *Ercc1* Null and Wt livers ($p= 0.56$ for 1-5 day group, $p= 0.1$ for 10-14 day group). However, at the age of 19-21 days, *Ercc1* Null livers showed a borderline significant difference in apoptosis levels when compared to Wt littermate controls (mean Null 0.61 ± 0.1, mean Wt 0.35 ± 0.1, $p= 0.054$, Table 9). This value might become significant with increased sample size and gives an indication of increased apoptosis in *Ercc1* Null livers with age. When all collected data were analysed, a significant difference in apoptosis between *Ercc1* Null and Wt livers could be observed, with increased levels of apoptosis in *Ercc1*- deficient livers (Null 0.9 ± 0.2, Wt 0.5 ± 0.1, $p= 0.046$, Table 9).

In conclusion, the striking polyploid liver phenotype in *Ercc1*- deficient animals was confirmed. Increased levels of apoptosis could also be detected in *Ercc1* Null livers when compared to Wt.

6.3 Detection of lipid accumulation in *Ercc1*- deficient liver by Oil Red O stain

Liver samples of 5 (ID # 29), 14 (ID #15) and 21 (ID #26) day old animals were taken and processed for Oil Red O staining. Lipid accumulated in the cytoplasm of all livers, irrespective of genotype at a young age, leading to the formation of micro- and macrovesicles (Figure 32). At 14 days of age, macro- and microvesicular lipid accumulation persisted in *Ercc1*- deficient liver with decreased levels of accumulated lipids being visible in *Ercc1* Wt littermates where microvesicular lipid accumulation was predominant. When Oil Red O staining was performed on livers of both

genotypes at the age of 21 days, micro- and macrovesicular lipid accumulation was still apparent in the cytoplasm of *Ercc1*- deficient liver. In contrast, only very small amounts of lipid were detectable in *Ercc1* Wt littermates (Figure 32). In conclusion, lipid accumulated in young livers independent of genotype with a gradual disappearance of cytoplasmic lipids in *Ercc1* Wt livers and persisting levels of lipid in *Ercc1* Null livers with age.

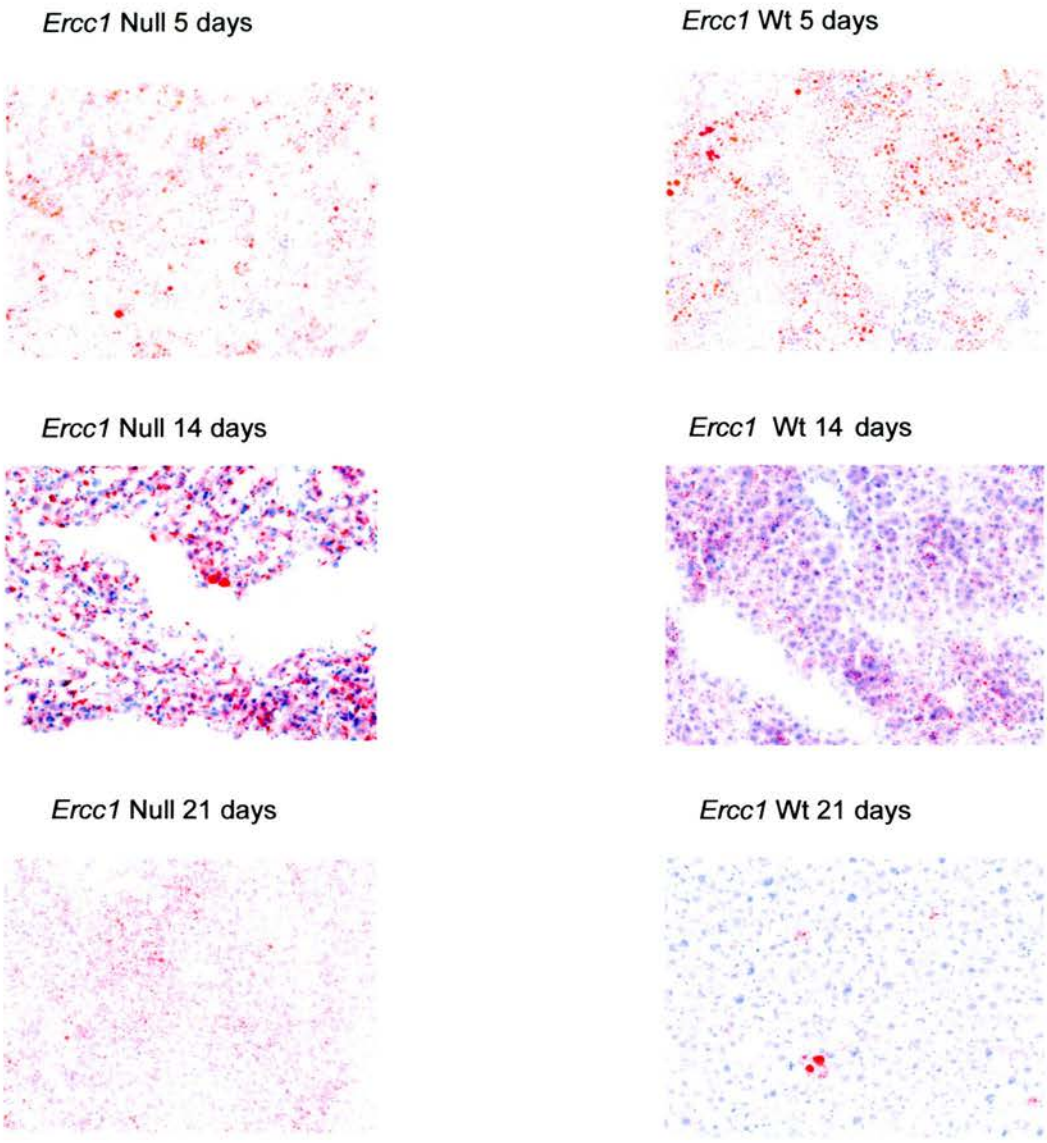

Figure 32: Lipid accumulation in *Ercc1*- deficient and Wt liver. Livers were stained with Oil Red O 5 (pair # 29), 14 (pair # 15) and 21 (pair # 26) days after birth. Pictures were taken with a 40x objective. Lipid vesicles are stained in red and cytoplasm and nuclei are stained in blue.

6.4 Characterisation of triglyceride content in *Ercc1*- deficient and Wt liver

In an attempt to further characterise the lipid accumulation seen in older *Ercc1* Null livers, we analysed the triglyceride content of 19-21 day old *Ercc1* Null and Wt livers (ID # 19, 23, 24, 26). Triglycerides are one of the lipids possibly accumulating in the cytoplasm of *Ercc1*- deficient livers with age as Oil Red O stains triglycerides and other hydrophobic lipids, such as cerebrosides and cholesterol esters. Cytoplasmic triglycerides are also found after CCl_4 induced damage to livers, where the damaged endoplasmic reticulum is found to reduce the release of triglycerides into the plasma and an accumulation takes place in the cytosol of hepatocytes (Weber et al. 2003). Higher triglyceride levels were detected in our *Ercc1*- deficient animals when compared to Wt littermate controls (Figure 33). However, this difference was not significant because of a high variability of triglyceride content observed in *Ercc1*- deficient livers ($p= 0.24$ by paired, two- tailed Student's t- test). An increase in sample number might lead to this difference becoming significant.

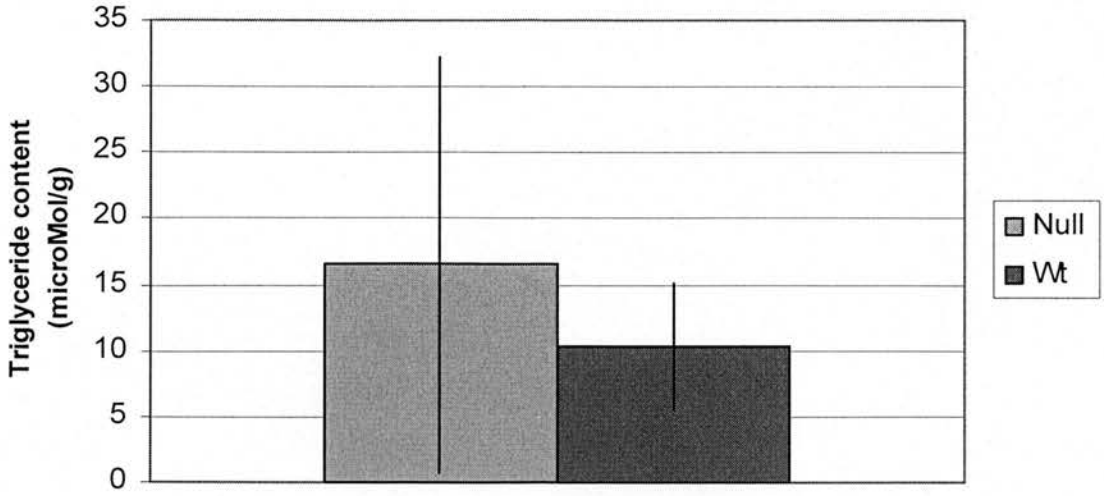

Figure 33: Triglyceride levels in *Ercc1*- deficient and Wt liver. Samples were taken from 19-21 day old animals (from littermate pairs with ID # 19, 23, 24 and 26). The amount of triglyceride is given as µMol/g of liver. The mean of four different samples is given. The SEM is indicated with error bars.

6.5 Characterisation of levels of reactive oxygen species in *Ercc1*- deficient and Wt livers

The amount of reactive oxygen species (ROS) was measured in *Ercc1*- deficient and Wt littermates of different age using the CM-H_2DCFDA – method. CM-H_2DCFDA is a cell permeable diacetate ester which fluoresces upon reaction with ROS. The assay was done on freshly isolated hepatocytes plated in 1x HBSS. The amounts of ROS were normalised to the amounts of cell protein measured per sample and were expressed on a relative scale giving the ratio of ROS in *Ercc1* Null versus Wt livers. For statistical analysis, we grouped animals into 2 age groups, from 5-7 days and 9-21 days. An increase in ROS could be detected in *Ercc1*- deficient liver at 5 and 7 days of age when compared to Wt littermates (Figure 34). Furthermore, this trend of increased ROS in *Ercc1* Null liver reversed with increased age, leading to higher amounts of ROS in *Ercc1* Wt livers when compared to the Null littermates. This increase in ROS in Null livers compared to Wt was not significant when both age groups were compared using the Wilcoxon matched pair test ($p= 0.08$). However, ROS levels in 12 day old *Ercc1* Null hepatocytes were surprisingly low and differed from all other data points of the same genotype. In conclusion, *Ercc1*- deficient livers show a trend towards higher levels of ROS at a young age compared to Wt littermates, but this difference is reversed in older animals.

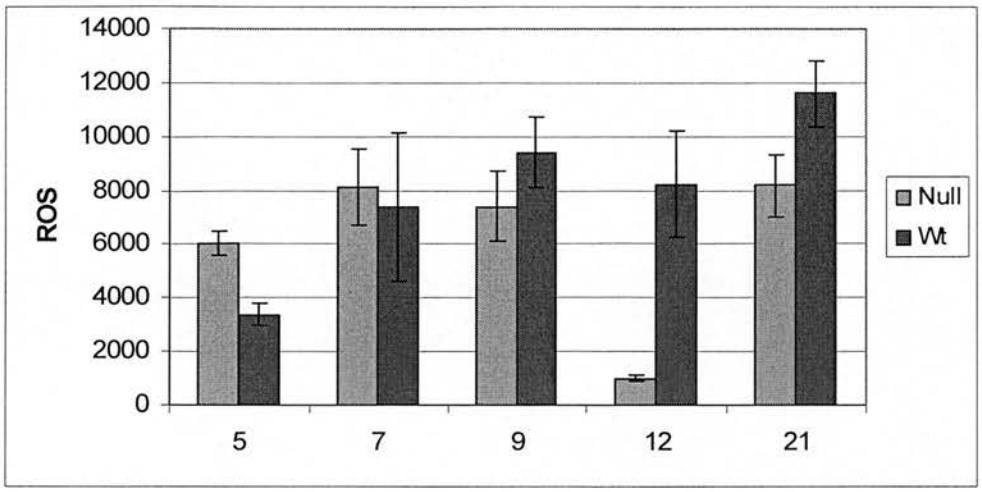

Figure 34: Reactive oxygen species in *Ercc1*- deficient and Wt hepatocytes. The amount of ROS normalised to the amount of protein in isolated Null and Wt hepatocytes is shown on a relative scale. The mean of 3 wells is given for each sample. The SEM is indicated with error bars. The age of the animals is given in days. Littermate pairs # 26 (21 days old), # 27 (12 days old), # 29 (5 days old), # 30 (7 days old) and # 31 (9 days old) are shown.

6.6 Analysis of malondialdehyde adducts in *Ercc1*- deficient and Wt livers

Malondialdehyde adducts are a form of DNA adduct found in an environment of high oxidative stress. The most common form of malondialdehyde adducts are malondialdehyde deoxyguanosine (M_1dG) DNA adducts. In addition, malondialdehydes can also react with DNA forming interstrand cross- links (Leuratti et al. 1998). We subjected *Ercc1*- deficient and Wt livers of different age to immunoslot blotting to determine the M_1dG content in liver DNA. 1 day after birth, nearly 2 times higher levels of M_1dG adducts could be detected in livers of *Ercc1*- deficient animals when compared to Wt littermates (n=2, Table 10). This difference was not significant resulting from a high variability in the amount of M_1dG adducts found in *Ercc1*- deficient livers ($p= 0.41$, Table 10). An increase of sample size could possibly result in this difference becoming significant. At 10 days of age, similarly low amounts of M_1dG DNA adducts were apparent in *Ercc1*- deficient and Wt livers (n=2, $p= 0.99$, Table 10). Moreover, 14-20 day old *Ercc1*- deficient animals showed nearly 2 times lower levels of M_1dG DNA adducts in their livers when compared to Wt littermates (n=3). This difference was significant with the p- value being < 0.01. In summary, *Ercc1*- deficient livers, when compared to Wt littermates, display high amounts of M_1dG adducts soon after birth. The levels of M_1dG DNA adducts are lower at the end of the maximum life span of the *Ercc1*- deficient animals, so that in 20 day old animals, levels of M_1dG DNA adducts are higher in Wt controls than in their *Ercc1*- deficient littermates.

Table 10: Malondialdehyde adducts in *Ercc1*- deficient and Wt liver. Levels of deoxyguanosine malondialdehyde adducts (M_1dG) are given per 10^8 nucleotides. Animals were grouped according to age and genotype. The three age groups consisted of animals being 1, 10 and 14-20 days old. ID numbers of littermate pairs are indicated for each group. The mean of malondialdehyde adducts is given for the different age groups. The SEM and the p-value, obtained from a paired t-test for the null hypothesis that there is no difference between genotypes, are given.

Genotype	ID #	Age (days)	M_1dG per 10^8 nucleotides (mean ± SEM)	p value
Null	20, 21	1	118.51 ± 71.7	
Wt	20, 21	1	67.86 ± 33.1	0.41
Null	13, 14	10	24.35 ± 14.2	
Wt	13, 14	10	24.3 ± 11.7	0.99
Null	15, 17, 19	14-20	68.16 ± 13.2	
Wt	15, 17, 19	14-20	113.62 ± 11.5	0.007

6.7 mRNA expression studies in *Ercc1*- deficient and Wt livers using RT Real- time PCR

RT Real- time PCR was performed on *Ercc1*- deficient livers and Wt littermates aged 4- 21 days. The expression of selected genes involved in cell cycle regulation, apoptosis and oxidative damage response was determined in duplicate experiments with the same set of samples. A normalisation factor was calculated from expression levels of the two reference genes, *Gapdh* and *Tbp*, for each sample following Vandesompele et al. (2002). The standard curve method was used, as reliable standard curves were produced for each run, and all calculations were performed following Larionov et al. (2004). The mean of both experiments was taken and the expression ratio of Null to Wt livers was plotted on a log scale. The SEM for each sample set is indicated with error bars.

6.7.1 Insulin- like growth factor binding protein 2 (IGFBP2)

IGFBP2 binds to insulin- like growth factor (IGF) I and II, thereby regulating the availability of IGF to a range of tissues. *Igfbp2* expression has been found to be upregulated in cell sorted fractions of polyploid hepatocyte nuclei compared to diploid nuclei from wild type mice (Pin et al. unpublished data). We examined the expression in 9 pairs of *Ercc1* Null and Wt livers aged 4-21 days. *Igfbp2* expression was upregulated in all *Ercc1*- deficient livers when compared to Wt littermate controls, independent of age (Figure 35). This upregulation resulted from increased levels of *Igfbp2* mRNA levels in Null livers with a more or less constant expression of *Igfbp2* in Wt livers in all but littermate pair # 15. The highest expression of *Igfbp2* was found in 14 day old *Ercc1* Null liver where the increase was found to be 25- fold (ID # 15). In this sample pair, *Igfbp2* mRNA levels were increased in Null liver with a slight decrease in Wt liver mRNA levels being apparent at the same time. The average increase in *Ercc1*- deficient livers was around 3- fold (ratio mean for all samples, excluding pair # 15: 3.3 ± 0.6; overall ratio mean: 5.7± 2.5). Overall,

increased *Igfbp2* mRNA levels were detected in *Ercc1* Null livers when compared to Wt control littermates.

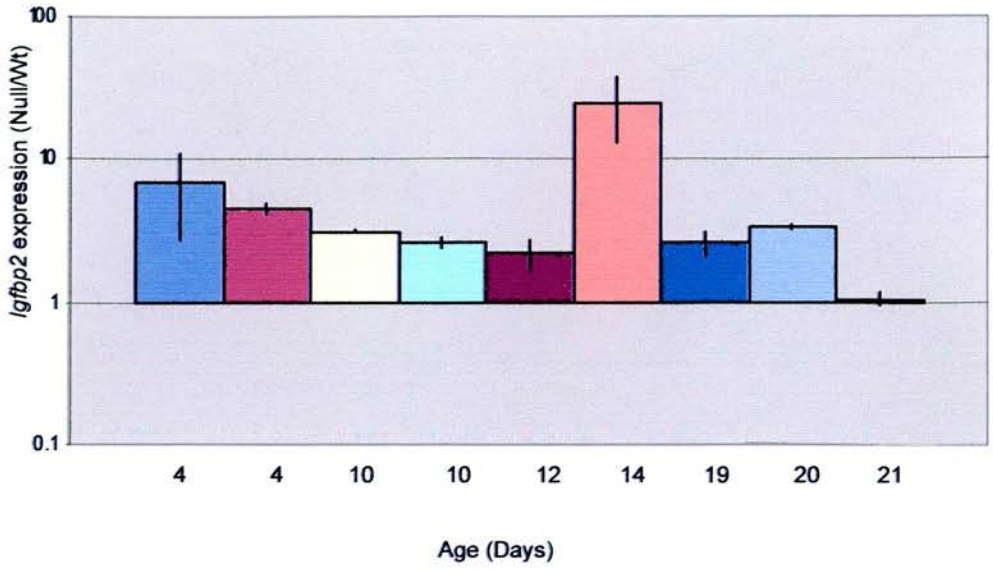

Figure 35: *Igfbp2* expression in *Ercc1*- deficient and Wt liver determined by RT- Real- time PCR. The ratio of Null versus Wt expression is given. A log scale is used to display the ratios. Each sample was run twice. The mean and the SEM are given for each pair. For each sample a normalisation factor was calculated for the reference genes *Gapdh* and *Tbp*. All samples were normalised before calculating the ratio of *Igfbp2* expression. Order of *Ercc1* Null/Wt pairs: *Ercc1* 4 days old (# 11); 4 days old (# 12); 10 days old (# 13); 10 days old (# 14); 12 days old (# 27); 14 days old (# 15); 19 days old (# 17); 20 days old (# 19); 21 days old (# 26).

6.7.2 p21

p21 is involved in cell cycle regulation and has been found to be upregulated in *Ercc1*- deficient, polyploid hepatocyte nuclei using immunohistochemistry and at the mRNA level using northern blotting (Chipchase et al. 2003, Nunez et al. 2000). This upregulation of *p21* was confirmed at the mRNA level in 4-20 day old *Ercc1* Null livers when compared to Wt littermates (Figure 36). The increase in *p21* expression resulted from an upregulation in Null livers with Wt livers expressing *p21* more or less constantly apart from in littermate pair # 13 where Null levels were constant and Wt levels changed. Again, the highest levels of *p21* mRNA were found in 14 day old *Ercc1*- deficient liver where a 30- fold increase was observed (ID # 15). The average level of *p21* expression lay typically around 2- fold (ratio mean for all samples, excluding pair # 15: 2 ± 0.3; overall ratio mean: 5.3± 3.3). *p21* was downregulated at 21 days of age where mRNA levels were 2- fold lower in *Ercc1*- deficient liver when compared to Wt (ID # 26). This decrease resulted from a decrease in *p21* mRNA expression in Null liver with Wt liver expressing similar levels compared to all other Wt livers examined. In summary, an upregulation of *p21* mRNA was detected in 4- 20 day old *Ercc1* deficient livers when compared to Wt littermates.

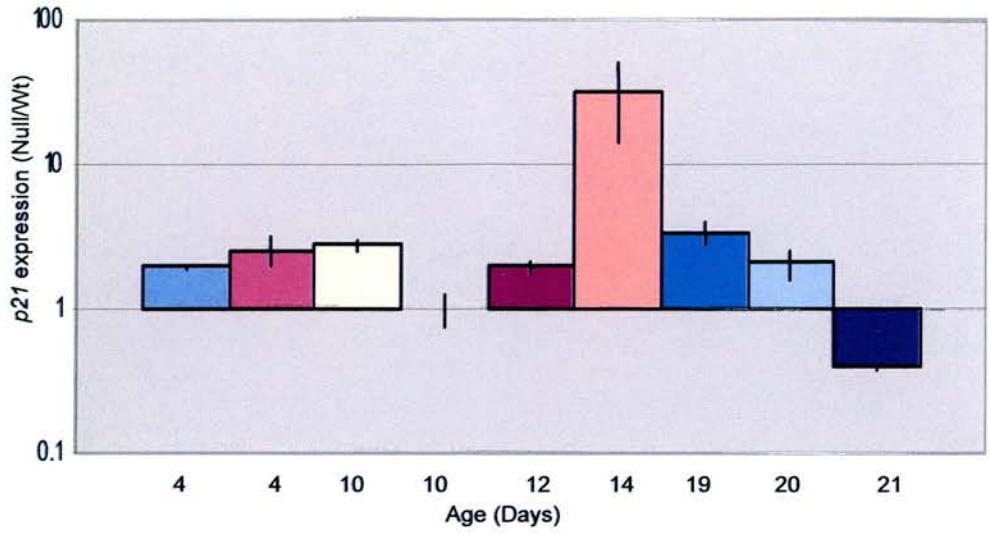

Figure 36: *p21* expression in *Ercc1*- deficient and Wt liver determined by RT- Real- time PCR. The ratio of Null versus Wt expression is given. A log scale is used to display the ratios. Each sample was run twice. The mean and the SEM are given for each pair. For each sample a normalisation factor was calculated for the reference genes *Gapdh* and *Tbp*. All samples were normalised before calculating the ratio of *p21* expression. Order of *Ercc1* Null/Wt pairs: *Ercc1* 4 days old (# 11); 4 days old (# 12); 10 days old (# 13); 10 days old (# 14); 12 days old (# 27); 14 days old (# 15); 19 days old (# 17); 20 days old (# 19); 21 days old (# 26).

6.7.3 Transforming growth factor β (TGF β)

TGF β is a multi- functional protein that is involved cell cycle regulation, modulation of differentiation, induction of apoptosis and angiogenesis and in maintenance of genome stability (Romero- Gallo et al. 2005). *Tgfβ* overexpression has been found to be a marker of liver cancer progression (Romero- Gallo et al. 2005). When *Tgfβ* mRNA levels were determined in *Ercc1* Null and Wt livers of different age, increased levels of *Tgfβ* were found in most younger *Ercc1* Null livers when compared to Wt controls (Figure 37). The highest levels were found in 4 day old *Ercc1* Null livers with 3- fold increased *Tgfβ* mRNA levels (ratio mean = 3 ± 0.95). On average *Tgfβ* was nearly 2- fold upregulated in 4-14 day old *Ercc1*- deficient livers (ratio mean = 1.9 ± 0.4) . The difference in expression was caused by upregulation of *Tgfβ* in Null livers in some littermate pairs and downregulation in Wt liver expression in others. In contrast, in 19-21 day old livers, Wt expression of *Tgfβ* mRNA was 2- fold higher compared to Nulls (ratio mean = 0.6 ± 0.06). In summary, high *Tgfβ* mRNA levels were apparent in young *Ercc1* Null livers with a decrease in older livers.

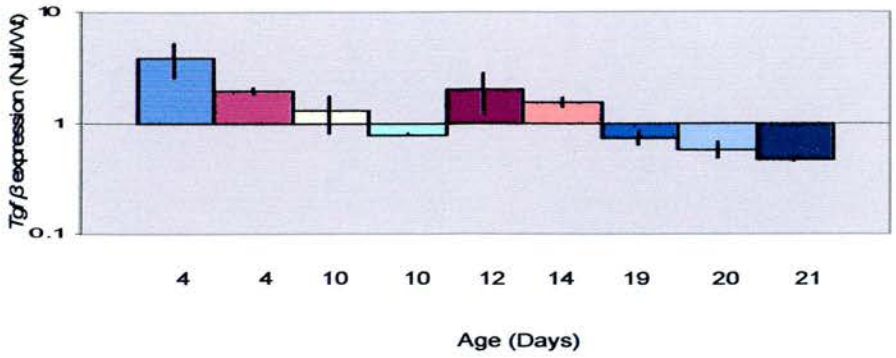

Figure 37: *Tgf β* expression in *Ercc1*- deficient and Wt liver determined by RT- Real- time PCR. The ratio of Null versus Wt expression is given. A log scale is used to display the ratios. Each sample was run twice. The mean and the SEM are given for each pair. For each sample a normalisation factor was calculated for the reference genes *Gapdh* and *Tbp*. All samples were normalised before calculating the ratio of *Tgf β* expression. Order of *Ercc1* Null/Wt pairs: *Ercc1* 4 days old (# 11); 4 days old (# 12); 10 days old (# 13); 10 days old (# 14); 12 days old (# 27); 14 days old (# 15); 19 days old (# 17); 20 days old (# 19); 21 days old (# 26).

6.7.4 BAX

BAX is a pro- apoptotic factor which has been shown to be downregulated in rat liver after exposure to oxidative damaging agents (Holmes et al. 2002). Expression studies of *Bax* in *Ercc1*- deficient livers and Wt littermates showed an upregulation of mRNA in 4-14 day old *Ercc1*- deficient livers (Figure 38). The highest levels of *Bax* mRNA were found in 14 day old *Ercc1* Null liver when compared to a Wt control with a 5- fold increase (ID # 15). The average increase in *Bax* expression was found to be around 2- fold in 4-12 day old *Ercc1*- deficient liver (ratio mean = 1.7 ± 0.1) . *Bax* mRNA levels decreased in *Ercc1* Null livers from 19 days of age onwards, showing a 1.5- fold downregulation when compared to Wt livers (ID # 17, 19, 26 ratio mean = 0.7 ± 0.2). The Wt liver *Bax* mRNA levels were consistent throughout, with changes in ratio being caused by differences in Null liver expression of *Bax* mRNA in all samples but littermate pair # 26. Surprisingly, at 21 days of age, slightly higher levels of *Bax* mRNA were found in *Ercc1* Null livers compared to Wt, but note the relatively large error bars associated with this ratio (ID # 26). In summary, 4-14 day old *Ercc1*- livers showed increased levels of *Bax* mRNA in comparison to Wt littermates, with a downregulation being apparent in older *Ercc1*- deficient livers.

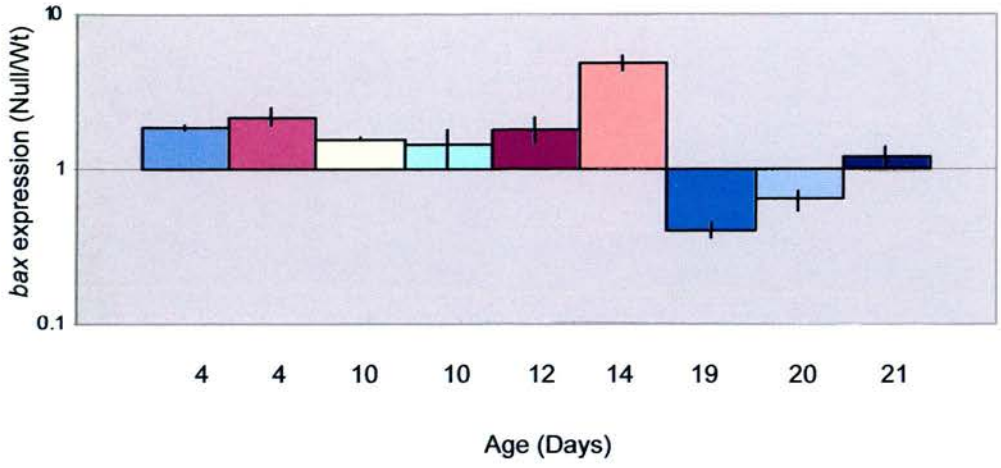

Figure 38: *Bax* expression in *Ercc1*- deficient and Wt liver determined by RT- Real- time PCR. The ratio of Null versus Wt expression is given. A log scale is used to display the ratios. Each sample was run twice. The mean and the SEM are given for each pair. For each sample a normalisation factor was calculated for the reference genes *Gapdh* and *Tbp*. All samples were normalised before calculating the ratio of *bax* expression. Order of *Ercc1* Null/Wt pairs: *Ercc1* 4 days old (# 11); 4 days old (# 12); 10 days old (# 13); 10 days old (# 14); 12 days old (# 27); 14 days old (# 15); 19 days old (# 17); 20 days old (# 19); 21 days old (# 26).

6.7.5 Proliferating cell nuclear antigen (PCNA)

PCNA is a processivity factor for polymerase δ and ε and is essential for DNA replication and repair. *Pcna* expression was found to be increased in rat liver in response to oxidative damage (Holmes et al. 2002). In addition, Hsia (2000) found increased levels of PCNA protein in *Ercc1*- deficient livers when compared to Wt samples. When *Ercc1*- deficient and Wt livers were compared for *Pcna* mRNA levels a slight downregulation was noted in all *Ercc1* Null livers from 4-21 days of age (Figure 39). The lowest levels of *Pcna* mRNA were found in 4 and 19-20 day old *Ercc1*- deficient livers with 1.5 – fold lower levels at 4 days of age (ratio mean = 0.7 ± 0.02) and nearly 3- fold lower levels at 20 days of age (ratio = 0.4). The difference in expression was caused by downregulation of *Pcna* in Null livers in some littermate pairs and upregulation of *Pcna* expression in Wt livers in others. In summary, a slight decrease in *Pcna* mRNA levels was detected in *Ercc1* Null livers.

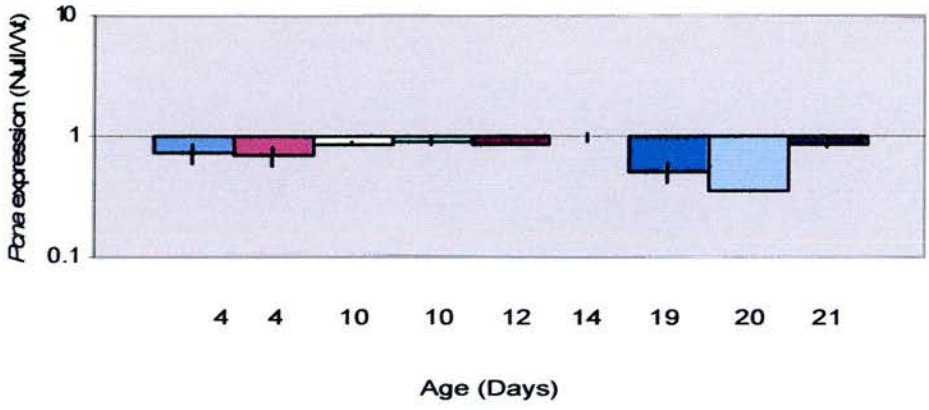

Figure 39: *Pcna* expression in *Ercc1*- deficient and Wt liver determined by RT- Real- time PCR. The ratio of Null versus Wt expression is given. A log scale is used to display the ratios. Each sample was run twice. The mean and the SEM are given for each pair. For each sample a normalisation factor was calculated for the reference genes *Gapdh* and *Tbp*. All samples were normalised before calculating the ratio of *Pcna* expression. Order of *Ercc1* Null/Wt pairs: *Ercc1* 4 days old (# 11); 4 days old (# 12); 10 days old (# 13); 10 days old (# 14); 12 days old (# 27); 14 days old (# 15); 19 days old (# 17); 20 days old (# 19); 21 days old (# 26).

6.7.6 Redox factor 1 (REF-1)

REF-1 is involved in the defence mechanism after oxidative injury as part of the BER pathway and has been shown to be upregulated in rat livers after challenge with oxidative damaging agents (Holmes et al. 2002). Previous immunohistochemistry studies in *Ercc1*- deficient livers suggested an upregulation of *Ref-1* in *Ercc1*-deficient livers when compared to Wt samples (Chipchase 2002). RT Real- time PCR studies using *Ercc1* Null and Wt livers aged 4-21 days could not reveal a trend in *Ref-1* expression with *Ref-1* mRNA levels showing a small increase in some *Ercc1*-deficient livers and a small decrease in others independent of age (Figure 40).

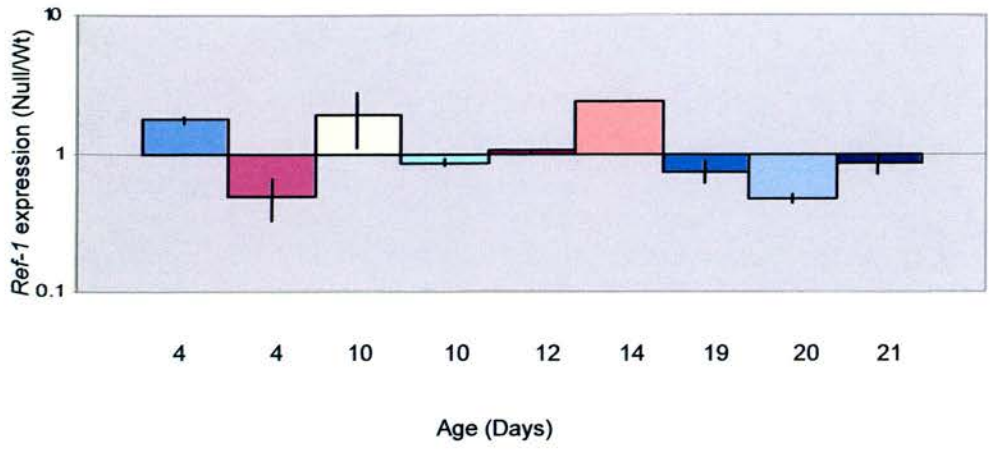

Figure 40: *Ref-1* expression in *Ercc1*- deficient and Wt liver determined by RT- Real- time PCR. The ratio of Null versus Wt expression is given. A log scale is used to display the ratios. Each sample was run twice. The mean and the SEM are given for each pair. For each sample a normalisation factor was calculated for the reference genes *Gapdh* and *Tbp*. All samples were normalised before calculating the ratio of *Ref-1* expression. Order of *Ercc1* Null/Wt pairs: *Ercc1* 4 days old (# 11); 4 days old (# 12); 10 days old (# 13); 10 days old (# 14); 12 days old (# 27); 14 days old (# 15); 19 days old (# 17); 20 days old (# 19); 21 days old (# 26).

6.7.7 Polymerase β

Polymerase β is involved in BER where it catalyses the filling of single nucleotide gaps after oxidative damage. *Polymerase β* mRNA levels were found to be upregulated in rat liver after exposure to oxidative stress (Holmes et al. 2002). When mRNA levels of *polymerase β* were determined in *Ercc1* Null and Wt livers of different age, no trend could be detected in mRNA expression between the genotypes (Figure 41).

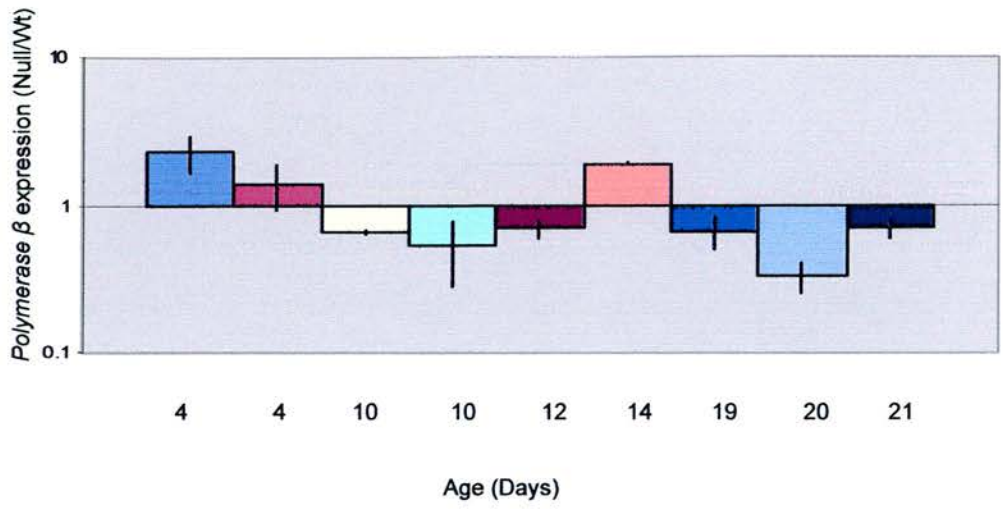

Figure 41: *Polymerase β* expression in *Ercc1*- deficient and Wt liver determined by RT-Real- time PCR. The ratio of Null versus Wt expression is given. A log scale is used to display the ratios. Each sample was run twice. The mean and the SEM are given for each pair. For each sample a normalisation factor was calculated for the reference genes *Gapdh* and *Tbp*. All samples were normalised before calculating the ratio of *polymerase β* expression. Order of *Ercc1* Null/Wt pairs: *Ercc1* 4 days old (# 11); 4 days old (# 12); 10 days old (# 13); 10 days old (# 14); 12 days old (# 27); 14 days old (# 15); 19 days old (# 17); 20 days old (# 19); 21 days old (# 26).

6.8 Discussion

Ercc1- deficient livers were further characterised to gain a better understanding of the mechanisms involved in the premature ageing phenotype of those mice. A hallmark of *Ercc1*- deficiency is the increase in levels of polyploid hepatocytes at a very young age which is comparable to levels seen in 2 year old Wt livers (McWhir et al. 1993, Weeda et al. 1998). We confirmed the increased levels of ploidy in our *Ercc1*- deficient livers aged 1- 21 days when compared to Wt littermates and established a time related pattern for the onset of polyploidy in *Ercc1* Null livers. At 1-5 days of age there was no significant difference in levels of polyploidy between the genotypes. This changed when 10- 14 day old livers of *Ercc1* Null and Wt animals were compared. Significant differences in tetraploidy become apparent at this time point. In addition, in 19-21 day old *Ercc1* Null livers, levels of tetra- an octaploidy were significantly increased when compared to Wt littermates. Overall, with increased age, an increase in polyploidy was observed in *Ercc1* Null livers. This could be caused by accumulating DNA damage with age, triggering polyploidisation as a protective mechanism (Weeda et al. 1998). In addition, *Ercc1*- deficiency might cause changes in nuclear gene regulation, leading to the onset of polyploidy over time. Interestingly, levels of octaploidy were lower in our *Ercc1*- deficient mice when compared to our previous results (McWhir et al. 1993, Nunez et al. 2000). In both cases there were high levels of tetraploid hepatocytes from 12 days of age onwards. The two studies were conducted more than 6 years apart in different mouse houses. Differences in milk composition due to changes in food given to the mothers could explain the differences in polyploidy levels. It has been shown that environmental factors such as food uptake play a role in ploidy levels of the liver (Gupta 2000). The animals are all on a non- inbred background which might have changed with time, leading to differences in levels of ploidy. In addition, 6 week old AdenoCre infected Flox/Null livers showed higher levels of octaploidy, but not tetraploidy, 1 week after infection when compared to infected Flox/Wt livers. This discrepancy between total levels of tetraploidy and octaploidy in *Ercc1*- deficient livers and AdenoCre infected Flox/Null livers could be explained by the difference in

age. AdenoCre infection occurs in 6 week old animals, where some polyploidisation has already occurred. AdenoCre infected animals of a younger age might give rise to a similar pattern of polyploidisation when compared to the simple *Ercc1*- deficient animals.

If oxidative damage was responsible for the liver failure in our *Ercc1*- deficient animals the life span of those animals could be improved by adding antioxidants such as Vitamin E and C to the food (Wu and Cederbaum 2003). The antioxidants should be passed on in the mother's milk to the pups and help to increase life span, rendering it possible to study the effects of *Ercc1*- deficiency in slightly older animals.

S- phase levels were high in young animals independent of genotype, decreasing with age. This decline in replication is to be expected as part of the normal maturation process and correlates with a decline of replicating haematopoietic cells, typically apparent in liver after birth (Gupta 2000). Nunez et al. (2000) found lower levels of replication in *Ercc1* Null livers when compared to Wt controls. However, this difference was not significant. Our data do not support the finding that replication is impaired in *Ercc1* Null livers. A difference in methodology could be the reason for this discrepancy as Nunez et al. (2000) used BrdU staining to determine replication potential whereas we used flow cytometry. As discussed earlier, BrdU staining is the more accurate method of S- phase determination. This might be particularly important given that only small changes in levels of S-phase would be predicted between the genotypes.

Although not always significant when the data were analysed by age, we observed a tendency towards increased levels of apoptosis in *Ercc1* Null livers when compared to Wt littermate controls using flow cytometry. Apoptosis could be triggered by increased levels of DNA damage using the p53 signalling pathway where polyploidisation does not provide sufficient protection. When all data were analysed

together significantly higher amounts of apoptosis were apparent in *Ercc1* Null livers compared to Wt. In fact, Dolle et al. (2006) suggest that one possible mechanism leading to liver failure in *Ercc1*- deficient animals could be increased rates of DNA damage- induced apoptosis. My in vivo data are in accordance with my previous findings which found increased levels of apoptosis in *Ercc1*- deficient hepatocyte cell cultures with time in culture. Artificial cell culture conditions might be responsible for a more pronounced effect seen in hepatocytes in vitro when compared to my in vivo results.

Lipid accumulation is a sign of malfunction of oxidative pathways in the liver. Free fatty acids are metabolised through β- oxidation in mitochondria with excess fat being converted to triglycerides and other hydrophobic lipids and stored in the cytoplasm (Patrick 2002). In addition, increased levels of ROS can damage respiratory chain components in the mitochondria through lipid peroxidation, leading to a defect in mitochondrial function (Fromenty et al. 2004). To help maintenance of mitochondrial function, repair mechanisms have evolved to guarantee genomic stability of the mtDNA. Recently, Achanta et al. (2005) found an involvement of p53 in mitochondria. A translocation of p53 into mitochondria was followed by interaction with mtDNA polymerase γ, enhancing replication and repair of the mitochondrial genome. We found elevated levels of lipid accumulation in young *Ercc1*- deficient and Wt livers. This accumulation of cytoplasmic lipids disappeared in older Wt livers, but persisted in *Ercc1*- deficient livers of a similar age. An increase in oxygen pressure at birth could be responsible for increased levels of oxidative stress in liver of both genotypes after birth, leading to accumulation of lipid which could be caused by mitochondrial damage. Where functional repair mechanisms are in place, lipid metabolism can be restored, resulting in a decrease of lipid vesicles in the cytoplasm. Another explanation might be that prior to birth, oxidation of lipids is inactive in the liver, leading to lipid accumulation. This lipid storage can then be used as a source of energy in Wt liver after birth, but not in *Ercc1* Null livers where repair pathways are abrogated, resulting in accumulation of DNA damage and mitochondrial dysfunction. This could lead to persistent, macrovesicular

lipid accumulation in *Ercc1*- deficient livers. In fact, Hsia (2000) found a disruption of the outer mitochondrial membrane in *Ercc1*- deficient livers when compared to Wt, showing that *Ercc1*- deficiency influences mitochondrial function in an indirect manner. Lipid accumulation in older livers has been noted in our conditional *Ercc1* knockout model using AdenoCre virus in vitro and in vivo. In addition, lipid accumulated in all cultures independent of genotype after DNA damage. Therefore, lipid accumulation seems to be a general feature of *Ercc1*- deficiency and liver DNA damage.

When triglyceride levels were compared between *Ercc1* Null and Wt livers, no significant difference in amount of accumulated lipids could be established between the genotypes. This was partly because of a high amount of variation in *Ercc1* Null livers. Alternatively, although triglycerides are a common form of lipid found in cytoplasmic vesicles, Oil Red O also stains other hydrophobic lipids such as cerebrosides and cholesterol esters (Lillie and Ashburn 1943). The macrovesicular lipid vesicles might therefore primarily contain other types of lipids in *Ercc1*-deficient liver when compared to Wt. Differences in lipid composition could also explain the variability in triglyceride content between *Ercc1* Null livers of similar age. The Oil Red O staining patterns are generally regarded as the more reliable indicator of differences in lipid accumulation between *Ercc1* Null and Wt livers.

ROS levels were determined in young *Ercc1*- deficient livers and Wt littermates. Higher amounts of ROS were found in *Ercc1* Null livers after birth. In older animals, this correlation was however inverted, with ROS being highest in Wt livers. In addition, higher levels of malondialdehyde adducts were established in young *Ercc1* Null livers when compared to Wt. This difference was not significant because of a high variability in M_1dG in Null livers. Older Wt livers showed higher levels of malondialdehyde adducts when compared to *Ercc1* Nulls. It seems that levels of ROS and malondialdehydes correlate in both genotypes which can be explained by the biological effects of ROS. During ROS generated lipid peroxidation, malondialdehyde adducts occur as a by-product (Niedernhofer et al. 1997). In

addition, arachidonic acid metabolism and synthesis of prostaglandins lead to malondialdehyde formation endogenously (Leuratti et al. 1998). Malondialdehyde is known to react with DNA at neutral pH forming deoxyguanosine (M_1dG) and, to a lesser extent deoxycytidine adducts, deoxyadenosine adducts and interstrand cross-links, in a variety of tissues including liver (Leuratti et al. 1998). Malondialdehyde adducts, especially the major adduct deoxyguanosine, are usually repaired by NER pathways (Singh et al. 2001). Background levels of M_1dG lie in the range of 50-120 adducts per 10^8 nucleotides in human disease free liver (Singh et al. 2001). In contrast, carbon tetrachloride treated rat livers displayed 38 M_1dG adducts per 10^8 nucleotides with base levels being around 21 M_1dG per 10^8 nucleotides in control animals showing inter- species differences in malondialdehyde adduct background levels (Singh et al. 2001).The M_1dG levels observed in young *Ercc1* Null animals and in old Wt livers lie within the range in human tissue, but are highly elevated when compared to rat malondialdehyde levels. Furthermore, even base levels in young Wt animals and older *Ercc1* Null animals are relatively high showing that oxidative stress might be apparent in both genotypes after birth and just before weaning. The fluctuation of both ROS and malondialdehyde adducts could be caused by differences in DNA repair capacity where disruption of various signalling pathways caused by unrepaired DNA damage leads to ROS and malondialdehyde accumulation in an indirect manner. Even though no significant difference in ROS and M_1dG levels could be established between genotypes, small differences in levels of oxidative stress and DNA damage could still have important physiological effects on hepatocytes. Overall, *Ercc1*- deficient mice show a premature aging phenotype with their elevated levels of liver polyploidy, accumulation of large lipid vesicles, runted appearance and premature death. These data fail to provide evidence that this is due to elevated levels of oxidative DNA damage. Premature ageing phenotypes have been created when the proof- reading capacity of mitochondrial polymerase γ was disabled, with mice showing reduced body weight, hair loss and premature death (Trifunovic et al. 2004, Kujoth et al. 2005). Although elevated levels of mtDNA mutations were apparent in those mice, an increase in markers of oxidative stress, such as ROS and malondialdehyde adducts, was not established. Instead the accelerated development of the ageing phenotype resulted in increased levels of

apoptosis which were thought to be responsible for tissue dysfunction (Kujoth et al. 2005). Similar mechanisms could be responsible for the phenotype in *Ercc1*-deficient livers. Therefore, the lack of significant differences in ROS and M_1dG levels between *Ercc1* Null and Wt animals could mean that increased levels of apoptosis, rather than oxidative stress leads to liver failure in *Ercc1*- deficient animals.

We further characterised *Ercc1*- deficiency in liver by using RT Real- time PCR to determine the expression of selected genes involved in cell cycle regulation, apoptosis and oxidative damage response. Glyceraldehyde 3- phosphate dehydrogenase (*Gapdh*) and Tata- binding protein (*Tbp*) were chosen as reference genes, as the use of one reference gene only can lead to 10-25% erroneous normalisation (Vandesompele et al. 2002). GAPDH has recently been shown to be regulated by mitogenic stimuli in a variety of experimental settings (Radonic et al. 2004). However, Vandesompele et al. (2002) examined several reference genes in a variety of tissues showing that GAPDH and TBP were stably expressed in liver. In addition, although TBP is found in low abundance in liver, it is also one of the reference genes with the lowest overall range of RNA transcription making it ideal as a second reference gene (Radonic et al. 2004).

Growth factors are multifunctional cell signalling units with insulin- like growth factor I (IGF) being involved in cell growth, regulation and differentiation. IGF II is responsible for degrading IGF I protein (Schneider et al. 2000). Their effect is mediated through cell surface receptors and insulin- like growth factor binding proteins (IGFBP) which bind IGF in biological fluids, thereby helping IGF circulation in the body (Scheider et al. 2000). In addition, IGFBP are thought to have autocrine and paracrine functions. IGFBP2 is expressed in a variety of tissues, but most abundantly in liver and kidney. It acts mainly as an inhibitor of IGF I bioactivity and its overexpression led to reduced growth capacity and a reduction in liver weight when compared to Wt littermates (Schneider et al. 2000). High serum levels of IGFBP2 are also associated with liver cirrhosis and diabetes mellitus

(Schneider et al. 2000). Wood et al. (2000) constructed *Igfbp2* knockout mice that displayed a reduction in male spleen weight and an increase in liver weight, showing that *Igfbp2* acts in a tissue- specific manner and that its loss can be counterbalanced by other Igf binding proteins. Pin et al. (unpublished data) showed that *Igfbp2* mRNA expression was highly upregulated in polyploid hepatocyte nuclei. Our findings are in accordance with this as we showed that *Igfbp2* mRNA expression was increased in *Ercc1* Null livers when compared to Wt littermates. IGFBP2 expression is influenced by hormones such as transforming growth factor β (TGFβ) and IGF (Hoeflich et al. 2001). Therefore, higher IGF levels stimulate cell growth and DNA replication, leading to upregulation of IGFBP2 at the same time. In addition, there is evidence that IGFBP2 itself may stimulate cell proliferation independent of IGF (Hoeflich et al. 2001). In conclusion, *Igfbp2* could be seen as a molecular marker for polyploidisation in the liver where increased levels of IGFBP2 lead to a decrease in IGF with a subsequent reduction in proliferation. This decline in proliferation might then favour polyploidisation. In addition, upregulation of Igfbp2 could contribute to the runted phenotype seen in *Ercc1* Null animals.

p21 is involved in cell cycle regulation and is a mediator of p53 pathways, with p53 independent pathways also existing (Kinoshita et al. 2002). It acts as a cyclin dependent kinase (CDK) inhibitor at different stages of the cell cycle and is classed as a Cip/Kip family member along with p27 and p57 (Luedde et al. 2003). *p21* mRNA levels were upregulated in *Ercc1* Null livers when compared to Wt littermates. This is in accordance with Chipchase et al. (2003) who found a correlation between enlarged hepatocyte nuclei and increased p21 expression in *Ercc1* Null and Wt liver using immunohistochemistry. As enlarged nuclei are mainly a phenotypic characteristic of *Ercc1*- deficient livers, an increased p21 expression is primarily expected in *Ercc1* Null livers. A G2 arrest has previously been found in enlarged nuclei of *Ercc1* Null hepatocytes and *p21*, which showed upregulation at the mRNA level, has been suggested as a possible mediator of the G2 arrest (Nunez et al. 2000). p21 along with proliferative stimuli, could be involved in the premature liver polyploidy in *Ercc1*- deficient animals. The variation observed in *p21* mRNA

expression between different littermate pairs has previously been observed by Chipchase et al. (2003) where immunohistochemistry revealed inter-nuclear differences of p21 expression. Especially in littermate pair # 14 the *Ercc1* Null liver showed very high levels of *p21* mRNA which probably reflects a real change, as the Wt liver *p21* mRNA levels in this littermate pair are comparable to Wt liver mRNA levels of the majority of Wt samples examined. In general, where major differences in expression between Wt and Null for a variety of genes have been observed, this difference is caused by variation in gene expression in Nulls, rather than changes in Wt livers.

Transforming growth factor β (TGF β) is a potent inhibitor of cell proliferation and known to be a tumour suppressor in a normal cellular context (Romero- Gallo et al. 2005). It is upregulated in response to partial hepatectomy, suppressing hepatocyte replication once liver mass is restored. TGF β signalling occurs through membrane associated serine threonine kinases (Stenvers et al. 2003). However, TGF β is also a known pro- metastatic factor and tumour promoter in a variety of tumours including hepatocellular carcinomas (HCC) (Tang et al. 2003, Romero- Gallo et al. 2005). This switch of function has been demonstrated in a breast cancer cell line in vitro (Tang et al. 2003). We investigated the expression patterns of *Tgfβ* in *Ercc1* Null and Wt livers of different age. In 4- 14 day old livers, *Tgfβ* mRNA seemed to be upregulated in *Ercc1*- deficient livers with a trend towards lower levels in older *Ercc1* Null livers when compared to Wt. *Tgfβ* mRNA upregulation in young *Ercc1* Null livers might be a mechanism trying to prevent cell proliferation of hepatocytes with unrepaired DNA damage.

Oxidative stress induced upregulation of proliferating cell nuclear antigen (PCNA), redox factor 1 (REF-1) and Polymerase β was observed in rat liver (Holmes et al. 2002). We therefore investigated the expression patterns of those oxidative stress markers in *Ercc1* Null and Wt livers. In addition, mRNA of the pro- apoptotic factor BAX was found to be downregulated in rat liver after treatment with an oxidative damage inducer (Holmes et al. 2002). BAX is a mediator of p53 induced apoptosis

and known to be a tumour suppressor (Knudson et al. 2001). BAX heterodimerises with anti- apoptotic family members rendering them inactive whilst a homodimerisation leads to activation of BAX and insertion into the mitochondrial membrane (Reed 1998). A translocation of BAX from the outer to the inner mitochondrial membrane helps to release mitochondrial cytochrome C during apoptosis. When we examined *Ercc1* Null and Wt livers, an upregulation of *Bax* mRNA was noted in 4- 14 day old livers with downregulation of *Bax* mRNA being apparent thereafter. In addition, an increase in apoptosis levels was indicated in older *Ercc1*Null livers when compared to Wt using flow cytometry. Accumulation of DNA damage and oxidative stress in *Ercc1* Null livers might lead to increases in apoptosis where polyploidisation cannot protect against rises in DNA damage. BAX has indeed been shown to be part of the cellular response to oxidative stress (Knudson et al. 2001). Increased survival might be necessary in older *Ercc1*- deficient liver to tolerate accumulating DNA damage to a certain extent. This would predict the observed downregulation of *Bax* mRNA and apoptotic mechanisms in old murine livers to counteract an otherwise fatal reduction of liver mass.

PCNA is a processing factor for polymerase γ and ε and also functions as a DNA clamp during translesion bypass when post- translationally modified, allowing the switch from a high fidelity polymerase to specialised polymerases (Friedberg 2005). Its subcellular localisation has been shown to change in response to oxidative stress (Holmes et al. 2002). In addition, p21 inhibits PCNA- mediated DNA polymerase activity upon binding (Jaime et al. 2002). No clear difference in *Pcna* mRNA expression was noted between young *Ercc1* Null and Wt animals. This is in agreement with the observation that S-phase levels did not differ between genotypes when examined by flow cytometry, showing that similar levels of DNA replication take place in both genotypes. Results obtained by Holmes et al. (2002) showing elevated levels of *Pcna* mRNA after oxidative stress in rat liver could not be confirmed. ROS levels in our *Ercc1* Null animals might not be high enough to trigger a PCNA response. In addition, species related differences in PCNA expression might be accountable for this difference. Furthermore, response to an external oxidative

damage inducer used by Holmes et al. (2002) in the liver might differ from mechanisms triggered by endogenous oxidative damage. Hsia (2000) found elevated PCNA protein levels in *Ercc1* Null livers using Western blotting. This discrepancy in *Pcna* mRNA and protein levels could be because of post- translational modifications of the protein, allowing higher levels of PCNA protein to persist in *Ercc1* Null livers without affecting mRNA levels.

Chipchase (2002) noted a possible upregulation of REF-1 in *Ercc1* Null liver compared to Wt using immunohistochemistry. In addition, an upregulation of *Ref-1* mRNA expression in rat liver was apparent after exposure to an oxidative damage inducer. We found a high variability in *Ref-1* mRNA expression between liver pairs and could therefore not see any trend in *Ref-1* mRNA levels between genotypes. REF-1 is involved in BER where its function as an AP endonuclease is essential (Meira et al. 2001). Apart from 5'- endonuclease activity, REF-1 also displays as a 3'-phosphodiesterase and 3'- phosphatase activity. Furthermore, REF-1 is required for redox activation of spontaneously oxidised transcription factors, highlighting its involvement in the cellular stress response (Raffoul et al. 2004). REF-1 expression could therefore be taken as an indirect indication of BER activity which does not seem to be upregulated in *Ercc1*- deficient livers where NER is abrogated. REF-1 has also been shown to recruit polymerase β to incised AP sites leading to insertion of new nucleotides (Raffoul et al. 2004, Sugo et al. 2004). Polymerase β, the smallest described polymerase with a single 39 kDa polypeptide, also mediates excision of abnormal 5'- dRP during BER, a rate- limiting property that can be enhanced upon REF-1 interaction (Esposito et al. 2000). No clear trend in *polymerase β* mRNA expression was noted in *Ercc1* Null and Wt livers, strengthening the observation that BER upregulation is not apparent in *Ercc1*- deficient livers. Because of the close relationship between the ubiquitously expressed Polymerase β and REF-1 similar, non- descript expression patterns in *Ercc1* Null and Wt livers should therefore not be surprising.

In conclusion, RT Real- time PCR revealed the upregulation of several proteins with a possible role in polyploidisation. An upregulation of *Igfbp2* and *p21* mRNA was found in *Ercc1* Null livers when compared to Wt and might help to mediate increases in tetra- and octaploidy observed in *Ercc1*- deficient livers. A tendency towards increased levels of apoptosis was apparent in *Ercc1* Null livers when compared to Wt controls. Moreover, *Bax* mRNA levels were highest in younger *Ercc1* Null livers and dropped below Wt levels from 19 days after birth. More accurate determination of apoptosis with for example caspases- 3 cleavage assays might help to understand the exact mechanism of apoptosis in more detail. The lack of increased oxidative damage, like malondialdehyde DNA adducts, in older *Ercc1*- deficient livers when compared to Wt controls agrees with the RT Real- time PCR analysis of oxidative stress markers. Oxidative stress markers did not display a rise in mRNA levels at any examined age, showing that the different amounts of ROS and malondialdehyde adducts in younger *Ercc1*- deficient animals did not cause a change in molecular expression patterns. However, malfunction of oxidative pathways which might be a cause of mitochondrial damage were apparent in the form of accumulating lipids in the cytoplasm of *Ercc1*- deficient livers. Measurement of mitochondrial membrane potential might give a more direct indicator of mitochondrial status in *Ercc1* Null livers.

7. Conclusions and future work

We conducted a study in an attempt to clarify the role of *Ercc1* in the liver in a conditional knockout system in vivo, in vitro and in complete knockout mice. The establishment of a conditional, transgenic, liver- specific knockout model proved more difficult than anticipated as TTRCre *Ercc1* Flox/Null and Flox/Wt mice only displayed very low and irreproducible levels of recombination upon tamoxifen administration. A lack of Cre recombinase expression, or rapid clearance of hepatocytes following tamoxifen administration, could explain these results. Western and northern blotting should help to determine the expression patterns of Cre recombinase in our mice in more detail. Caspase cleavage and TUNEL assays might be able to elucidate the levels of apoptosis after tamoxifen administration.

One conclusion from this study is that *Ercc1* seems to be essential for liver maintenance and that a lack of protein resulted in possible rapid clearance of hepatocytes in vivo. The higher amounts of apoptosis in infected *Ercc1* Flox/Null cultures spontaneously and after exposure to UV and GO highlights the involvement of *Ercc1* in hepatocyte survival. Both its function in the NER pathway and in oxidative damage repair seem to be required for hepatocyte maintenance. In addition, Oil Red O data in 6 week old AdenoCre infected mice suggest a clearance of infected Flox/Null hepatocytes that accumulate large amounts of lipid in the cytoplasm 3 weeks after infection. Moreover, *Ercc1* knockout animals displayed an upregulation of *Bax*, a pro- apoptotic factor, at the mRNA level in younger animals. It would be interesting to examine *Bax* mRNA levels in AdenoCre infected *Ercc1* Flox/Null and Flox/Wt livers 1 and 3 weeks after infection to clarify the amounts of apoptosis caused by *Ercc1* downregulation. Other apoptosis markers such as caspase cleavage might help to determine the apoptotic status in *Ercc1* knockout livers in more detail. In general, it seems that apoptosis is a mechanism of protection in liver at an early stage during *Ercc1*- deficiency before other mechanisms of protection can occur. Alternatively, apoptosis and polyploidy could act at the same time helping to protect *Ercc1*- deficient livers.

Polyploidisation is another response to *Ercc1* deficiency in the liver. As a consequence of the short survival of *Ercc1*- deficient hepatocytes in vitro, the development of polyploidisation could not be followed up in primary hepatocyte cultures. In addition, polyploidisation was only apparent in some AdenoCre infected Flox/Null animals where higher levels of octaploidy correlated with higher amounts of cytoplasmic lipid accumulation 1 week after infection. This polyploidisation is a rather striking finding given that recombination levels were found to be below 25% in those livers. Polyploidisation was apparent in *Ercc1* knockout livers from 10 days of age where increased levels of tetraploidy became established. Small rises in octaploidy were visible towards the maximum life span of the animals. These findings underline the importance of polyploidisation as a mechanism of protection in the liver. The difference in polyploidy patterns between complete *Ercc1* knockout livers and AdenoCre infected livers might be explained by the difference in age of AdenoCre administration. The upregulation of IGFBP2, which regulates the availability of IGF, in *Ercc1*- deficient liver could be taken as a marker for polyploidy status as IGFBP2 levels have previously been implicated with higher polyploid status in hepatocyte nuclei (Pin et al. unpublished data). In addition, p21 mRNA was upregulated in *Ercc1*- deficient livers. It has previously been suggested that p21 is implicated in G2 arrest found in *Ercc1*- deficient livers thereby helping to establish polyploidisation in hepatocytes (Nunez et al. 2000, Chipchase et al. 2003). Polyploidisation is most pronounced at later stages (3 week old) suggesting that there is a greater requirement for this protective (but ultimately unsuccessful) mechanism in the later stages of *Ercc1* deficiency in mice.

Another common feature of *Ercc1*- deficient livers is the accumulation of cytoplasmic lipid. In older infected *Ercc1* Flox/Null hepatocyte cultures this accumulation of lipid becomes apparent in the form of microvesicles in the cytoplasm. Furthermore, after UV irradiation all hepatocyte cultures accumulate lipid vesicles independent of genotypes. These vesicles disappear in infected *Ercc1* Flox/Wt and uninfected *Ercc1* Flox/Null cultures with time. A similar pattern of lipid accumulation was observed in *Ercc1*- deficient livers and Wt littermates where

macrovesicular lipid accumulation was evident in young livers. This lipid accumulation persisted in *Ercc1* Null livers with age, but a disappearance of lipid was noted in Wt littermate controls. In 6 week old AdenoCre infected Flox/Null livers, macrovesicular lipid accumulation was noted 1 week after infection and disappeared 3 weeks after virus infection, possibly indicating clearance of *Ercc1*-deficient hepatocytes. In summary, lipid accumulation seems to be a feature caused by DNA damage in the liver. Repair of damaged DNA leads to lipids being used during mitochondrial oxidative pathways, but lipids persist where repair mechanisms are disturbed. Hsia (2000) found a disruption of the outer mitochondrial membrane suggesting that mitochondrial dysfunction, as an indirect consequence of loss of *Ercc1*, might be responsible for the cytoplasmic lipid accumulation observed. It would be interesting to examine the mitochondrial membrane potential between *Ercc1* Null and Wt animals to clarify the relationship between mitochondrial membrane damage and accumulated cytoplasmic lipid in more detail. This could be done using a flow cytometry based assay and the JC-1 dye. This dyes changes from mono- to polymers when changes in mitochondrial membrane potential are apparent. Lipid accumulation seems to be an early response to loss of *Ercc1* in the liver, even appearing before polyploidisation occurs. Lipid accumulation was apparent in all our models of *Ercc1* deficiency. Therefore, a lack of polyploidy in vitro and in some AdenoCre infected animals in vivo does not mean that different mechanisms are operating in the different models.

Lipid accumulation in the liver was apparent in some patients undergoing oxaliplatin treatment for ovarian cancer (D. Jodrell, personal communication). Differences in *ERCC1* status might be involved in the response to oxaliplatin treatment and the increased side effects of the drug as manifested in lipid accumulation in the liver. The outcome of the treatment might be predictable by determining *ERCC1* status in patients. In addition, our cell culture system could be used to compare the response of *Ercc1*- deficient hepatocytes to oxaliplatin treatment in more detail.

A sudden increase in oxygen pressure at birth might be responsible for accumulation of lipids in young animals independent of genotype. Higher levels of ROS and MDA adducts in young *Ercc1*- deficient livers could result from this sudden rise in oxygen pressure with alternative mechanisms of repair becoming important at later stages of *Ercc1* deficiency. However, a rise in ROS and MDA level occurs in Wt livers with age. In older *Ercc1* Null mice, ROS and MDA levels are reduced when compared to the Wt controls. This could be an indirect marker of malfunctioning liver metabolism where high levels of DNA damage start contributing to the liver failure observed in *Ercc1* Null mice toward their maximum life span. Indeed, increased levels of albumin have previously been found in those mice pointing to malfunction of liver metabolism (McWhir et al. 1993).

More and more evidence suggests an involvement of *ERCC1* deregulation in cancer. *ERCC1* polymorphisms, although silent, have been associated with worse prognosis of colon and ovarian cancer (Ford et al. 2000, Isla et al. 2004). Overexpression of *ERCC1* was also found in HCC (Fautrel et al. 2005). In addition, *Ercc1* seems to play a special role in the liver as response to loss is much more severe compared to loss in for example skin. Therefore, more research will be needed to elucidate the exact role of *Ercc1* in the liver.

In general, conclusions drawn from a comparison of individual mice between the two *Ercc1* genotypes should be taken as an indication of possible molecular events only. All our *Ercc1* animals are on a mixed genetic background which can lead to variation between individual animals of the same genotype, regardless of experimental setting. In addition, the health status of the individual animal might be important as *Ercc1* Null animals can die before reaching their maximal life span of 3 weeks. Molecular events in unhealthy animals are likely to differ from those obtained from healthy mice. Gender differences have so far not been noted in our *Ercc1* Null and Wt animals but might play a role when comparing individual animals only. To overcome these limitations, an increase in sample size would be necessary, comparing a number of animals for each treatment and time point. Experiments could be better

designed by reducing the amount of time points at which experiments are carried out. In addition, one treatment, for example amount of virus given per animal, rather than several different treatments will increase sample size and might help to elucidate the role of *Ercc1* in the liver more clearly.

8. References

1. 1989. *The UFAW Handbook on the Care and Management of Laboratory Animals*. Edited by Poole, T. 6 ed. Bath: Longman Scientific and Technical.

2. 1994. *The molecular biology of The Cell*. Edited by Alberts, B Bray D. Lewis J. Raff M. Roberts K. Watson J. D. 3 ed. New York: Garland Publishing.

3. [Anon]. 2002. The mouse genome. *Nature* 420, no. 6915:510.

4. Achanta, G., R. Sasaki, L. Feng, J. S. Carew, W. Lu, H. Pelicano, M. J. Keating, and P. Huang. 2005. Novel role of p53 in maintaining mitochondrial genetic stability through interaction with DNA Pol gamma. *EMBO J.* 24, no. 19:3482-3492.

5. Adair, G. M. Rolig R. L. Moore-Faver D. Zabelshansky M. Wilson J. H. Nairn R. S. 2000. Role of ERCC1 in removal of long non-homologous tails during targeted non-homologous recombination. *The Embo Journal* 19, no. 20:5552-5561.

6. Addison, C. L., M. Hitt, D. Kunsken, and F. L. Graham. 1997. Comparison of the human versus murine cytomegalovirus immediate early gene promoters for transgene expression by adenoviral vectors. *J.Gen.Virol.* 78 (Pt 7):1653-1661.

7. Akagi, K., V. Sandig, M. Vooijs, der Van, V, M. Giovannini, M. Strauss, and A. Berns. 1997. Cre-mediated somatic site-specific recombination in mice. *Nucleic Acids Res.* 25, no. 9:1766-1773.

8. Anantharaju, A. Feller A. Chedid A. 2002. Aging liver. *Gerontology* 48:343-353.

9. Andressoo, J. O. and J. H. Hoeijmakers. 2005. Transcription-coupled repair and premature ageing. *Mutat.Res.* 577, no. 1-2:179-194.

10. Anton, M. and F. L. Graham. 1995. Site-specific recombination mediated by an adenovirus vector expressing the Cre recombinase protein: a molecular switch for control of gene expression. *J.Virol.* 69, no. 8:4600-4606.

11. Bellamy, C. O. C. Clarke A. R. Wyllie A. H. Harrison D. J. 1997. p53 deficiency in liver reduces local control of survival and proliferation, but does not affect apoptosis after DNA damage. *The FASEB Journal* 11:591-599.

12. Biesterfeld, S., K. Gerres, G. Fischerwein, and A. Bocking. 1994. Polyploidy in Nonneoplastic Tissues. *Journal of Clinical Pathology* 47, no. 1:38-42.

13. Bosch, F. X., J. Ribes, M. Diaz, and R. Cleries. 2004. Primary liver cancer: Worldwide incidence and trends. *Gastroenterology* 127, no. 5:S5-S16.

14. Buermeyer, A. B. Deschenes S. M. Baker J. M. Liskay R. M. 1999. Mammalian DNA mismatch repair. *Annual Review of Genetics* 33:533-564.

15. Chipchase, M. D. 2001. *The effects of ERCC1 deficiency on mouse hepatocytes in vitro*. Edinburgh: Ph.D. Thesis, University of Edinburgh.

16. Chipchase, M. D., M. O'Neill, and D. W. Melton. 2003. Characterization of premature liver polyploidy in DNA repair (Ercc1)-deficient mice. *Hepatology* 38, no. 4:958-966.

17. Chipchase, M.D., D.W. Melton. 2002. The formation of UV-induced chromosome aberrations involves ERCC1 and XPF but not other nucleotide excision repair genes. *DNA Repair* 1:335-340.

18. Comai, L. 2005. The advantages and disadvantages of being polyploid. *Nat.Rev.Genet.* 6, no. 11:836-846.

19. Cooke, M. S., M. D. Evans, M. Dizdaroglu, and J. Lunec. 2003. Oxidative DNA damage: mechanisms, mutation, and disease. *FASEB J.* 17, no. 10:1195-1214.

20. Danielian, P. S., R. White, S. A. Hoare, S. E. Fawell, and M. G. Parker. 1993. Identification of residues in the estrogen receptor that confer differential sensitivity to estrogen and hydroxytamoxifen. *Mol.Endocrinol.* 7, no. 2:232-240.

21. de Boer, J. Hoeijmakers J. H. J. 2000. Nucleotide excision repair and human syndromes. *Carcinogenesis* 21, no. 3:453-460.

22. de Laat, W. L. Sijbers A. M. Odijk H. Jaspers N. G. J. Hoeijmakers J. H. J. 1998. Mapping of interaction domains between human repair proteins ERCC1 and XPF. *Nucleic Acids Research* 26, no. 18:4146-4152.

23. Demple, B. and J. S. Sung. 2005. Molecular and biological roles of Ape1 protein in mammalian base excision repair. *DNA Repair (Amst)* 4, no. 12:1442-1449.

24. Dirkx, R., I. Vanhorebeek, K. Martens, A. Schad, M. Grabenbauer, D. Fahimi, P. Declercq, P. P. Van Veldhoven, and M. Baes. 2005. Absence of peroxisomes in mouse hepatocytes causes mitochondrial and ER abnormalities. *Hepatology* 41, no. 4:868-878.

25. Doig, J., C. Anderson, N. J. Lawrence, J. Selfridge, D. G. Brownstein, and D. W. Melton. 2006. Mice with skin-specific DNA repair gene (Ercc1) inactivation are hypersensitive to ultraviolet irradiation-induced skin cancer and show more rapid actinic progression. *Oncogene*. Epub ahead of print.

26. Dolle, M. E. T., R. A. Busuttil, A. M. Garcia, S. Wijnhoven, E. van Drunen, L. J. Niedernhofer, G. van der Horst, J. H. J. Hoeijmakers, H. van Steeg, and J. Vijg. 2006. Increased genomic instability is not a prerequisite for shortened lifespan in DNA repair deficient mice. *Mutation Research-Fundamental and Molecular Mechanisms of Mutagenesis* 596, no. 1-2:22-35.

27. Dunkern, T. R. Fritz G. Kaina B. 2001. Ultraviolet light-induced DNA damage triggers apoptosis in nucleotide excision repair-deficient cells via Bcl-2 decline and caspase-3/-8 activation. *Oncogene* 20:6026-6038.

28. Eldridge, S. R. Tilburry L. F. Goldsworthy T. L. Butterworth B. E. 1990. Measurement of chemically induced cell proliferation in rodent liver and kidney: a comparison of 5-bromo-2'-deoxyuridine and 3H thymidine administered by injection or osmotic pump. *Carcinogenesis* 11, no. 12:2245-2251.

29. Enzlin, J. H. Scharer O. D. 2002. The active site of the DNA repair endonuclease XPF-ERCC1 forms a highly conserved nuclease motif. *The Embo Journal* 21, no. 8:2045-2053.

30. Esposito, G., G. Texido, U. A. K. Betz, H. Gu, W. Muller, U. Klein, and K. Rajewsky. 2000. Mice reconstituted with DNA polymerase beta-deficient foetal liver cells are able to mount a T cell-dependent immune response and mutate their Ig genes normally. *Proceedings of the National Academy of Sciences of the United States of America* 97, no. 3:1166-1171.

31. Fautrel, A., L. Andrieux, O. Musso, K. Boudjema, A. Guillouzo, and S. Langouet. 2005. Overexpression of the two nucleotide excision repair genes ERCC1 and XPC in human hepatocellular carcinoma. *J.Hepatol.* 43, no. 2:288-293.

32. Fawell, S. E., J. A. Lees, R. White, and M. G. Parker. 1990. Characterization and colocalization of steroid binding and dimerization activities in the mouse estrogen receptor. *Cell* 60, no. 6:953-962.

33. Feil, R., J. Brocard, B. Mascrez, M. LeMeur, D. Metzger, and P. Chambon. 1996. Ligand-activated site-specific recombination in mice. *Proc.Natl.Acad.Sci.U.S.A* 93, no. 20:10887-10890.

34. Ford, B. N., C. C. Ruttan, V. L. Kyle, M. E. Brackley, and B. W. Glickman. 2000. Identification of single nucleotide polymorphisms in human DNA repair genes. *Carcinogenesis* 21, no. 11:1977-1981.

35. Friedberg, E.C. 2001. How nucleotide excision repair protects against cancer. *Nature Reviews Cancer* 1, no. 1:22-33.

36. Friedberg, E. C. 2005. Suffering in silence: the tolerance of DNA damage. *Nat.Rev.Mol.Cell Biol.* 6, no. 12:943-953.

37. Fromenty, B., M. A. Robin, A. Igoudjil, A. Mansouri, and D. Pessayre. 2004. The ins and outs of mitochondrial dysfunction in NASH. *Diabetes Metab* 30, no. 2:121-138.

38. Gage, R., R. F. Venn, M. A. Bayliss, A. M. Edgington, S. J. Roffey, and B. Sorrell. 2000. Fluorescence determination of sulphobutylether-beta-cyclodextrin in human plasma by size exclusion chromatography with inclusion complex formation. *J.Pharm.Biomed.Anal.* 22, no. 5:773-780.

39. Gillet, L. C. and O. D. Scharer. 2006. Molecular mechanisms of mammalian global genome nucleotide excision repair. *Chem.Rev.* 106, no. 2:253-276.

40. Gorla, G. R., H. Malhi, and S. Gupta. 2001. Polyploidy associated with oxidative injury attenuates proliferative potential of cells. *Journal of Cell Science* 114, no. 16:2943-2951.

41. Gratchev, A., P. Strein, J. Utikal, and G. Sergij. 2003. Molecular genetics of Xeroderma pigmentosum variant. *Exp.Dermatol.* 12, no. 5:529-536.

42. Guicciardi, M. E. and G. J. Gores. 2005. Apoptosis: a mechanism of acute and chronic liver injury. *Gut* 54, no. 7:1024-1033.

43. Guidotti, J. E. Bregerie O. Robert A. Debey P. Brechot C. Desdouets C. 2003. Liver cell polyploidisation: a pivotal role of binuclear hepatocytes. *Journal of Biological Chemistry* 278, no. 21: 19095-19101

44. Gupta, S. 2000. Hepatic polyploidy and liver growth control. *Seminars in Cancer Biology* 10:161-171.

45. Han, X. L. and J. G. Liehr. 1992. Induction of covalent DNA adducts in rodents by tamoxifen. *Cancer Res.* 52, no. 5:1360-1363.

46. Heller, R. C. and K. J. Marians. 2006. Replication fork reactivation downstream of a blocked nascent leading strand. *Nature* 439, no. 7076:557-562.

47. Hirsimaki, P Aaltonen A. Mantyla E. 2002. Toxicity of antiestrogens. *The Breast Journal* 8, no. 2:92-96.

48. Hoeflich, A., S. Nedbal, W. F. Blum, M. Erhard, H. Lahm, G. Brem, H. J. Kolb, R. Wanke, and E. Wolf. 2001. Growth inhibition in giant growth hormone transgenic mice by overexpression of insulin-like growth factor-binding protein-2. *Endocrinology* 142, no. 5:1889-1898.

49. Holmes, E. W., C. M. Bingham, and M. L. Cunningham. 2002. Hepatic expression of polymerase beta, Ref-1, PCNA, and Bax in WY 14,643-exposed rats and hamsters. *Exp.Mol.Pathol.* 73, no. 3:209-219.

50. Hsia, K. T. 2000. *Use of gene targeting to study the mouse Ercc1 gene*. Edinburgh: Ph.D. thesis, University of Edinburgh.

51. Imai, T., P. Chambon, and D. Metzger. 2000. Inducible site-specific somatic mutagenesis in mouse hepatocytes. *Genesis.* 26, no. 2:147-148.

52. Ishikawa, T., S. S. M. Zhang, X. S. Qin, Y. Takahashi, H. Oda, Y. Nakatsuru, and F. Ide. 2004. DNA repair and cancer: Lessons from mutant mouse models. *Cancer Science* 95, no. 2:112-117.

53. Isla, D., C. Sarries, R. Rosell, G. Alonso, M. Domine, M. Taron, G. Lopez-Vivanco, C. Camps, M. Botia, L. Nunez, M. Sanchez-Ronco, J. J. Sanchez, M. Lopez-Brea, I. Barneto, A. Paredes, B. Medina, A. Artal, and P. Lianes. 2004. Single nucleotide polymorphisms and outcome in docetaxel-cisplatin-treated advanced non-small-cell lung cancer. *Annals of Oncology* 15, no. 8:1194-1203.

54. Jackson, s. P. 2002. Sensing and repairing DNA double-strand breaks. *Carcinogenesis* 23, no. 5:687-692.

55. Jaime, M., M. J. Pujol, J. Serratosa, C. Pantoja, N. Canela, O. Casanovas, M. Serrano, N. Agell, and O. Bachs. 2002. The p21(Cip1) protein, a cyclin inhibitor, regulates the levels and the intracellular localization of CDC25A in mice regenerating livers. *Hepatology* 35, no. 5:1063-1071.

56. Kalinina, O. A., S. A. Kalinin, E. W. Polack, I. Mikaelian, S. Panda, R. H. Costa, and G. R. Adami. 2003. Sustained hepatic expression of FoxM1B in transgenic mice has minimal effects on hepatocellular carcinoma development but increases cell proliferation rates in preneoplastic and early neoplastic lesions. *Oncogene* 22, no. 40:6266-6276.

57. Kanzler, S. Galle P. R. 2000. Apoptosis and the liver. *Seminars in Cancer Biology* 10:173-184.

58. Kellendonk, C., C. Opherk, K. Anlag, G. Schutz, and F. Tronche. 2000. Hepatocyte-specific expression of Cre recombinase. *Genesis.* 26, no. 2:151-153.

59. Kinoshita, A., H. Wanibuchi, S. Imaoka, M. Ogawa, C. Masuda, K. Morimura, Y. Funae, and S. Fukushima. 2002. Formation of 8-hydroxydeoxyguanosine and cell-cycle arrest in the rat liver via generation of oxidative stress by phenobarbital: association with expression profiles of p21(WAF1/Cip1), cyclin D1 and Ogg1. *Carcinogenesis* 23, no. 2:341-349.

60. Klungland, A. Hollenbach S. Larsen E. Daly G. Epe B. Seeberg E. Lindahl T. Barnes D. E. 1999. Accumulation of premutagenic DNA lesions in mice defective in removal of oxidative base damage. *PNAS* 96, no. 23:13300-13305.

61. Klungland, A. Hoss M. Gunz D. Constantinou A. Clarkson S. G. Doetsch P. W. Bolton P. H. Wood R. D. Lindahl T. 1999. Base excision repair of oxidative DNA damage activated by XPG protein. *Molecular Cell* 3:33-42.

62. Knudson, C. M., G. M. Johnson, Y. Lin, and S. J. Korsmeyer. 2001. Bax accelerates tumorigenesis in p53-deficient mice. *Cancer Res.* 61, no. 2:659-665.

63. Krokan, H. E. Nilsen H. Skorpen F. Otterlei M. Slupphaug G. 2000. Base excision repair of DNA in mammalian cells. *FEBS* 476:73-77.

64. Kujoth, G. C., A. Hiona, T. D. Pugh, S. Someya, K. Panzer, S. E. Wohlgemuth, T. Hofer, A. Y. Seo, R. Sullivan, W. A. Jobling, J. D. Morrow, H. Van Remmen, J. M. Sedivy, T. Yamasoba, M. Tanokura, R. Weindruch, C. Leeuwenburgh, and T. A. Prolla. 2005. Mitochondrial DNA mutations, oxidative stress, and apoptosis in mammalian aging. *Science* 309, no. 5733:481-484.

65. Kuraoka, I. Romieu A. Wood R. D. Lindahl T. 2000. Removal of oxygen free radical induced 5', 8'-purine cyclodeoxynucleosides from DNA by the nucleotide excision-repair pathway in human cells. *PNAS* 97, no. 8:3832-3837.

66. Lan, L., T. Hayashi, R. M. Rabeya, S. Nakajima, S. Kanno, M. Takao, T. Matsunaga, M. Yoshino, M. Ichikawa, H. Riele, S. Tsuchiya, K. Tanaka, and A. Yasui. 2004. Functional and physical interactions between ERCC1 and MSH2 complexes for resistance to cis-diamminedichloroplatinum(II) in mammalian cells. *DNA Repair (Amst)* 3, no. 2:135-143.

67. Lanier, T. L., E. K. Berger, and P. I. Eacho. 1989. Comparison of 5-bromo-2-deoxyuridine and [3H]thymidine for studies of hepatocellular proliferation in rodents. *Carcinogenesis* 10, no. 7:1341-1343.

68. Larionov, A., A. Krause, and W. Miller. 2005. A standard curve based method for relative real time PCR data processing. *BMC Bioinformatics* 6, no. 1:62.

69. Larsen, N. B., M. Rasmussen, and L. J. Rasmussen. 2005. Nuclear and mitochondrial DNA repair: similar pathways? *Mitochondrion* 5, no. 2:89-108.

70. Leuratti, C., R. Singh, C. Lagneau, P. B. Farmer, J. P. Plastaras, L. J. Marnett, and D. E. Shuker. 1998. Determination of malondialdehyde-induced DNA damage in human tissues using an immunoslot blot assay. *Carcinogenesis* 19, no. 11:1919-1924.

71. Lillie, RD and LL Ashburn. Super-saturated solutions of fat stains in dilute isopropanol for demonstration of acute fatty degenerations not shown by Herxheimer technique. Archives of Pathology 36, 432. 1943.
Ref Type: Generic

72. Lim, I. K. 2002. Spectrum of molecular changes during hepatocarcinogenesis induced by DEN and other chemicals in Fischer 344 male rats. *Mech.Ageing Dev.* 123, no. 12:1665-1680.

73. Lindahl.T. 1993. Instability and decay of the primary structure of DNA. *Nature* 362:709-715.

74. Liu, Z. Hossain G. S. Islas-Osuna M. A. Mitchell D. L. Mount D. W. 2000. Repair of UV damage in plants by nucleotide excision repair: Arabidopsis UVH1 DNA repair gene is a homolog of Saccharomyces cerevisiae Rad1. *The Plant Journal* 21, no. 6:519-528.

75. Loft, S., X. S. Deng, J. Tuo, A. Wellejus, M. Sorensen, and H. E. Poulsen. 1998. Experimental study of oxidative DNA damage. *Free Radic.Res.* 29, no. 6:525-539.

76. Lombard, D. B., K. F. Chua, R. Mostoslavsky, S. Franco, M. Gostissa, and F. W. Alt. 2005. DNA repair, genome stability, and aging. *Cell* 120, no. 4:497-512.

77. Luedde, T., M. E. Rodriguez, F. Tacke, Y. Xiong, D. A. Brenner, and C. Trautwein. 2003. p18(INK4c) collaborates with other CDK-inhibitory proteins in the regenerating liver. *Hepatology* 37, no. 4:833-841.

78. Marti, T. M. Kunz C. Fleck O. 2002. DNA mismatch repair and mutation avoidance pathways. *Journal of Cellular Physiology* 191:28-41.

79. McWhir, J. Selfridge J. Harrison D. J. Squires S. Melton D. W. 1993. Mice with DNA repair gene (ERCC1) deficiency have elevated levels of p53, liver nuclear abnormalities and die before weaning. *Nature Genetics* 5:217-224.

80. Meira, L. B., S. Devaraj, G. E. Kisby, D. K. Burns, R. L. Daniel, R. E. Hammer, S. Grundy, I. Jialal, and E. C. Friedberg. 2001. Heterozygosity for the mouse Apex gene results in phenotypes associated with oxidative stress. *Cancer Research* 61, no. 14:5552-5557.

81. Melton, D. W. and Nunez F. Bonatti-Abbondandolo S. Abbondandolo A. Squires S. Johnson R. T. Ketchen A.-M. 1998. Cells from ERCC1-deficient mice show increased genome instability and a reduced frequency of S-phase-dependent illegitimate chromosome exchange but a normal frequency of homologous recombination. *Journal of Cell Science* 111:395-404.

82. Melton, D. W. 2002. Gene-targeting strategies. In *Transgenesis Techniques*, edited by A.R.Clarke 2 ed. Vol. 180, (Totowa, NJ: Humana Press Inc.).

83. Metzger, D. and P. Chambon. 2001. Site- and time-specific gene targeting in the mouse. *Methods* 24, no. 1:71-80.

84. Mitaka, T. 1998. The current status of primary hepatocyte culture. *International Journal of Experimental Pathology* 79:393-409.

85. Moreno, V., F. Gemignani, S. Landi, L. Gioia-Patricola, A. Chabrier, I. Blanco, S. Gonzalez, E. Guino, G. Capella, and F. Canzian. 2006. Polymorphisms in genes of nucleotide and base excision repair: Risk and prognosis of colorectal cancer. *Clinical Cancer Research* 12, no. 7:2101-2108.

86. Morton, N.M., J.M. Paterson, H. Mosuzaki, M.C. Holmes, B. Staels, C. Filvet, B.R. Walker, J.S. Flier, J.J. Mullins, J.R. Seckl. 2004. Novel adipose tissue- mediated resistance to diet- induced visceral obesity in 11 β-Hydroxysteroid dehydrogenase type 1- deficient mice. *Diabetes* 53, no. 4: 931-938.

87. Mossin, L., H. Blankson, H. Huitfeldt, and P. O. Seglen. 1994. Ploidy-dependent growth and binucleation in cultured rat hepatocytes. *Exp.Cell Res.* 214, no. 2:551-560.

88. Mueller, S., K. Pantopoulos, C. A. Hubner, W. Stremmel, and M. W. Hentze. 2001. IRP1 activation by extracellular oxidative stress in the perfused rat liver. *J.Biol.Chem.* 276, no. 25:23192-23196.

89. Niedernhofer, L. J., M. Riley, N. Schnetz-Boutaud, G. Sanduwaran, A. K. Chaudhary, G. R. Reddy, and L. J. Marnett. 1997. Temperature-dependent formation of a conjugate between tris(hydroxymethyl)aminomethane buffer and the malondialdehyde-DNA adduct pyrimidopurinone. *Chem.Res.Toxicol.* 10, no. 5:556-561.

90. Nohmi, T. and K. Masumura. 2005. Molecular nature of intrachromosomal deletions and base substitutions induced by environmental mutagens. *Environ.Mol.Mutagen.* 45, no. 2-3:150-161.

91. Nunez, F. Chipchase M. D. Clarke A. R. Melton D. W. 2000. Nucleotide excision repair gene (ERCC1) deficiency causes G2 arrest in hepatocytes and a reduction in liver binucleation: the role of p53 and p21. *The FASEB Journal* 14, no. 9:1073-1082.

92. O'Driscoll, M. and P. A. Jeggo. 2006. The role of double-strand break repair - insights from human genetics. *Nat.Rev.Genet.* 7, no. 1:45-54.

93. Ostling, O. and K. J. Johanson. 1984. Microelectrophoretic study of radiation-induced DNA damages in individual mammalian cells. *Biochem.Biophys.Res.Commun.* 123, no. 1:291-298.

94. Paques, F. and J. E. Haber. 1999. Multiple pathways of recombination induced by double-strand breaks in Saccharomyces cerevisiae. *Microbiol.Mol.Biol.Rev.* 63, no. 2:349-404.

95. Patrick, L. 2002. Nonalcoholic fatty liver disease: relationship to insulin sensitivity and oxidative stress. *Alternative medicine review* . 7, no. 4: 276-291.

96. Petit, C. Sancar A. 1999. Nucleotide excision repair: from E.coli to man. *Biochimie* 81:15-25.

97. Pfaffl, M. W. 2004. *A- Z of quantitative PCR*. Edited by Bustin, S. A. La Jolla: International University Line.

98. Postic, C. and M. A. Magnuson. 2000. DNA excision in liver by an albumin-Cre transgene occurs progressively with age. *Genesis.* 26, no. 2:149-150.

99. Prasher, J. M., A. S. Lalai, C. Heijmans-Antonissen, R. E. Ploemacher, J. H. Hoeijmakers, I. P. Touw, and L. J. Niedernhofer. 2005. Reduced hematopoietic reserves in DNA interstrand crosslink repair-deficient Ercc1(-/-) mice. *Embo Journal* 24, no. 4:861-871.

100. Prolla, T. A. 1998. DNA mismathc repair and cancer. *Current Opinion in Cell Biology* 10:311-316.

101. Prost, S. Ford J. M. Taylor C. Doig J. Harrison D. J. 1998. Hepatitis B x protein inhibits p53-dependent DNA repair in primary mouse hepatocytes. *The Journal of Biological Chemistry* 273, no. 50:33327-33332.

102. Prost, S. Sheahan S. Rannie D. Harrison D. J. 2001. Adenovirus-mediated Cre deletion of floxed sequences in primary mouse cells is an efficient alternative for studies of gene deletion. *Nucleic Acids Research* 29, no. 16:e80.

103. Radonic, A., S. Thulke, I. M. Mackay, O. Landt, W. Siegert, and A. Nitsche. 2004. Guideline to reference gene selection for quantitative real-time PCR. *Biochem.Biophys.Res.Commun.* 313, no. 4:856-862.

104. Raffoul, J. J., D. C. Cabelof, J. Nakamura, L. B. Meira, E. C. Friedberg, and A. R. Heydari. 2004. Apurinic/apyrimidinic endonuclease (APE/REF-1) haploinsufficient mice display tissue-specific differences in DNA polymerase beta-dependent base excision repair. *Journal of Biological Chemistry* 279, no. 18:18425-18433.

105. Ramirez, A., A. Page, A. Gandarillas, J. Zanet, S. Pibre, M. Vidal, L. Tusell, A. Genesca, D. A. Whitaker, D. W. Melton, and J. L. Jorcano. 2004. A keratin K5Cre transgenic line appropriate for tissue-specific or generalized Cre-mediated recombination. *Genesis.* 39, no. 1:52-57.

106. Reed, J. C. 1998. Dysregulation of apoptosis in cancer. *Cancer J.Sci.Am.* 4 Suppl 1:S8-14.

107. Romero-Gallo, J., E. G. Sozmen, A. Chytil, W. E. Russell, R. Whitehead, W. T. Parks, M. S. Holdren, M. F. Her, S. Gautam, M. Magnuson, H. L. Moses, and W. M. Grady. 2005. Inactivation of TGF-beta signaling in hepatocytes results in an increased proliferative response after partial hepatectomy. *Oncogene* 24, no. 18:3028-3041.

108. Ryding, A. D. S. Sharp M. G. F. Mullins J. J. 2001. Conditional transgenic technologies. *Journal of Endocrinology* 171:1-14.

109. Saffran, W. A., S. Ahmed, S. Bellevue, G. Pereira, T. Patrick, W. Sanchez, S. Thomas, M. Alberti, and J. E. Hearst. 2004. DNA repair defects channel interstrand DNA crosslinks into alternate recombinational and error-prone repair pathways. *J.Biol.Chem* 279, no. 35: 36462-36469.

110. Sancar, A. 1996. DNA excision repair. *Annual Review of Biochemistry* 65:43-81.

111. Sargent, R. G. Brenneman Wilson J. H. 1997. Repair of site-specific double-strand breaks in a mammalian chromosome by homologous and illegitimate recombination. *Molecular and Cellular Biology* 17, no. 1:267-277.

112. Sarkar, S., A. A. Davies, H. D. Ulrich, and P. J. McHugh. 2006. DNA interstrand crosslink repair during G1 involves nucleotide excision repair and DNA polymerase zeta. *EMBO J.* 25, no. 6:1285-1294.

113. Schneider, M. R., H. Lahm, M. Wu, A. Hoeflich, and E. Wolf. 2000. Transgenic mouse models for studying the functions of insulin-like growth factor-binding proteins. *FASEB J.* 14, no. 5:629-640.

114. Schulze-Bergkamen, H., M. Schuchmann, B. Fleischer, and P. R. Galle. 2006. The role of apoptosis versus oncotic necrosis in liver injury: Facts or faith? *J.Hepatol.* 44, no. 5: 984-993.

115. Seglen, P. O. 1997. DNA ploidy and autophagic protein degradation as determinants of hepatocellular growth and survival. *Cell Biol.Toxicol.* 13, no. 4-5:301-315.

116. Selfridge, J., K. T. Hsia, N. J. Redhead, and D. W. Melton. 2001. Correction of liver dysfunction in DNA repair-deficient mice with an ERCC1 transgene. *Nucleic Acids Research* 29, no. 22:4541-4550.

117. Sheahan, S., C. O. Bellamy, L. Treanor, D. J. Harrison, and S. Prost. 2004. Additive effect of p53, p21 and Rb deletion in triple knockout primary hepatocytes. *Oncogene* 23, no. 8:1489-1497.

118. Sigal, S. H., P. Rajvanshi, G. R. Gorla, R. P. Sokhi, R. Saxena, D. R. Gebhard, Jr., L. M. Reid, and S. Gupta. 1999. Partial hepatectomy-induced polyploidy attenuates hepatocyte replication and activates cell aging events. *Am.J.Physiol* 276, no. 5 Pt 1:G1260-G1272.

119. Sijbers, A. M. van den Spek P. J. Odijk H. van den Berg J. van Duin M. Westerveld A. Jaspers N. G. J. Bootsma D. Hoeijmakers J. H. J. 1996. Mutational analysis of the human nucleotide excision repair gene ERCC1. *Nucleic Acids Research* 24, no. 17:3370-3380.

120. Singh, N. P., M. T. McCoy, R. R. Tice, and E. L. Schneider. 1988. A simple technique for quantitation of low levels of DNA damage in individual cells. *Exp.Cell Res.* 175, no. 1:184-191.

121. Singh, R., C. Leuratti, S. Josyula, M. A. Sipowicz, B. A. Diwan, K. S. Kasprzak, H. A. Schut, L. J. Marnett, L. M. Anderson, and D. E. Shuker. 2001. Lobe-specific increases in malondialdehyde DNA adduct formation in the livers of mice following infection with Helicobacter hepaticus. *Carcinogenesis* 22, no. 8:1281-1287.

122. Southern, E. M. 1975. Detection of specific sequences among DNA fragments separated by gel electrophoresis. *J.Mol.Biol.* 98, no. 3:503-517.

123. Stec, D. E., R. L. Davisson, R. E. Haskell, B. L. Davidson, and C. D. Sigmund. 1999. Efficient liver-specific deletion of a floxed human angiotensinogen transgene by adenoviral delivery of Cre recombinase in vivo. *J.Biol.Chem.* 274, no. 30:21285-21290.

124. Stenvers, K. L., M. L. Tursky, K. W. Harder, N. Kountouri, S. Amatayakul-Chantler, D. Grail, C. Small, R. A. Weinberg, A. M. Sizeland, and H. J. Zhu. 2003. Heart and liver defects and reduced transforming growth factor beta 2 sensitivity in transforming growth factor beta type III receptor-deficient embryos. *Molecular and Cellular Biology* 23, no. 12:4371-4385.

125. Sugo, N., N. Niimi, Y. Aratani, K. Takiguchi-Hayashi, and H. Koyama. 2004. p53 deficiency rescues neuronal apoptosis but not differentiation in DNA polymerase beta-deficient mice. *Molecular and Cellular Biology* 24, no. 21:9470-9477.

126. Suzme, R., F. Gurdol, G. Deniz, and T. Ozden. 2001. Response in DNA ploidy of hepatocytes to tamoxifen and/or melatonin in vivo. *Res.Commun.Mol.Pathol.Pharmacol.* 109, no. 5-6:275-286.

127. Tang, B., M. Vu, T. Booker, S. J. Santner, F. R. Miller, M. R. Anver, and L. M. Wakefield. 2003. TGF-beta switches from tumor suppressor to prometastatic factor in a model of breast cancer progression. *J.Clin.Invest* 112, no. 7:1116-1124.

128. Tannour-Louet, M. Porteu A. Vaulont S. Kahn A. Vasseur-Cognet M. 2002. A tamoxifen-inducible chimeric cre recombinase specifically effective in the foetal and adult mouse liver. *Hepatology* 35, no. 5:1072-1081.

129. Tateno, C. Takai-Kajihara K. Yamasaki C. Sato H. Yoshizato K. 2000. Heterogeneity of growth potential of adult rat hepatocytes in vitro. *Hepatology* 31, no. 1:65-74.

130. Taub, R. 2004. Liver regeneration: from myth to mechanism. *Nat.Rev.Mol.Cell Biol.* 5, no. 10:836-847.

131. Taylor, A.M., P.J. Byrd. 2005. Molecular pathology of axtaxia telangiectasia. *Journal of Clinical Pathology* 58, no. 10:1009-1015.

132. Thacker, J. 1999. The role of homologous recombination processes in the repair of severe froms of DNA damage in mammalian cells. *Biochimie* 81:77-85.

133. Thacker, J. 2005. The RAD51 gene family, genetic instability and cancer. *Cancer Lett.* 219, no. 2:125-135.

134. Tian, M., R. Shinkura, N. Shinkura, and F. W. Alt. 2004. Growth retardation, early death, and DNA repair defects in mice deficient for the nucleotide excision repair enzyme XPF. *Molecular and Cellular Biology* 24, no. 3:1200-1205.

135. Torres, S., B. P. Diaz, J. J. Cabrera, J. C. Diaz-Chico, B. N. Diaz-Chico, and A. Lopez-Guerra. 1999. Thyroid hormone regulation of rat hepatocyte proliferation and polyploidization. *Am.J.Physiol* 276, no. 1 Pt 1:G155-G163.

136. Trifunovic, A., A. Wredenberg, M. Falkenberg, J. N. Spelbrink, A. T. Rovio, C. E. Bruder, Y. Bohlooly, S. Gidlof, A. Oldfors, R. Wibom, J. Tornell, H. T. Jacobs, and N. G. Larsson. 2004. Premature ageing in mice expressing defective mitochondrial DNA polymerase. *Nature* 429, no. 6990:417-423.

137. Tripsianes, K., G. Folkers, E. Ab, D. Das, H. Odijk, N. G. Jaspers, J. H. Hoeijmakers, R. Kaptein, and R. Boelens. 2005. The structure of the human ERCC1/XPF interaction domains reveals a complementary role for the two proteins in nucleotide excision repair. *Structure* 13, no. 12:1849-1858.

138. van Duin, M. de Wit J. Odijk H. Westerveld A. Yasui A. Koken M. H. M. Hoeijmakers J. H. J. Bootsma D. 1986. Molecular characterisation of the human excision repair gene. *Cell* 44:913-923.

139. van Duin, M. Koken M. H. M. van den Tol J. ten Dijke P. Odijk H. Westerveld A. Bootsma D. Hoeijmakers J. H. J. 1987. Genomic characterisation of the human DNA excision repair gene ERCC-1. *Nucleic Acids Research* 15, no. 22:9195-9213.

140. van Duin, M. van den Tol J. Warmerdam and Odijk H. Westerveld A. Bootsma D. Hoeijmakers J. H. J. P. 1988. Evolution and mutagenesis of the mammalian excision repair gene ERCC-1. *Nucleic Acids Research* 16, no. 12:5305-5323.

141. Vandesompele, J., K. De Preter, F. Pattyn, B. Poppe, N. Van Roy, A. De Paepe, and F. Speleman. 2002. Accurate normalization of real-time quantitative RT-PCR data by geometric averaging of multiple internal control genes. *Genome Biol.* 3, no. 7:RESEARCH0034.

142. Verrou, C., Y. Zhang, C. Zurn, W. W. Schamel, and M. Reth. 1999. Comparison of the tamoxifen regulated chimeric Cre recombinases MerCreMer and CreMer. *Biol.Chem.* 380, no. 12:1435-1438.

143. Videla, L. A., R. Rodrigo, J. Araya, and J. Poniachik. 2004. Oxidative stress and depletion of hepatic long-chain polyunsaturated fatty acids may contribute to nonalcoholic fatty liver disease. *Free Radic.Biol.Med.* 37, no. 9:1499-1507.

144. Vindelov, L. L. 1977. Flow microfluorometric analysis of nuclear DNA in cells from solid tumors and cell suspensions. A new method for rapid isolation and straining of nuclei. *Virchows Arch.B Cell Pathol.* 24, no. 3:227-242.

145. Weaver, D. T. 2003. V(D)J recombination and double-strand break repair. *Advances in immunology* 58:29-85.

146. Weber, L. W., M. Boll, and A. Stampfl. 2003. Hepatotoxicity and mechanism of action of haloalkanes: carbon tetrachloride as a toxicological model. *Crit Rev.Toxicol.* 33, no. 2:105-136.

147. Weeda, G. Donker I. de Wit J. Morreau H. Janssens R. Vissers C. J. Nigg A. van Steeg H. Bootsma D. Hoeijmakers J. H. J. 1997. Disruption of mouse ERCC1 results in a novel repair syndrome with growth failure, nuclear abnormalities and senescence. *Current Biology* 7:427-439.

148. Westerveld, A. Hoeijmakers J. H. J. van Duin M. de Wit J. Odijk H. Wood R. D. Bootsma D. 1984. Molecular cloning of human DNA repair gene. *Nature* 310:425-429.

149. Wheelhouse, N. M., Y. S. Chan, S. E. Gillies, H. Caldwell, J. A. Ross, D. J. Harrison, and S. Prost. 2003. TNF-alpha induced DNA damage in primary murine hepatocytes. *Int.J.Mol.Med.* 12, no. 6:889-894.

150. Winter, A. G., C. Dorgan, and D. W. Melton. 2005. Expression of a splicing variant in the 5'-UTR of the human ERCC1 gene is not cancer related. *Oncogene* 24, no. 12:2110-2113.

151. Wirth, K. G., R. Ricci, J. F. Gimenez-Abian, S. Taghybeeglu, N. R. Kudo, W. Jochum, M. Vasseur-Cognet, and K. Nasmyth. 2004. Loss of the anaphase-promoting complex in quiescent cells causes unscheduled hepatocyte proliferation. *Genes Dev.* 18, no. 1:88-98.

152. Wood, T. L., L. E. Rogler, M. E. Czick, A. G. Schuller, and J. E. Pintar. 2000. Selective alterations in organ sizes in mice with a targeted disruption of the insulin-like growth factor binding protein-2 gene. *Mol.Endocrinol.* 14, no. 9:1472-1482.

153. Wu, D. F. and A. I. Cederbaum. 2003. Role of p38 MAPK in CYP2E1-dependent arachidonic acid toxicity. *Journal of Biological Chemistry* 278, no. 2:1115-1124.

154. Wu, H., M. Wade, L. Krall, J. Grisham, Y. Xiong, and T. Van Dyke. 1996. Targeted in vivo expression of the cyclin-dependent kinase inhibitor p21 halts hepatocyte cell-cycle progression, postnatal liver development and regeneration. *Genes Dev.* 10, no. 3:245-260.

155. Xu, H. Swoboda I. Bhalla P. L. Sijbers A. M. Zhao C. Ong E. K. Hoeijmakers J. H. J. Singh M. B. 1998. Plant homologue of human excision repair gene ERCC1 points to conservation of DNA repair mechanisms. *The Plant Journal* 13, no. 6:823-829.

156. Yan, Q. W., E. Reed, X. S. Zhong, K. Thornton, Y. Guo, and J. J. Yu. 2006. MZF1 possesses a repressively regulatory function in ERCC1 expression. *Biochemical Pharmacology* 71, no. 6:761-771.

157. Yu, J. J., K. B. Lee, C. J. Mu, Q. D. Li, T. V. Abernathy, F. Bostick-Bruton, and E. Reed. 2000. Comparison of two human ovarian carcinoma cell lines (A2780/CP70 and MCAS) that are equally resistant to platinum, but differ at codon 118 of the ERCC1 gene. *International Journal of Oncology* 16, no. 3:555-560.

158. Yu, J. J., K. Thornton, Y. Guo, H. Kotz, and E. Reed. 2001. An ERCC1 splicing variant involving the 5 '-UTR of the mRNA may have a transcriptional modulatory function. *Oncogene* 20, no. 52:7694-7698.

159. Zafonte, B. T. Hulit J. Amanatullah D. F. Albanese C. Wang C. Rosen E. Reutens A. Sparano J. A. Lisanti M. P. Pestell R. G. 2000. Cell-cycle dysregulation in breast cancer: breast cancer therapies targeting the cell-cycle. *Frontiers in Bioscience* 5:938-361.

160. Zhang, Y., C. Riesterer, A. M. Ayrall, F. Sablitzky, T. D. Littlewood, and M. Reth. 1996. Inducible site-directed recombination in mouse embryonic stem cells. *Nucleic Acids Res.* 24, no. 4:543-548.

161. Zheng, H., X. Wang, R.J. Legerski, P.M. Glazer, L. Li. 2006. Repair of DNA interstrand cross- links: interaction between homology- dependent and homology- independent pathways. *DNA repair* 5, no. 5: 566-574.

162. Zienolddiny, S., D. Campa, H. Lind, D. Ryberg, V. Skaug, L. Stangeland, D. H. Phillips, F. Canzian, and A. Haugen. 2006. Polymorphisms of DNA repair genes and risk of non-small cell lung cancer. *Carcinogenesis* 27, no. 3:560-567.